GA-A14243
UC-77

GAS TURBINE HTGR PROGRAM

QUARTERLY PROGRESS REPORT FOR THE PERIOD ENDING DECEMBER 31, 1976

by
PROJECT STAFF

Prepared under
Contract EY-76-C-03-0167
Project Agreement No. 46
for the San Francisco Operations Office
U.S. Energy Research and Development Administration

GENERAL ATOMIC PROJECT 3227

DATE PUBLISHED: JANUARY 1977

ABSTRACT

This report describes work performed under ERDA Contract EY-76-C-03-167, Project Agreement No. 46, for the period October 1, 1976 through December 31, 1976. The ERDA program effort is directed at completing a conceptual design of the gas turbine HTGR that will satisfy U.S. requirements and allow participation in international cooperative investigations related to establishing plant configuration and application incentives.

The studies reported here include refinements to the design and performance of the General Atomic Company 3-loop, 3000 MW(t) dry-cooled plant having a delta arrangement. This design was evaluated in 1976 by A. D. Little, Inc. The recuperator, precooler, and turbomachinery designs were compared with those by the German-Swiss High Temperature Reactor with Helium Turbine (HHT) Project. The comparisons are presented herein.

CONTENTS

FIGURES

FIGURES (Continued)

TABLES

TABLES (Continued)

1. INTRODUCTION AND SUMMARY

This report describes progress of the Gas Turbine High-Temperature Gas-Cooled Reactor (GT-HTGR) Program, Contract E(04-3)-167 (now Contract EY-76-C-03-0167), Project Agreement No. 46, for the period October 1, 1976, through December 31, 1976. The purpose of this report is to cover activity relating to plant conceptual design and to review designs by General Atomic Company (GA) and the German/Swiss High Temperature Reactor with Helium Turbine (HHT) Project. The studies on materials for the direct-cycle HTGR performed at GA are separately reported. Previous results from the ERDA GT-HTGR program are described in Refs. 1, 2, and 3.

The three horizontal turbomachines (one for each power-conversion loop) have been rearranged into a delta configuration inside the PCRV below the HTGR core in the latest GA design evolution (Fig. 1-1). The precooler and recuperator heat exchangers, each in a separate vertical cavity, surround the core cavity. This arrangement together with the system parameters selected about a year ago was evaluated by independent consultants for ERDA (Ref. 4). Their conclusion was that the GT-HTGR is potentially the lowest cost converter reactor.

The direct-cycle HTGR designs by the German/Swiss HHT Project have evolved somewhat differently from the GA design of the GT-HTGR for the U.S. The respective plant designs result from the lower electric generation frequency of 50 Hz in Europe vs 60 Hz in the U.S., differences in climate, utility load profile, and licensing, as well as differences in design approach. The HHT Project is currently investigating: 1) a 3000 MW(t)/1200 MW(e) dry-cooled plant with a single intercooled helium turbomachine and two parallel trains of heat exchangers integrated into the PCRV (designated as INT), and 2) a 3000 MW(t)/1200 MW(e) wet-cooled combined-cycle plant consisting of an integrated single nonintercooled helium turbomachine

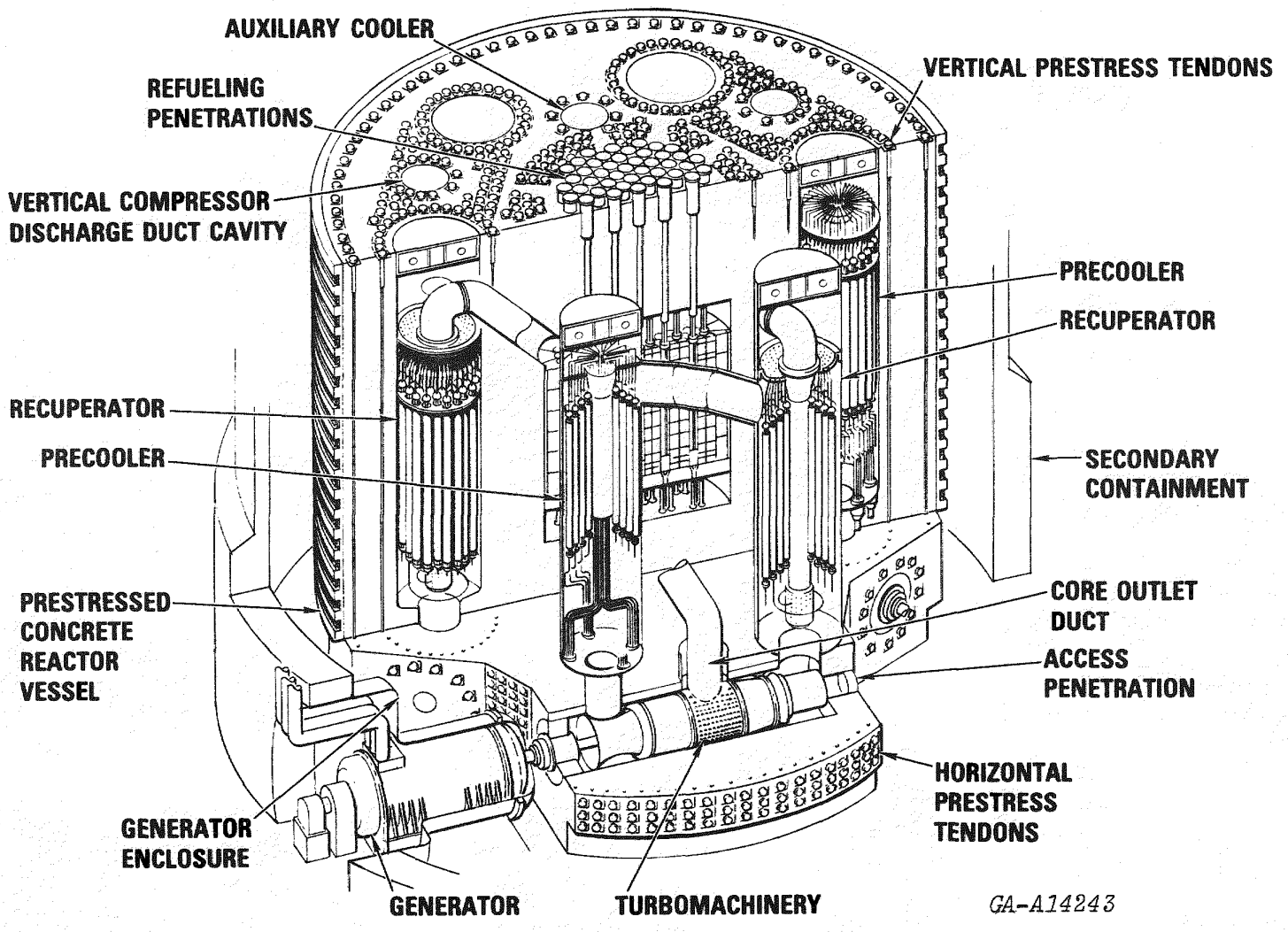

Fig. 1-1. 3 loop 3000 MW(t) GT-HTGR power plant

with a steam generator heated by the helium turbine exhaust and an external steam turbine plant (designated KD). Both the INT and KD plants have essentially the same thermal efficiency and output as the GA 3-loop design. The INT HHT plant has been the primary subject of GA comparisons with the GA 3-loop GT-HTGR plant.

It is clear that further commonality between the U.S. and European direct-cycle HTGR designs will improve the results achievable with current resources and will enhance future development work. Hence, portions of the ERDA program reported here include reviews and comparisons of GT-HTGR and HHT designs with the objective of increased technical commonality.

The work reported here has concentrated on completing outstanding items from the previous work and providing comparisons between the GA and HHT Project designs. Section 2 describes the plant performance incorporating the latest pressure loss estimates, seal leakages, and turbomachine component efficiency estimates. The resulting performance shows little change from that reported in Refs. 1 and 4.

The larger cost uncertainties in the plant are associated with the balance-of-plant (BOP). Accordingly, as a part of the utility program, a BOP study has been initiated at United Engineers and Constructors (UE&C). The BOP design requirements were prepared under the ERDA Project Agreement 46 program and layout criteria were issued as GA Document GTC-2-3, "GT-HTGR Design Criteria: Plant Layout Criteria."

Various system studies are reported in Section 3, including 1) a flashing steam bottoming cycle that was investigated as a way of increasing efficiency and as an alternative to intercooling, 2) loop pressure loss calculations, 3) thermal transients accompanying the startup of a down loop, 4) preliminary wet/dry cooling tower studies, and 5) the use of the helium purification system for inventory control. The latter appears to have quite promising performance for only a modest cost increase. The seismic response of the PCRV without the previous ring support structure is also discussed in Section 3.

Comparisons of component designs are presented in Section 4, including precooler, recuperator, and turbomachinery. New design work in these areas includes conceptual studies of a recuperator with integral return tubes in each module for the heated high-pressure helium instead of a single central duct, and of a precooler that is supported from the bottom. Differences in heat-transfer and pressure-loss calculations by GA and the HHT Project are reviewed. The approach to heat exchanger installation and removal is also discussed.

Section 4.3 describes PCRV design studies. Of particular significance is the work on cold and warm liner arrangements in which the liner is left bare, which is of interest as one of several ways to achieve inspection and monitoring of the liner. An effort to clarify the ASME Boiler and Pressure Vessel Code, Section III, Division 2, with respect to rules for a multipressure, multicavity PCRV has been initiated. This clarification offers significant potential for cost reduction. Finally, modest design changes to the PCRV are discussed, including a revised tendon layout, improved integration of the control valves into the PCRV, and core cavity cooling with a down loop.

2. PERFORMANCE STUDIES

2.1 REVISED PLANT PERFORMANCE

Revised performance predictions for the 3000 MW(t) GT-HTGR with a reactor outlet temperature (ROT) of 850°C (1562°F) were determined. These data are for the existing plant design, but use new, revised component performance estimates and up-to-date estimates of seal leakages. The plant efficiency is 39.6% when dry-cooled by ISO atmosphere at 15°C (59°F). If the plant is designed to European ground rules of 10°C (50°F) ambient air temperature the efficiency would be 40.16%. No changes were made to the existing plant design. Major design parameters for the dry cooled plant are shown in Table 2-1.

The reactor core pressure loss used in the performance estimates is consistent with a 10-row fuel block instead of the original 8-row block. This change results in a smaller coolant hole pitch and diameter and increased core flow resistance, but does not alter the reactor core size. The smaller, more numerous coolant holes improve cooling as is required for the core outlet temperature of 850°C. Two other parameters influencing the plant performance are the component pressure losses at design conditions and the plant leakage/cooling flows. Table 2-2 shows complete component pressure losses at design conditions for the 3000 MW(t), 850°C GT-HTGR. Data pertaining to the turbomachinery are provided by UTC and the rest by GA. The 3-loop delta plant arrangement shown in Dwg SK-92C was used to determine the GA pressure loss data.

Table 2-3 lists leakage flows in the plant and the turbine cooling flow. The leakage flows in the recuperator shroud seal and in the turbomachinery cavity seals are increased over earlier estimates. A leakage flow of 0.1% was attributed to the primary bypass control valve past its

TABLE 2-1
MAJOR DESIGN PARAMETERS FOR 3000 MW(t) 850°C GT-HTGR - DRY COOLED

Turbine inlet temperature	850°C (1562°F)
Ambient air temperature	15°C (59°F)
Compressor pressure ratio	2.5
Compressor inlet temperature	26.1°C (79°F)
Compressor discharge pressure	7.93 MPa (1150 psia)
System pressure loss ratio	0.0672
Recuperator effectiveness	0.898
Turbine isentropic efficiency	91.8%
Compressor isentropic efficiency	89.8%
Generator efficiency	98.8%
Primary system heat loss	18.9 MW(t)
Station auxiliary power	11 MW(e)
Station efficiency	39.55%
Net electrical output	1186.5 MW(e)
Reactor thermal power	3000 MW(t)
Compressor helium flow rate per loop	571.3 kg/sec (4,537,450 lb/hr)

TABLE 2-2
PRESSURE LOSSES AT DESIGN CONDITIONS FOR
3000 MW(t), 850°C DELTA DESIGN GT-HTGR

Segment	Source of Estimate	Pressure Loss (%) $\Delta P/P$[a]
Compressor Exit Diffuser	UTC	0.470
Compressor Exit Diffuser Dump	UTC	0.230
Compressor Exit Interface (Shell Holes)	UTC	0.030
Compressor Exit Contraction	UTC	0.000
Compressor Exit Interface to Recuperator Inlet	GA	0.141
Within Recuperator (Cold Side)	GA	0.620
Recuperator Exit to Reactor Inlet	GA	0.522
Within Reactor	GA	1.110
Reactor Exit to Gas Turbine Inlet Interface	GA	0.108
Turbine Inlet Interface	UTC	0.000
Turbine Inlet Volute	UTC	0.364
Turbine Exit Case Struts	UTC	0.040
Turbine Exhaust Diffuser	UTC	0.090
Turbine Exit Interface or Dump Loss	UTC	0.320
Turbine Exit Contraction	UTC	0.010
Turbine Exit Interface to Recuperator Inlet	GA	0.387
Within Recuperator (Hot Side)	GA	1.22
Recuperator Exit to Precooler Inlet	GA	0.245
Within Precooler	GA	0.99
Precooler Exit to Compressor Inlet Interface	GA	0.008
Compressor Inlet Interface	UTC	0.000
Compressor Inlet Volute	UTC	0.250

[a] Pressure loss values, $\Delta P/P$, are not additive.

TABLE 2-3
LEAKAGE AND TURBINE COOLING FLOWS FOR
3000 MW(t), 850°C GT-HTGR

Leakage From	Leakage (%)
Recuperator Shroud Seal	0.50
Precooler Shroud Seal	0.25
Compressor to Turbine Cavity Seal	0.40
Compressor Exit to Inlet Cavity Seal	0.40
Primary Bypass Control Valve Seat	0.10
Compressor Discharge to Turbine Inlet Duct Flange Seal	0.14
Turbine Cooling Flow from Compressor Outlet	3.6

seat, and, similarly, a leakage of 0.14% was attributed through the bellows seal from the compressor discharge into the turbine inlet. Turbine cooling and sealing flows amount to 3.6%, compared with 2.5% estimated previously.

The compressor inlet temperature selected for the design point is 26.1°C (79°F). This temperature is consistent with a 15°C (59°F) dry bulb temperature with dry cooling. The GT-HTGR project expects utilities with winter peak demand to desire such low design point temperature. (Winter peaks are more common in Europe than in the U.S.) For summer peaks, one of two different approaches would be taken. The plant design point could be adjusted for a higher compressor inlet temperature, which might require new turbomachine blading designs. Alternatively, wet/dry cooling could be used, in which case the 26.1°C (79°F) compressor inlet temperature should be appropriate.

A schematic GT-HTGR cycle is shown in Fig. 2-1 which identifies locations referred to in Table 2-4. Table 2-4 lists the cycle data for a dry-cooled single 3000 MW(t) 850°C GT-HTGR plant.

2.2 THERMAL TRANSIENTS DURING STARTUP

Studies performed earlier for various plant startup schemes for a 3000 MW(t) GT-HTGR indicated potential problems from transient temperature gradients in the plant components, particularly in the recuperator unit. For example, during the transient of a single loop starting up from shutdown with the other two loops operating, a sharp gradient was observed in the transient temperature profile at the low-pressure recuperator inlet (Fig. 2-2). The present study therefore was directed to alleviate this problem by suitably revising the attemperation control logic and so generate moderate temperature transients in the plant components.

The condition of starting up a single turbomachine with the other machines running at significant speed could exist after the machine has been shutdown (for a variety of reasons; i.e., loop trip, maintenance). The

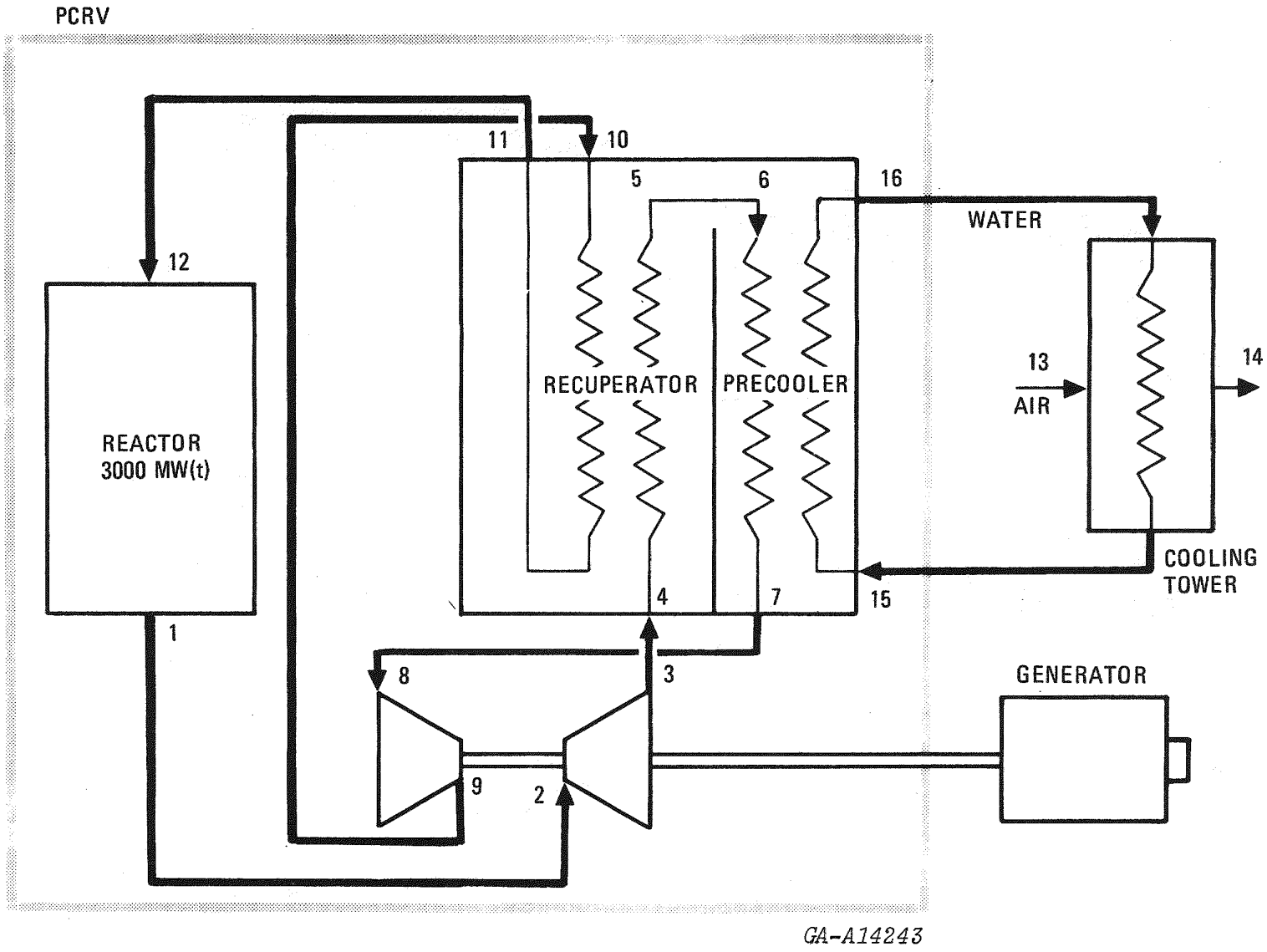

Fig. 2-1. Gas Turbine HTGR cycle diagram

TABLE 2-4
3000 MW(t) GT-HTGR CYCLE DATA FOR CORE OUTLET TEMPERATURE OF 850°C

Station Number From Fig. 2-1	Position	Pressure [MPa (psia)]	Temperature [°C (°F)]	Flow/Loop [kg/sec (lb/hr)]
12	Reactor Inlet	7.76 (1126.1)	498.1 (928.5)	1634.4 (12,981,354)
1	Reactor Outlet	7.68 (1113.6)	850.0 (1562.1)	1634.4 (12,981,354)
	Duct Inlet	7.68 (1113.6)	850.0 (1562.1)	544.8 (4,327,118)
	Duct Outlet	7.64 (1108.9)	850.0 (1562.0)	544.8 (4,327,118)
2	Turbine Inlet	7.64 (1108.9)	849.0 (1560.2)	545.6 (4,333,471)
3	Turbine Outlet	3.28 (475.6)	536.5 (997.7)	566.2 (4,496,819)
	Duct Inlet	3.28 (475.6)	535.0 (994.9)	569.0 (4,519,300)
	Duct Outlet	3.26 (472.2)	534.9 (994.9)	569.0 (4,519,300)
4	Recuperator Hot Inlet	3.26 (472.2)	534.8 (994.7)	566.1 (4,496,703)
5	Recuperator Hot Outlet	3.22 (466.4)	223.3 (434.0)	566.1 (4,496,703)
	Duct Inlet	3.22 (466.4)	223.2 (433.8)	569.0 (4,519,300)
	Duct Outlet	3.21 (465.3)	223.2 (433.8)	569.0 (4,519,300)
6	Precooler Inlet	3.21 (465.3)	223.2 (433.5)	567.6 (4,508,002)

TABLE 2-4 (Continued)

Station Number From Fig. 2-1	Position	Pressure [MPa (psia)]	Temperature [°C (°F)]	Flow/Loop [kg/sec (lb/hr)]
7	Precooler Outlet	3.18 (460.7)	26.1 (79.0)	567.6 (4,508,002)
	Duct Inlet	3.18 (460.7)	26.1 (79.0)	569.0 (4,519,300)
	Duct Outlet	3.17 (460.0)	26.1 (79.0)	569.0 (4,519,300)
8	Compressor Inlet	3.17 (460.0)	26.7 (80.1)	571.3 (4,537,450)
9	Compressor Outlet	7.93 (1150.0)	174.5 (346.2)	571.3 (4,537,450)
	Duct Inlet	7.93 (1150.0)	174.4 (346.2)	545.3 (4,331,450)
	Duct Outlet	7.85 (1138.5)	174.2 (346.1)	545.3 (4,331,450)
10	Recuperator Cold Inlet	7.85 (1138.5)	174.2 (346.1)	545.3 (4,331,450)
11	Recuperator Cold Outlet	7.80 (1131.4)	498.1 (928.6)	545.3 (4,331,450)
	Duct Inlet	7.80 (1131.4)	498.1 (928.6)	545.3 (4,331,450)
	Duct Outlet	7.76 (1126.1)	498.1 (928.5)	545.3 (4,331,450)
	Cooling Water Inlet	[1.99 avg (289.2 avg)]	20.60 (69.0)	9331.0 (74,113,660)
	Cooling Water Outlet	[1.99 avg (289.2 avg)]	167.8 (334.0)	9331.0 (74,113,660)

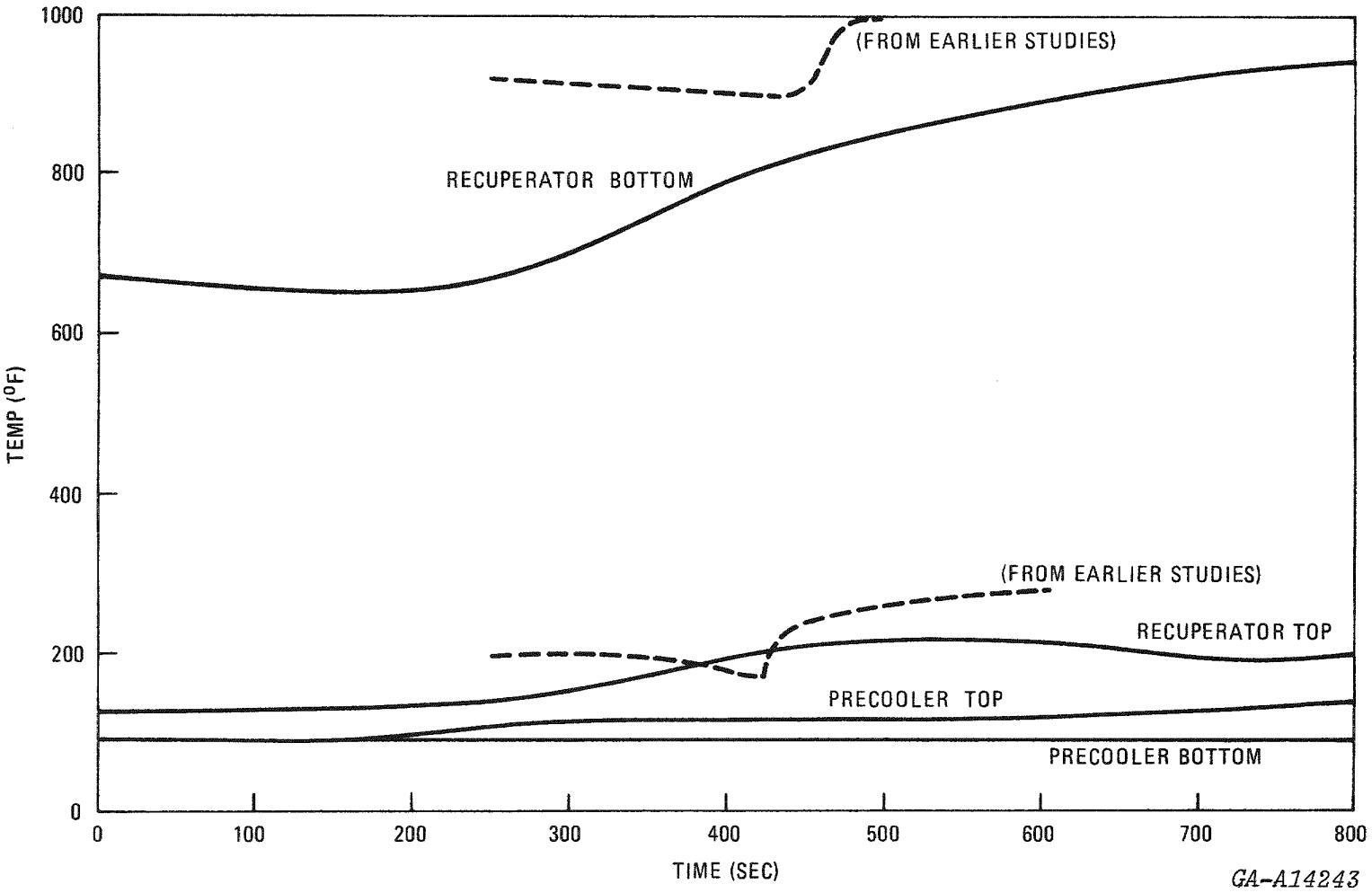

Fig. 2-2. 3000 MW(t) GT-HTGR heat exchanger metal temperatures during single loop startup

most severe condition would be when the two operating loops were at full speed and carrying the largest possible electrical load, and this is the condition discussed here.

Two conditions were chosen for the single-loop startup scheme for determining the worst-case implications of thermal cycling. They were 1) with partial helium inventory in the plant (approximately 62.5% full inventory), and 2) with full inventory in the plant. The reduced helium inventory startup technique decreases the motoring power requirements, whereas full inventory determines an upperbound of the required starting power.

The REALY2 computer code (Ref. 5) was used to analyze the startup conditions. The reactor core outlet temperature was lowered and held at 593.3°C (1100°F). The electrical loads on two operating loops were reduced commensurately with the lower core outlet temperature, and the turbomachines were held at full speed of 3600 rpm. The third loop was shut down for some time, simulating a steady-state condition. Reverse flow was fully established in the down loop.

From this condition, the turbomachine speed in the down loop was ramped up at the rate of 2 rpm/sec. Reactor power started increasing and the turbine started generating power as its speed was increased. The turbomachine was eventually brought to its full speed of 3600 rpm, then synchronized to pick up the electric load.

The startup condition simulated in the present study is typical up to about 700 sec, but after that the simulation is not representative. The results obtained from this study are valid between 200 and 700 sec, the period during which the flow switches direction and the generator is still being motored. The helium flow, which was initially in the reverse direction in the downloop, switches its flow to the conventional forward direction as the turbomachine speed increases. After the switch in the flow direction, rapid temperature changes occur in the plant components.

In the original control system design, the control system monitors recuperator temperatures at its low-pressure inlet and high-pressure outlet. Whenever the sum of the two temperatures exceed the sum determined at its full-load or part-load steady-state design point operation (depending on scheduled plant load operation), the attemperation valve opens. The open valve diverts the relatively cold helium gas at one compressor outlet to the low-pressure recuperator inlet, preventing the metal from attaining excessive temperatures. This attemperation control lacked one feature to control potential rapid temperature gradients in the plant components, however, such as those encountered during a single loop startup such as is being studied. In the present study the attemperation logic was revised to include an additional feature to control this event.

The attemperation temperature demand value was set to be not greater than the sum of the transient temperatures at the low-pressure recuperator inlet and high-pressure recuperator outlet plus 10°F. The attemperation valve will remain closed whenever the measured temperatures are less than the demand. Conditions might exist where the system could force the measured temperatures below the normal load set temperature demand. In such situations the revised attemperation control will keep the temperatures from rising too rapidly from their lower values later. The selection of 10°F in excess of the measured temperatures is arbitrary. The objective was to initiate the opening of the attemperation valve as soon as the point of inflection was reached and limit the temperature transient. The results of the study indicate that the demand profile selected to follow the measured value down yielded a moderate temperature transient (Fig. 2-2). Thus, by having the demand follow the measured value down and then only allowing a fixed rate of demand increase, the good limiting of temperature transients by attemperation control is accomplished. The upper bound on the attemperation temperature demand value was set equal to the sum at full-load design point condition as in the original control system, which precluded excessive temperatures in the plant components.

Figure 2-2 shows the full and Fig. 2-3 shows the partial helium inventory transient temperature profiles at the low-pressure recuperator

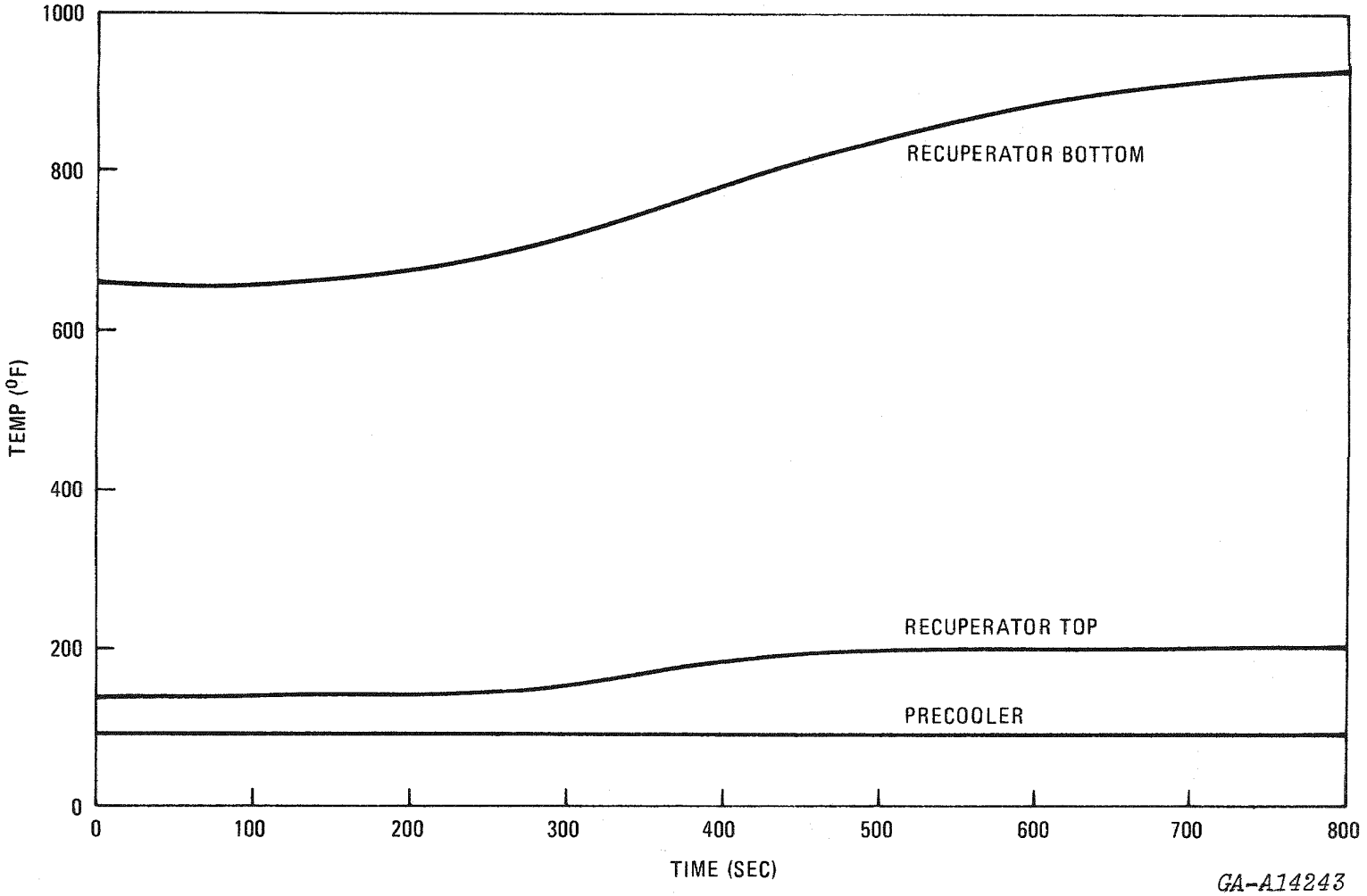

Fig. 2-3. 3000 MW(t) GT-HTGR heat exchanger metal temperatures during single loop startup at partial inventory

entry during the single-loop startup. It appears from the temperature profiles shown that they are relatively gradual; local gradients in the profiles are quite modest.

Figure 2-4 illustrates the single-loop startup behavior with full helium inventory in the plant. All time periods referred to herein are reckoned from loop startup. The attemperation valve opening starts at about 205 sec to effect a gradual temperature increase in the recuperator material. When the turbomachine attains a speed of 1400 rpm, the motoring power is reduced to zero, ending the region of typical startup operation. With turbine outlet temperature decreasing, the low-pressure recuperator inlet temperature also starts lowering, and the attemperation valve remains closed after 780 sec. In the actual controlled startup operation, the primary bypass valve will start opening to control the single-loop turbomachine speed as the electrical motoring input power goes to zero.

Figure 2-5 illustrates the transient behavior of the single loop during startup with reduced inventory. At about 200 sec the attemperation valve starts opening to control the recuperator temperature increases at the hot end. The valve begins closing near 780 sec. Again, the operation beyond this time is not typical, but the actual transient is expected to be moderate for times beyond 780 sec.

2.3 WET/DRY COOLING

Results of a very preliminary investigation of wet/dry cooling are reported in Ref. 6 and summarized here. This brief study serves to quantify the effect of wet/dry cooling on the economic competitiveness of the GT-HTGR.

A reference wet/dry cooling system for the GT-HTGR was selected to minimize the design impact on the existing dry-cooled GT-HTGR design and to expedite a preliminary evaluation of the economics of the system. The reference system is identical to the all-dry system, except that a wet cooling tower further cools the water from the dry cooling tower via an intermediate water-to-water heat exchanger.

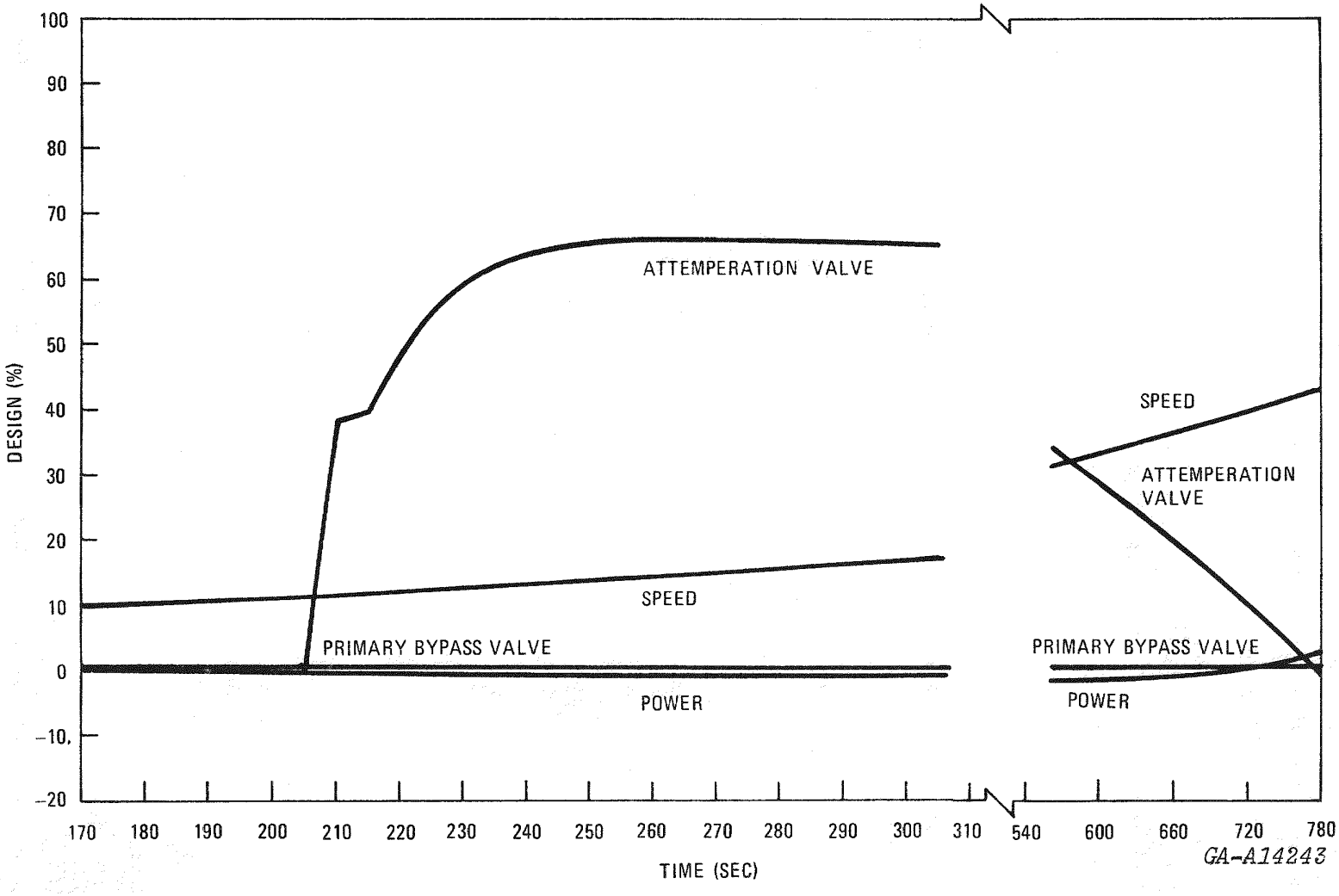

Fig. 2-4. Transient performance of 3000 MW(t) GT-HTGR during single loop startup at full inventory

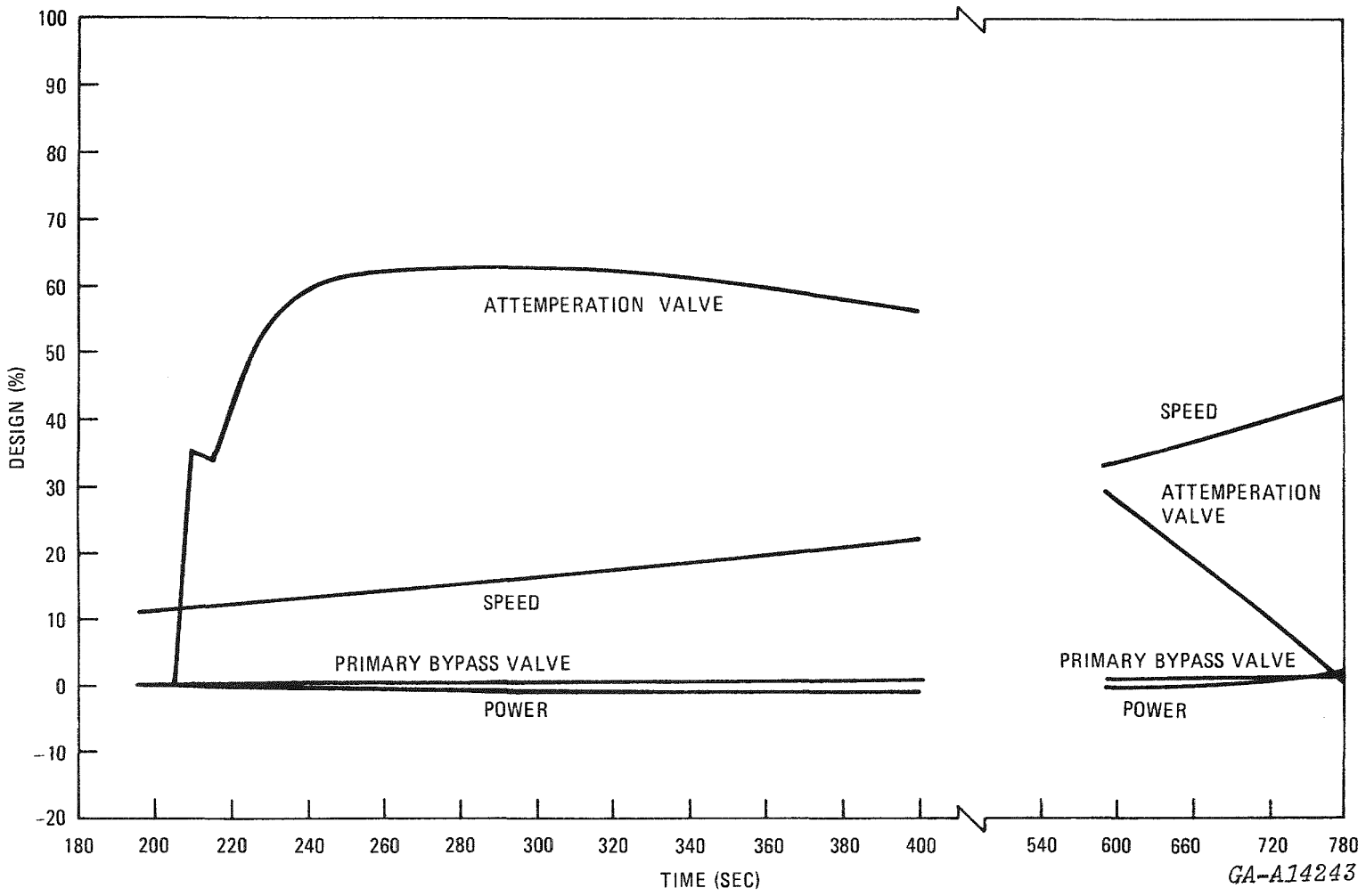

Fig. 2-5. Transient performance of 3000 MW(t) GT-HTGR during single loop startup at reduced inventory

The GT-HTGR investigations are based on the study of wet/dry cooled LWR plants performed by United Engineers & Constructors (UE&C) (Ref. 7). Economic results for the GT-HTGR can be compared with the LWR plants. Preliminary comparisons show that the GT-HTGR can reduce its evaluated costs in changing from all-dry to wet/dry cooling as much as can an LWR. Therefore, the large economic incentives previously demonstrated for the all-dry-cooled GT-HTGR are believed to exist when both plants are compared on a wet/dry-cooled basis. Wet/dry cooling should not affect the competitive position of the GT-HTGR.

The GT-HTGR obtains its savings due to shifting from dry to wet/dry cooling in a manner different from the LWRs. As shown in the UE&C report, capital costs of a wet/dry-cooled LWR increase compared to an all-dry-cooled plant. Savings for LWRs are achieved by reducing the large penalties for lost performance. In contrast, the GT-HTGR has lower capital costs with wet/dry cooling, but saves slightly less in penalties for lost performance.

The penalties for lost performance dominate preliminary economic evaluation. Because the effect of wet/dry cooling on performance is more easily and accurately determined, the conclusions are not especially sensitive to the conceptual nature of these design and capital cost estimates.

2.4 FLASHING STEAM BOTTOMING CYCLE

2.4.1 Summary

Flashing steam was evaluated in a GA-funded comprehensive study, which led to the selection of the reference binary system using ammonia. New calculations have been performed and are described here.

Figure 2-6 shows the conditions for a flashing steam cycle using the existing precooler. Penalties such as steam/water pressure losses, turbine exit losses, additional station auxiliary loads (although main feedpump

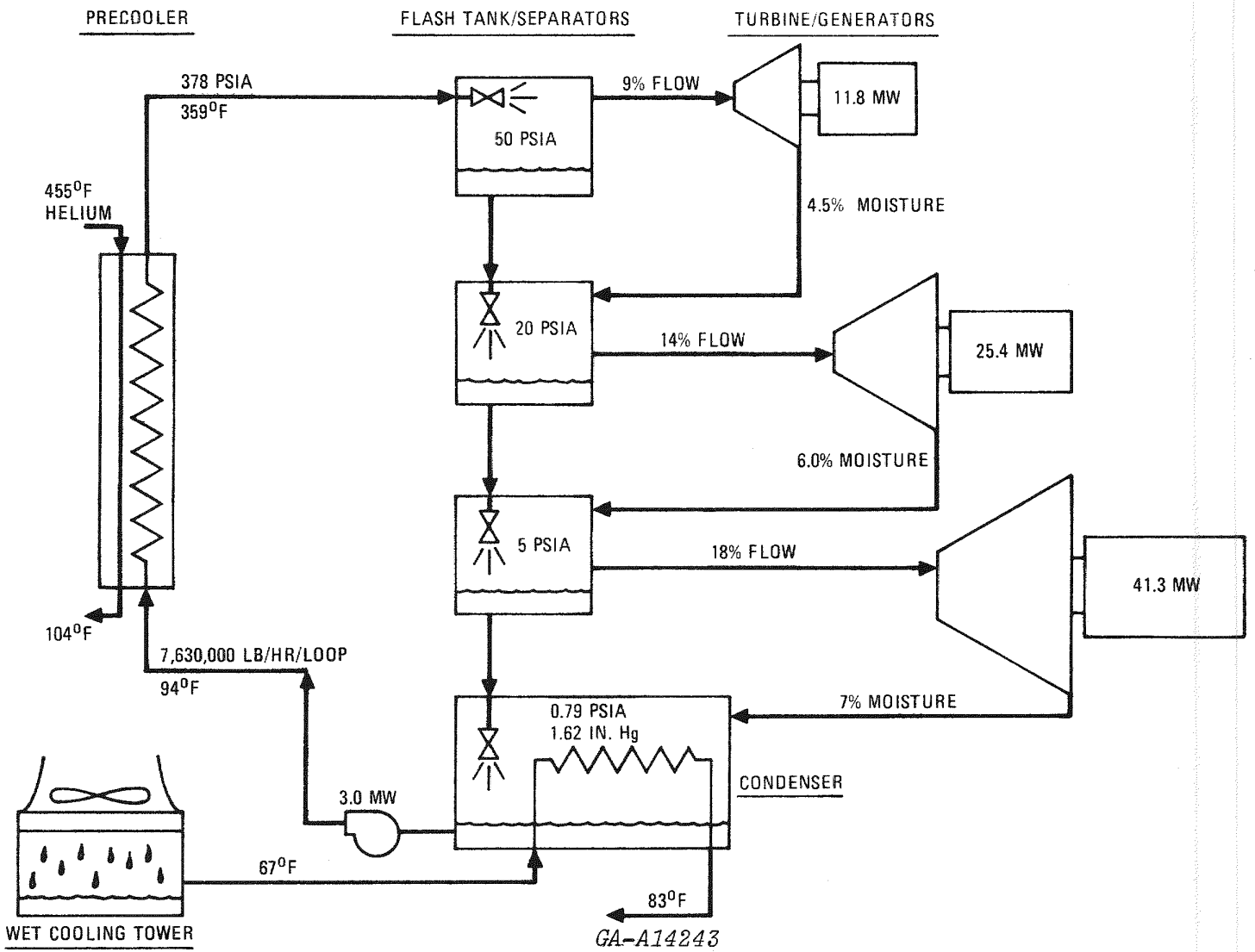

Fig. 2-6. Flashing steam bottoming cycle with conventional precooler

power is included), heat losses, etc. were not included. Subsequent studies based on this cycle, accounting for the penalties described, resulted in an efficiency estimate of 44.5%. (The configuration with three separate turbines as shown in Fig. 2-6 was chosen to simplify cycle calculations. In practice, the turbines - with multiple extractors and inlets - would probably be placed on a single shaft with one generator.)

An alternative arrangement was also investigated with the objective of keeping the primary helium compressor inlet temperature at the low reference level, using an additional precooler section to independently cool the compressor inlet helium. An additional 0.7 percentage point again is possible. The performance gain may be substantially offset by 1) increased system complexity and capital cost, and 2) added helium system pressure losses with the two-stage precooler.

2.4.2 Ammonia Bottoming Cycle Efficiency

The efficiency calculated for the ammonia bottoming cycle has decreased since the conceptual studies (Ref. 2) were performed, primarily because more detailed calculations were used.

An additional decrease in binary plant efficiency has been identified but not yet included in the reference efficiency numbers. New (believed to be more accurate) fluid properties data have been obtained, which reduced the plant efficiency by 1.1 percentage points. This would put the ammonia binary cycle efficiency near 47% for a primary system core outlet temperature of 850°C.

2.4.3 Dry Cooling Potential

The efficiency estimates for both ammonia and flashing steam systems are based on evaporative cooling at the same ambient wet-bulb temperature. The flashing steam system differs from normal condensing cycles in that it produces a large quantity of low-pressure hot water that cannot in any

practical way produce more electricity. While this water represents a thermodynamic efficiency loss, it does allow some fraction of the heat to be rejected with economical dry cooling towers.

Although the wet-bulb air temperature is lower than the dry-bulb air temperature, it is characteristic of condensing systems used with both GT-HTGR steam and ammonia that they cause the compressor inlet temperature to rise from its dry-cooled value without a bottoming cycle.

3. SYSTEM STUDIES

3.1 SYSTEM PRESSURE LOSS

The efficiency of a closed-cycle gas turbine plant is very sensitive to the system pressure loss, because for given cycle parameters, it establishes the turbine expansion ratio and thus power output (i.e., $\Sigma(\Delta P/P) = 1 - Rt/Rc$). In the GA 3-loop reference plant design, close attention has been given to the design of the major components and the geometry of the gas flow paths within the PCRV to minimize pressure loss. In this phase of the design program, a limited study was carried out to refine the pressure loss estimates, particularly the losses associated with the primary system ducting.

Figure 3-1 outlines the stations and boundaries within the primary system for computation of pressure losses. Details of the direct pressure losses, consistent with Fig. 3-1 for the internal gas flow paths, are shown on Tables 3-1 and 3-2. The summation of pressure losses within the primary system ducting is 1.41%. It is interesting that frictional losses in the ducting represent only about 10% of the duct loss; the bulk of the losses are associated with expansion and contraction. A summation of all the losses in the power-conversion loop is given on Table 3-3.

Emphasis has been placed on establishing exactly how much low-pressure loss occurs in the components in laying out the primary system to give good flow path geometries. The 3-loop reference design with the delta PCRV layout results in good performance because the overall system pressure loss is low.

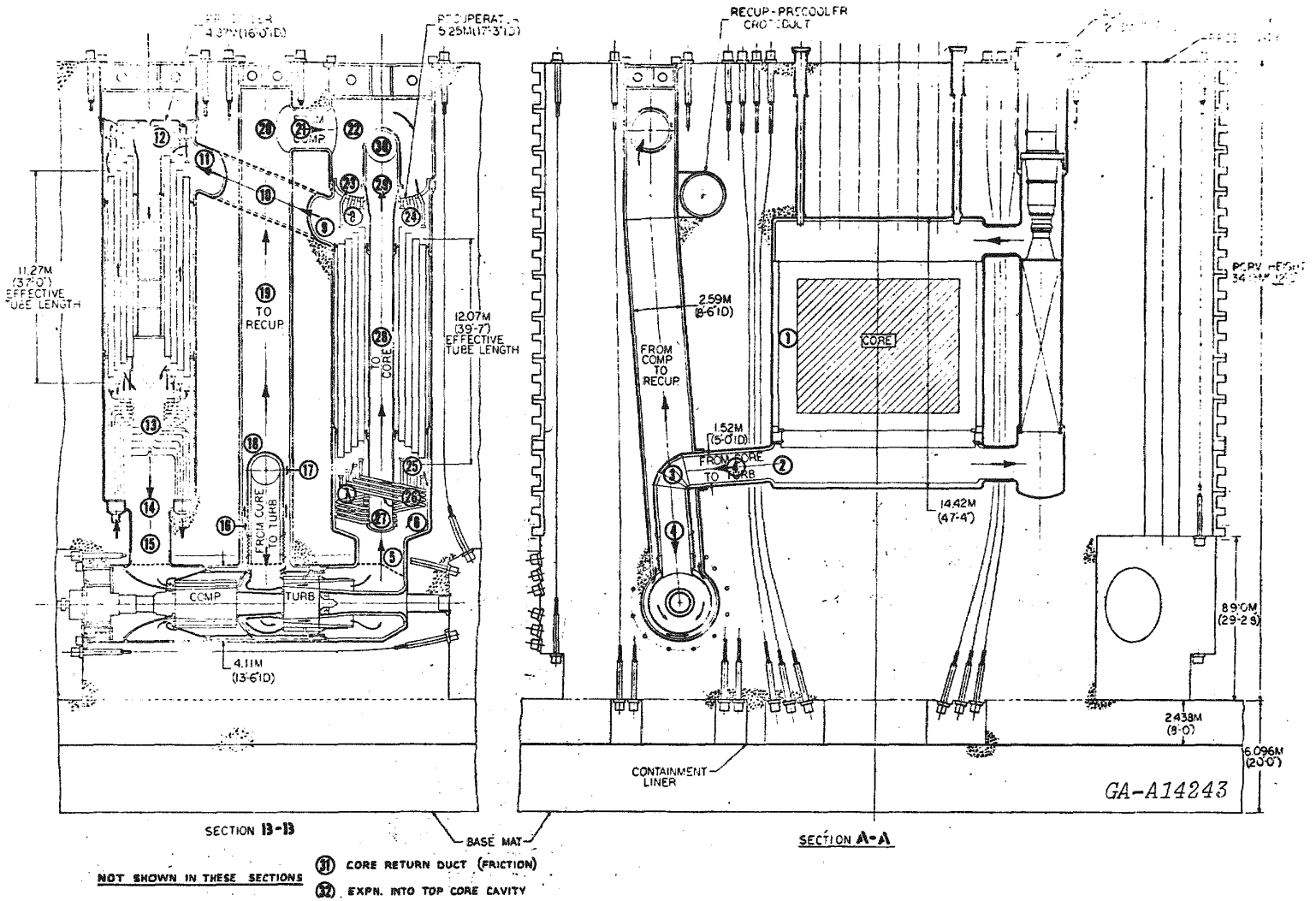

Fig. 3-1. System pressure loss plane definition

TABLE 3-1
SYSTEM PRESSURE LOSS PARAMETERS FOR REFERENCE PLANT DESIGN

GT-MTGR DUCT LOSSES ** 850 DEG C ** 3 LOOP CONFIGURATION

	DESCRIPTION	L FT	D FT	A SQ FT	K	T DEG F	P PSIA	W MM LBS/HR	VISC LB/FT HR
1	CORE	.00	.00	.00	.000	1562.	1130.	4.44	.119
2	CONTRACTION	.00	5.00	.00	.025	1562.	1130.	4.44	.119
3	90 DEG BEND	.00	5.00	.00	.510	1562.	1130.	4.44	.119
4	FRICTION	35.00	5.00	.00	.000	1562.	1130.	4.44	.119
5	FRICTION	4.00	8.00	.00	.000	1012.	474.	4.56	.096
6	EXPANSION	.00	8.00	.00	3.000	1012.	474.	4.56	.096
7	TUBE DRAG	10.50	14.15	.00	2.000	1012.	474.	4.55	.096
8	TUBE DRAG	.00	8.00	.00	.500	430.	468.	4.55	.068
9	CONTRACTION	.00	7.00	.00	.025	430.	468.	4.55	.068
10	FRICTION	27.00	7.00	.00	.000	430.	468.	4.56	.068
11	EXPANSION	.00	7.00	.00	1.000	430.	468.	4.55	.068
12	TUBE DRAG	.00	8.00	.00	1.000	430.	468.	4.55	.068
13	TUBE DRAG	21.00	15.37	.00	2.000	79.	463.	4.55	.048
14	CONTRACTION	.00	15.37	.00	.025	79.	463.	4.56	.048
15	FRICTION	9.00	6.50	33.18	.000	79.	460.	4.56	.048
16	ANNULUS	17.00	5.90	27.52	.000	348.	1150.	4.44	.064
17	BLOCKAGE	.00	5.15	20.86	.010	348.	1150.	4.44	.064
18	EXPANSION	.00	5.15	20.86	.490	348.	1150.	4.44	.064
19	FRICTION	60.00	8.50	.00	.000	347.	1143.	4.44	.063
20	PLUGGED TEE	.00	8.50	.00	1.500	347.	1143.	4.44	.063
21	FRICTION	7.00	6.50	33.18	.000	347.	1143.	4.44	.063
22	EXPANSION	.00	6.50	33.18	3.000	347.	1143.	4.44	.063
23	CONTRACTION	.00	.46	.00	.300	347.	1143.	.03	.063
24	FRICTION	4.50	.46	.00	.000	347.	1143.	.03	.063
25	FRICTION	25.00	.46	.00	.000	944.	1133.	.03	.093
26	315 DEG BEND	.00	.46	.00	.300	944.	1133.	.03	.093
27	EXPANSION	.00	.46	.00	.800	944.	1133.	.03	.093
28	FRICTION	53.00	4.00	.00	.000	944.	1133.	4.44	.093
29	DIFFUSOR	5.25	4.00	.00	.100	944.	1133.	4.44	.093
30	140 DEG BEND	.00	5.50	.00	.350	944.	1133.	4.44	.093
31	FRICTION	35.00	5.50	.00	.000	944.	1133.	4.44	.093
32	EXPANSION	.00	5.50	.00	3.000	944.	1133.	4.44	.093

TABLE 3-2
DUCT PRESSURE LOSS DATA FOR REFERENCE PLANT DESIGN

GT-MTGR DUCT LOSSES ** 850 DEG C ** 3 LOOP CONFIGURATION

	DESCRIPTION	DEN LB/CU FT	A SQ FT	F	RE	VELOCITY FT/SEC	Q PSI	FL/D	K	ΔP PSI	ΔP/P %	SUM ΔP/P %
1	CORE	.208	.000	.009	.000	0.	.000	.000	.000	.000	.000	.000
2	CONTRACTION	.208	19.635	.009	.953+07	301.	2.041	.000	.025	.051	.005	.005
3	90 DEG BEND	.208	19.635	.009	.953+07	301.	2.041	.000	.510	1.041	.092	.097
4	FRICTION	.208	19.635	.009	.953+07	301.	2.041	.063	.000	.129	.011	.108
5	FRICTION	.120	50.266	.009	.760+07	210.	.570	.005	.000	.003	.001	.109
6	EXPANSION	.120	50.266	.009	.760+07	210.	.570	.000	3.000	1.710	.361	.469
7	TUBE DRAG	.120	157.255	.010	.428+07	67.	.058	.008	2.000	.116	.025	.494
8	TUBE DRAG	.196	50.266	.009	.107+08	128.	.348	.000	.500	.174	.037	.531
9	CONTRACTION	.196	38.485	.009	.122+08	167.	.593	.000	.025	.015	.003	.534
10	FRICTION	.196	38.485	.009	.122+08	168.	.595	.035	.000	.021	.004	.539
11	EXPANSION	.196	38.485	.009	.122+08	167.	.593	.000	1.000	.593	.127	.665
12	TUBE DRAG	.196	50.266	.009	.107+08	128.	.348	.000	1.000	.348	.074	.739
13	TUBE DRAG	.320	185.540	.009	.781+07	21.	.016	.013	2.000	.031	.007	.746
14	CONTRACTION	.320	185.540	.009	.783+07	21.	.016	.000	.025	.000	.000	.746
15	FRICTION	.318	33.180	.009	.185+08	120.	.494	.012	.000	.006	.001	.748
16	ANNULUS	.531	27.520	.009	.150+08	84.	.408	.026	.000	.011	.001	.749
17	BLOCKAGE	.531	20.860	.009	.172+08	111.	.710	.000	.010	.007	.001	.749
18	EXPANSION	.531	20.860	.009	.172+08	111.	.710	.000	.490	.348	.030	.779
19	FRICTION	.528	56.745	.009	.105+08	41.	.096	.064	.000	.006	.001	.780
20	PLUGGED TEE	.528	56.745	.009	.105+08	41.	.096	.000	1.500	.145	.013	.793
21	FRICTION	.528	33.180	.009	.137+08	70.	.282	.010	.000	.003	.000	.793
22	EXPANSION	.528	33.180	.009	.137+08	70.	.282	.000	3.000	.846	.074	.867
23	CONTRACTION	.528	.165	.013	.136+07	99.	.558	.000	.300	.167	.015	.882
24	FRICTION	.528	.165	.013	.136+07	99.	.558	.128	.000	.072	.006	.888
25	FRICTION	.301	.165	.014	.931+06	174.	.979	.769	.000	.752	.066	.954
26	315 DEG BEND	.301	.165	.014	.931+06	174.	.979	.000	.300	.294	.026	.980
27	EXPANSION	.301	.165	.014	.931+06	174.	.979	.000	.800	.783	.069	1.049
28	FRICTION	.301	12.566	.009	.153+08	326.	3.450	.119	.000	.411	.036	1.086
29	DIFFUSOR	.301	12.566	.009	.153+08	326.	3.450	.012	.100	.386	.034	1.120
30	180 DEG BEND	.301	23.758	.009	.111+08	172.	.965	.000	.350	.338	.030	1.149
31	FRICTION	.301	23.758	.009	.111+08	172.	.965	.057	.000	.055	.005	1.154
32	EXPANSION	.301	23.758	.009	.111+08	172.	.965	.000	3.000	2.896	.256	1.410

TABLE 3-3
SYSTEM PRESSURE LOSSES FOR 3-LOOP
GA REFERENCE PLANT DESIGN

Component or System	Pressure Loss ($\Delta P/P$, %)
Turbomachine Inlets and Exits	
Compressor Inlet	0.25
Compressor Exit	0.73
Turbine Inlet	0.36
Turbine Exit	0.46
Σ Turbomachine Losses	1.80
Recuperator (HP side)	0.62
Recuperator (LP side)	1.22
Precooler	0.99
System Duct Losses	1.41
Core Loss (10 row block)	1.11
Primary System Loss Summation	7.15[(a)]

[(a)] This direct summation is not strictly valid, but the low value is indicative of a well designed closed-cycle system. In the cycle calculations the overall system pressure loss is given by:

$$\Sigma\ (\Delta P/P) = 1 - \frac{Rt}{Rc}) \times 100 = 6.8\%$$

3.2 HELIUM INVENTORY CONTROL

The GT-HTGR can achieve very high part-load efficiency by controlling helium inventory. The use of the helium purification system to match changes in load demand by inventory control for the GT-HTGR has been examined.

3.2.1 Objective of Helium Inventory Control

Nuclear power plants thus far have been base loaded. Nuclear power will someday supply a large part of the nation's electricity, and when it does, part-load operation of nuclear plants will be necessary for following the normal daily and weekly load changes. Because high part-load efficiency will save fuel cycle costs, plants with high-part load efficiency will have an advantage.

The objective of the helium inventory control system is therefore to save fuel costs. Savings in fuel costs, including benefits of fuel resource conservation, must justify any expenditures on the inventory control system. Figure 3-2 illustrates the change in plant efficiency with helium inventory.

3.2.2 Performance Requirements

Helium transfer from the primary coolant system to storage during helium inventory control is made via the helium purification system to ensure that only purified helium is returned to storage. The removal rate for the primary coolant system to the helium storage system is limited by the helium purification system. The low temperature absorbers can be damaged if the volumetric flow rate exceeds the design flow for extended periods of time. Although the detailed design of the helium purification system for the GT-HTGR has not been prepared, the design requirements have been identified and the system would be designed on the basis of the steam-cycle HTGR.

The reference design helium flow (Ref. 8) was selected to be a maximum of 0.13 m^3/sec, 310 acfm (measured at the interface between the purification system outlet and the helium storage system inlet). The filters,

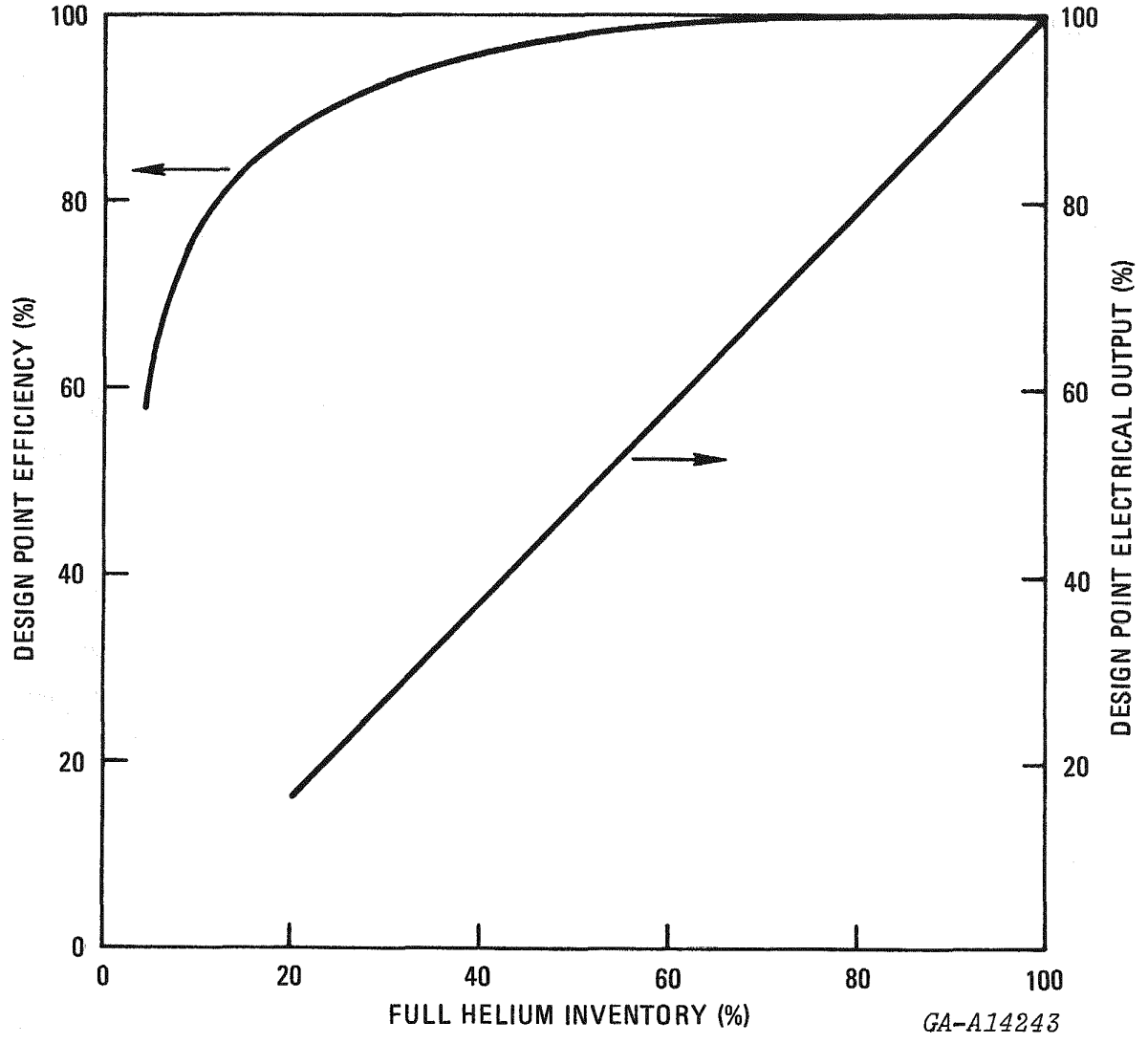

Fig. 3-2. Relationship between helium inventory, plant output and efficiency

absorbers, and transfer compressors are sized to this selected value. Holding the volumetric flow constant during helium inventory control results in a variable mass flow rate through the system because of the reduction in primary coolant pressure. The net helium flow rate for helium inventory control is the total flow minus the helium flow makeup requirements for the PCRV seal and purge system and other auxiliaries. The helium makeup flow varies in direct proportion to the power output. At 100% power rating, approximately 0.83 kg/sec (6650 lbm/hr) is required for makeup.

Figure 3-3 shows the net removal rate for the reference system and for a hypothetical system with twice the flow capacity. One method of increasing the helium purification capacity by two times its reference design value is to operate the additional standby purification train during the power ramp reductions. This method would require no additional equipment over the reference design.

Figure 3-4 shows the ramp reduction capabilities of the reference and double capacity systems. The daily load demand curve for a so-called typical utility is given in Fig. 3-5. This curve can be simplified by assuming 8 hr at maximum power, 8 hr at reduced power, and two 4-hr transition periods with linear power rates of change.

The maximum power ramp decrease illustrated in Fig. 3-5 is approximately 0.15%/min of full power. This value is within the capability of the present system, performance of which is illustrated in Fig. 3-4, namely, a 0.2%/min maximum, or 0.15%/min average. The double-capacity would provide even greater margin.

3.2.3 Proposed Operation of Helium Purification System for Load Following

The procedure below would be used for all load reductions:

1. The initial load reduction would be handled by the bypass control valve.

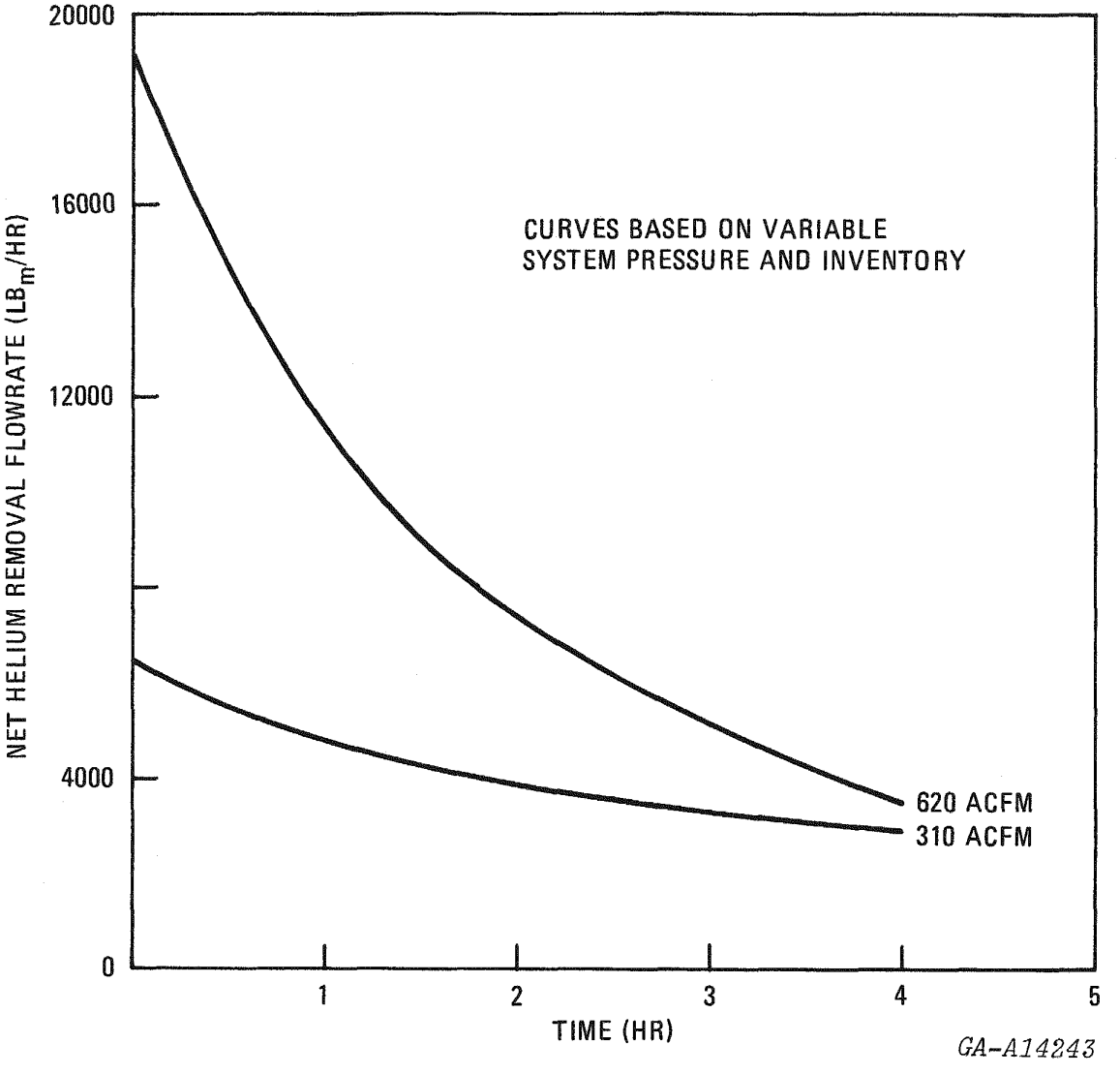

Fig. 3-3. Helium removal rate during helium inventory control for various purification capacities

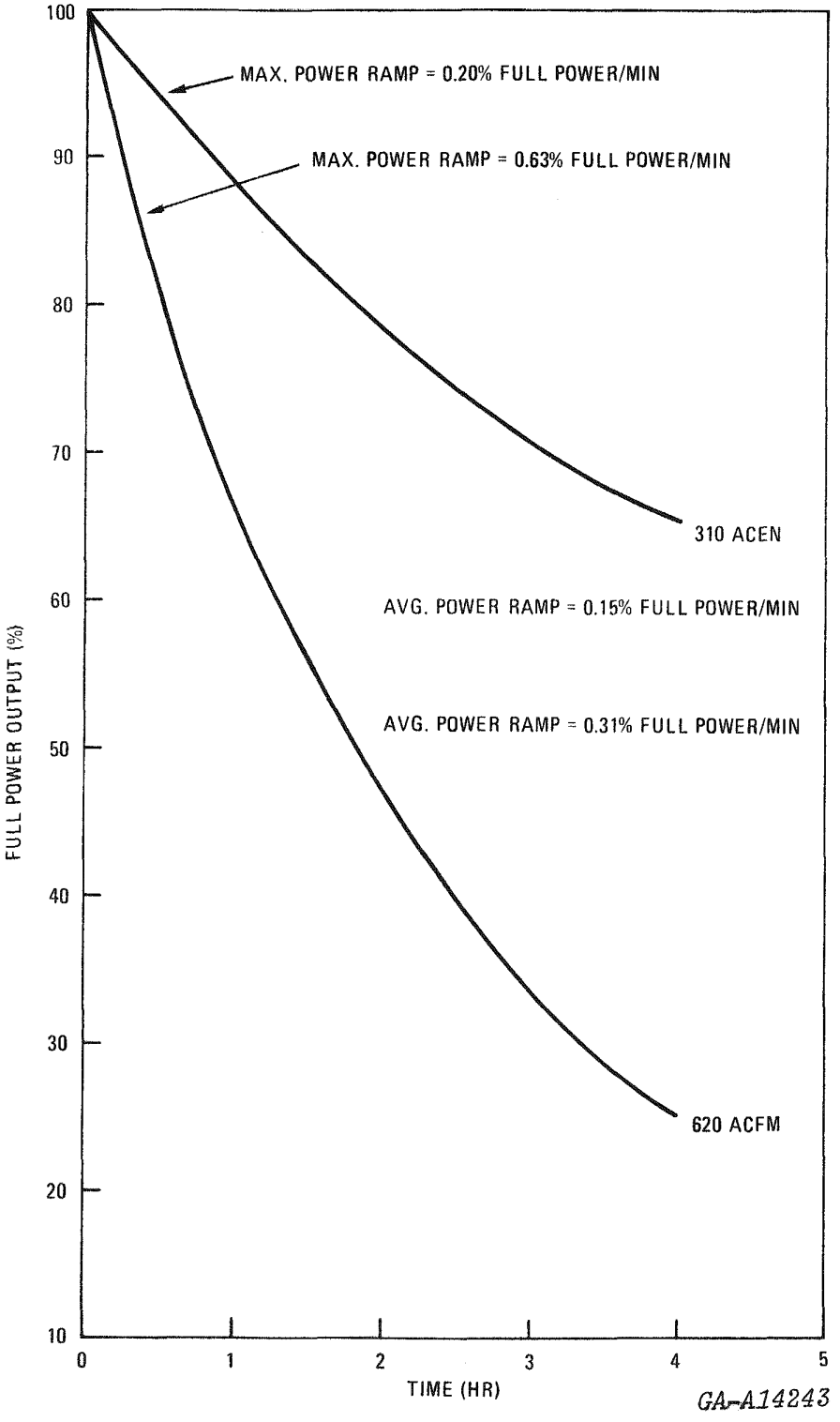

Fig. 3-4. Ramp decrease in full power output using helium inventory control

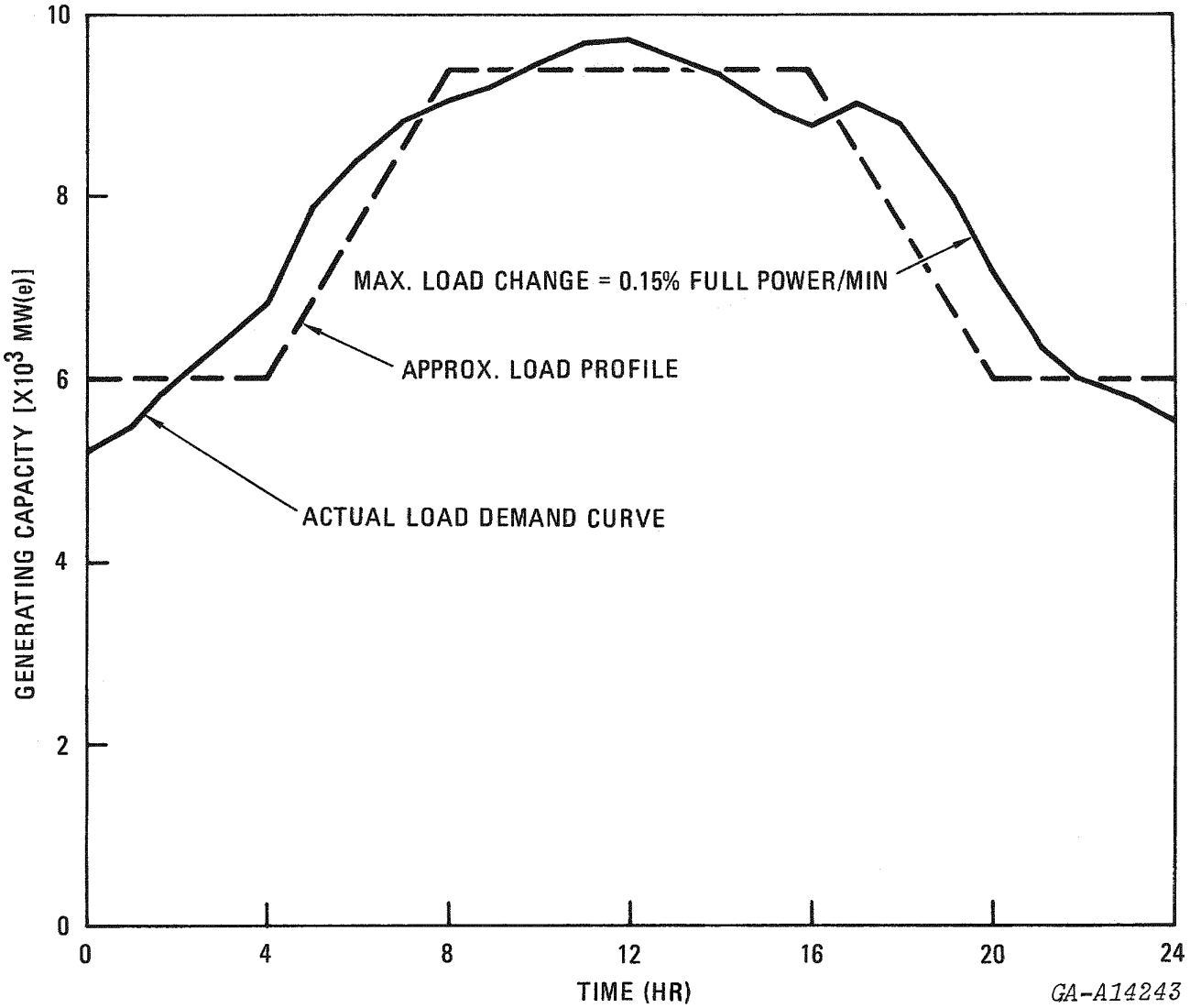

Fig. 3-5. Daily load variations of a typical utility

2. Concurrent with the load reduction, the helium purification system would begin pumping helium out of the PCRV to high-pressure storage tanks. The bypass control valve would close as inventory is reduced.

3. The helium storage system would be readied for possible load increases before the bypass control valve stops its control capability.

The following procedure would be followed for 10% step load increases:

1. Helium would be injected into the PCRV from that portion of the purified helium storage system designated to accommodate the 10% step increase.

2. The helium storage system would be readied for a subsequent 10% step increase within a 2-hr period.

The procedure for all sustained load increases would be to inject helium into the PCRV at the required rate.

Continuous operation of the trim valve would be required for fine load control; no helium inventory control system would be adequate to replace the trim valve. Therefore, some small excess of helium would always be required in the PCRV for a margin in which the trim valve could operate. It would be expected that an excess of helium would be injected and the control valves would be used to match the load exactly, until the load demand and helium inventory stabilize.

Implicit in the operating procedures is the requirement that helium be stored at such pressures and in such quantities that it can be reinjected at sufficient rates to meet load increases. Control will be maintained with the bypass control valve sufficient to return to 100% at any time and at

any required rate, until the helium storage system is made ready to do so. Transfer of control capability from the bypass valve to the helium inventory control system is envisioned as a continuous process.

3.3 SEISMIC RESPONSE OF PCRV WITHOUT SUPPORT STRUCTURE

A preliminary seismic analysis of the PCRV and reactor containment building (RCB) for the GT-HTGR was reported in Ref. 1. The GT-HTGR plant configuration has now changed so that the PCRV is directly supported by the RCB base mat, rather than supported by the PCRV ring support as in the previous analysis. The change of the PCRV bottom head to the three delta cavities has for purposes of PCRV seismic response evaluation, been assumed to be negligible.

The purpose of these design changes was twofold:

1. To reduce the RCB height.

2. To reduce, if possible, the mismatch between the turbomachine and the generator during a seismic event.

To assess the effects of these design changes on the dynamic response of the GT RCB/PCRV, a seismic model without the PCRV ring support was prepared as shown in Fig. 3-6. Data such as lumped masses and sectional properties of the connecting bar required for the seismic model were assumed to be the same as those reported in Ref. 1.

A seismic analysis of the GT RCB/PCRV model, Fig. 3-6, was performed using the SAP IV program, Ref. 9. This multipurpose program is capable of performing static as well as dynamic analysis. The comparisons of the various dynamic parameters, in particular time history response between two seismic runs (one reported in Ref. 1; one the results of this analysis) are discussed in the following paragraphs.

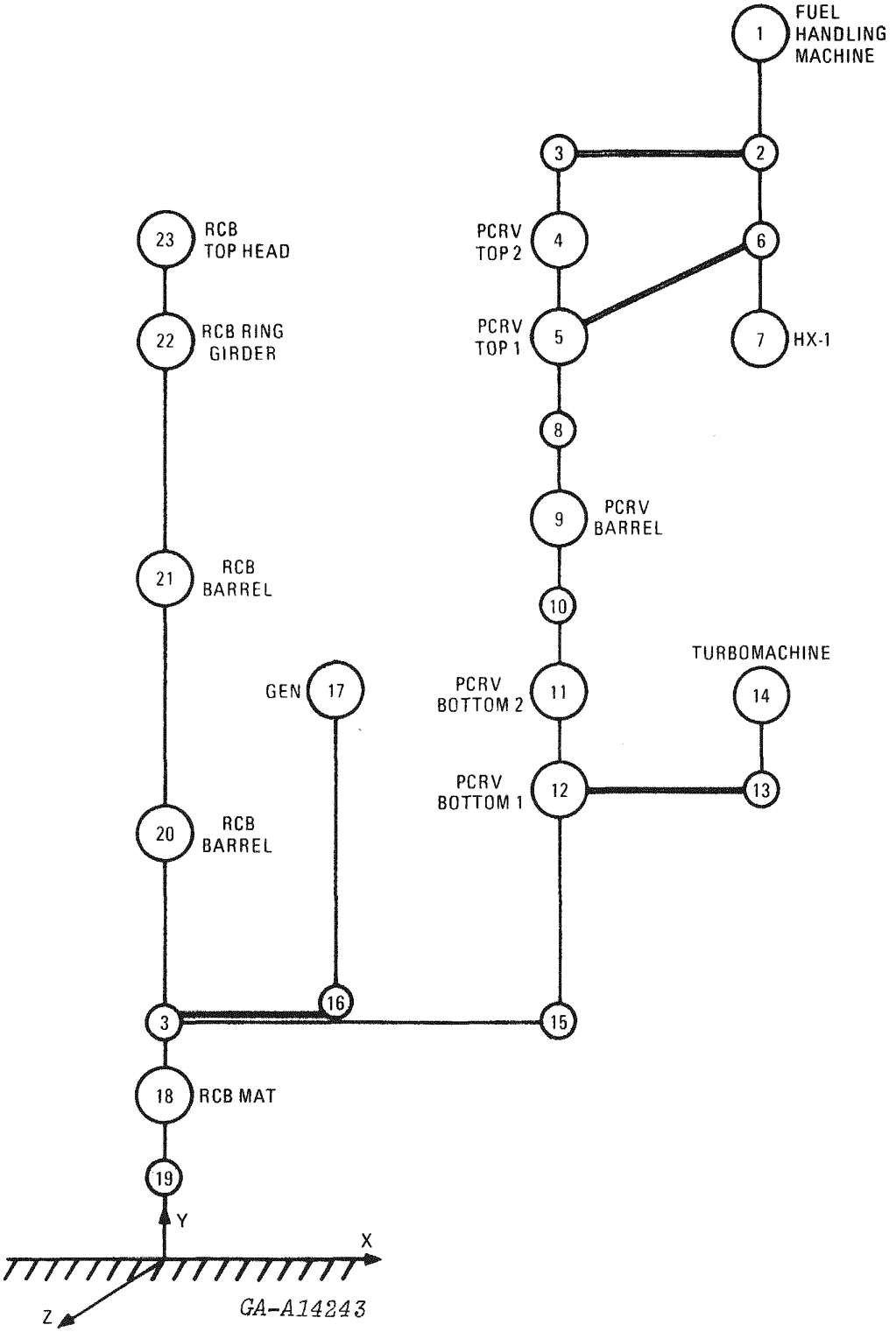

Fig. 3-6. GT-RCB/PCRV new seismic model without PCRV ring support

Time history analyses were performed to generate the in-structural response spectra at the various RCB/PCRV location. For this analysis the in-structural response spectra were also generated for the different soil conditions based on the method outlined in Ref. 1. For the response spectra analyses, the following RCB/PCRV locations were selected:

1. Turbomachine support
2. Reactor core support
3. Heat exchanger support
4. PCRV top head (fuel handling machine support)
5. RCB support (top of base mat)

The comparison of the in-structural response spectrum curve at the turbomachinery support between two seismic runs, one with the PCRV ring support and the other without the PCRV ring support, is shown in Fig. 3-7. Based on this plot, it can be concluded that the response spectrum maxima for the latter run are less than or equal to those reported in Ref. 1, and that frequency at which the maxima occur is also found to be higher. Nevertheless, the effect of this design change, i.e., removal of PCRV support ring, is considered to have beneficial effects on the in-structural response spectra.

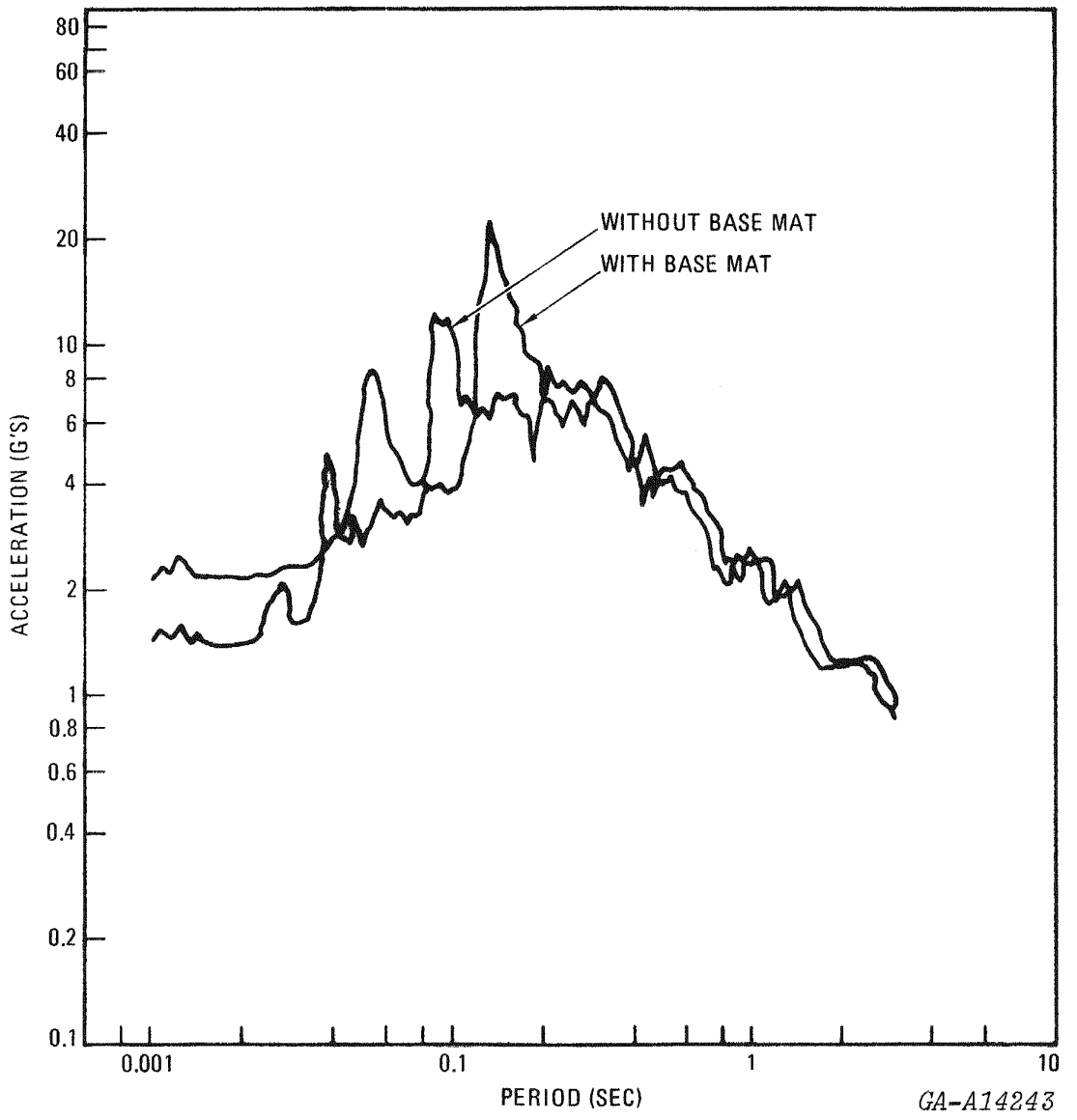

Fig. 3-7. Turbomachinery support floor horizontal response spectra rock soil (OBE)

4. DESIGN STUDIES

4.1 HEAT EXCHANGER DESIGNS

4.1.1 Introduction and Summary

In this phase of the program the heat exchanger design effort was essentially limited to 1) refining the GA designs for improved performance and/or simpler mechanical arrangements, and 2) comparing the GA and HHT configurations as a step toward increased design commonality. Heat exchanger design activities also included a review of the HHT design concepts and generation of data for the GA arrangements, particularly for heat exchanger installation and removal. Additional work and discussion by GA and HHT is needed on the desirability of compact heat exchanger designs and of the fabrication cost increments associated with compact designs.

Both the GA and HHT heat exchangers embody straight tube counterflow arrangements consisting of a multiplicity of modular assemblies. By virtue of the much higher loop rating of the HHT plant, the recuperator is much larger than the GA design (and this is even further accentuated by the higher effectiveness chosen for the HHT plant). Because of the different cycles (HHT incorporating an intercooler), no direct precooler comparison is possible, even though both plants utilize axial flow arrangements, with the water inlet and outlet headering pipes at the bottom of the exchanger assemblies.

In comparing the thermal-hydraulic designs it was observed that, while different heat transfer and friction correlations are used by GA and HHT, there was, in general, good agreement on the heat exchanger thermal sizing.

The GA designs are characterized by a more compact modular array made possible by the conical subheadering configuration, which permits a contiguous modular assembly. This arrangement leads to efficient utilization of flow frontal area (i.e., higher packing efficiency) with an attendant reduction in pressure loss.

The HHT recuperator embodies integral return lead tubes, which has the advantages of 1) simplification of headering areas, 2) full utilization of cavity for heat-transfer elements, and 3) increased height availability in exchanger cavities. Thermal expansion (both from ambient to operating temperature, and module-to-module differential thermal expansion) is accommodated in the GA concept by incorporating a sliding piston ring seal or bellows assembly in each module. While recognizing the merits of a recuperator configuration with integral return tubes, many mechanical design areas must be resolved before an optimum configuration can be identified and recommended for the GA reference plant design. The results of an initial conceptual design study are included herein. The results are encouraging, and further design studies in this area are planned.

The significant differences between GA and HHT in the precooler design policy are manifest in different mechanical arrangements. One of the basic GA ground rules has been that repair of the precooler (in the event of a failed tube) must be possible from outside the PCRV, without man access. This led to a design embodying 144 modules, such that in the event of a failed tube, the module would be isolated by plugging the lead tube, either manually or remotely with a tube plugging machine, outside the PCRV. The GA 3-loop reference plant design incorporates this feature. The HHT plant has but only 7 very large modules in the precooler, the maintenance philosophy being that man access into the precooler cavity is possible for direct plugging of individual tubes (after removal of water manifolds, cover plates, etc.). In the HHT plant the precooler is supported from the bottom, and this has the advantages of 1) simplified lead tube geometries, 2) increased volume availability in the cavity for heat-transfer surface, and 3) freedom from constraint of the exchanger at both ends. A limited design study

of a bottom-supported precooler (HHT approach) for the GA plant is included in this report. It has many simplifying features that warrant its selection for the plant reference design.

4.1.2 Recuperator Design Comparison

The comparison studies performed on the GA GT-HTGR and HHT recuperator designs during this report period are steps taken in cooperation aimed toward achieving heat exchanger design commonality. Although the respective designs until now have been developed independently, they possess a great deal of similarity. Both recuperators are counterflow tubular heat exchangers embodying modular construction. They are both top-supported, employ similar size tubing and pitching within hexagonal modules, and use similar flow circuitry orientation and arrangement. While there is modest disagreement on some of the analytical procedures and mechanical design approaches for packaging of the heat-transfer matrix, the chief differences between the two designs are obviously their overall sizes and performance requirements, both of which are directly influenced by policy considerations (site vs factory fabrication, man-access, etc.). Table 4-1 presents a summary comparison of the current HHT INT plant and GA GT-HTGR 3-loop plant recuperator designs. Aspects of this comparison addressed specifically during the report period are discussed below, and a GA assessment of the internal return tube approach employed in the HHT recuperator design is presented in Section 4.1.3.

4.1.2.1 Module Packaging. The importance of efficient frontal area utilization in heat exchanger designs for an integrated plant arrangement is fully appreciated by both the HHT and GT-HTGR projects. With heat exchanger sizes large enough to mandate mechanical designs based on modular construction, both projects recognized the need to select a module frontal size and shape and subheader configuration, resulting in a heat exchanger design with an overall packing efficiency approaching that of a homogeneous tube field. These considerations produced general agreement on the shape of the modules (hexagonal), but there are packaging inconsistencies between

TABLE 4-1
RECUPERATOR DESIGN COMPARISON

	Plant	
	GT-HTGR (3 Loop)	HHT/INT
Hx Rating, MW(t)	1000	1500
Number per Plant	3	2
Diameter, m (ft), ITB	5.26 (17.25)	6.5 (21.3)
Overall Length, m (ft)	18.9 (61.9)	33.5 (109.9)
Weight, tonne (ton)	430 (474)	1250 (1378)
Effectiveness	0.898	0.929
$\Sigma \Delta P/P_1$	0.0218[a]	0.0539
Flow Configuration	Counterflow	Counterflow
Surface Geometry	Tubular	Tubular
Construction	Modular	Modular
Module Shape	Hexagonal	Hexagonal
Number of Modules	144	84
Tubes per Module	547	1224
Tube Material	2-1/4 Cr - 1 Mo Ferritic	Unspecified Ferritic
Packaging Approach	Contiguous	Noncontiguous
Packing Efficiency, %	78	64.5
Orientation	Vertical	Vertical
Support Method	Top support	Top support
Main Tubesheet Configuration	Torospherical	Spherical
Subheader Tubesheet Configuration	Conical	Flat
Tubeside Fluid	High-pressure helium	High-pressure helium
Shellside Fluid	Low-pressure helium	Low-pressure helium
Low-pressure flow circuit	Bottom entry, top exit	Bottom entry, top exit
High-pressure Flow Circuit	Top entry and exit	Top entry and exit
High-pressure Return Circuit Approach	Center duct	Module integral return tubes
Fabrication Location	Factory	Modules fabricated in factory
Maintenance	Module lead tube plugging	Final assembly at site
Man-Access Provisions	Not required	Design requirement
Safety Class	NNS; SC-2 Center duct	--
ASME Code	Section VIII	--

the GA and HHT designs. These inconsistencies are probably because of differences of opinion on 1) subheadering techniques, 2) module size, and 3) module partition (shroud) thickness. With regard to 1), GA has taken the steps necessary to confine the subheader peripheral envelope within the projected envelope of the hexagonal tube bundle. This eliminates the need for gaps (and thus bypass-prevention seals) between modules and creates the possibility of having the module tube bundles contained within a latticework of hexagonal cells, instead of having the bundles individually shrouded. The latticework provides additional stiffness of the module array, and the mutually-shared partitions of the lattice have less frontal area blockage than do individual shrouds. Provisions for intermodule shell-side mixing (for attenuation of temperature streaks) are available through perforation of the partition panels in the lattice.

Both the GA recuperator and precooler current designs, shown in Figs. 4-1 and 4-2, are based on a novel subheadering approach that accomplishes the module packaging goals set forth above. Instead of relying upon flat tubesheets, the subheaders have conical tubesheets with machined internal circumferential ledges for the tube welds. With this approach, the tubes penetrate the header surface at an acute rather than perpendicular angle to reduce the amount of tube bending required to get the tubes to meet the tube/tubesheet interface.

The contiguous module packaging afforded by the use of the conical subheaders has produced an overall frontal area packing efficiency (based on ITB, the PCRV cavity diameter inside the thermal barrier) of 78% in the GT-HTGR recuperator design, which compares with the 64.5% corresponding efficiency obtained in the HHT recuperator design based on flat tubesheet subheaders. It is also notable that previous GA recuperator designs using subheaders with flat tubesheets developed packing efficiencies in the 60 to 65% range.

The issue, therefore, seems to lie in whether to accept the additional fabrication cost and complexity in the novel GA subheader approach to

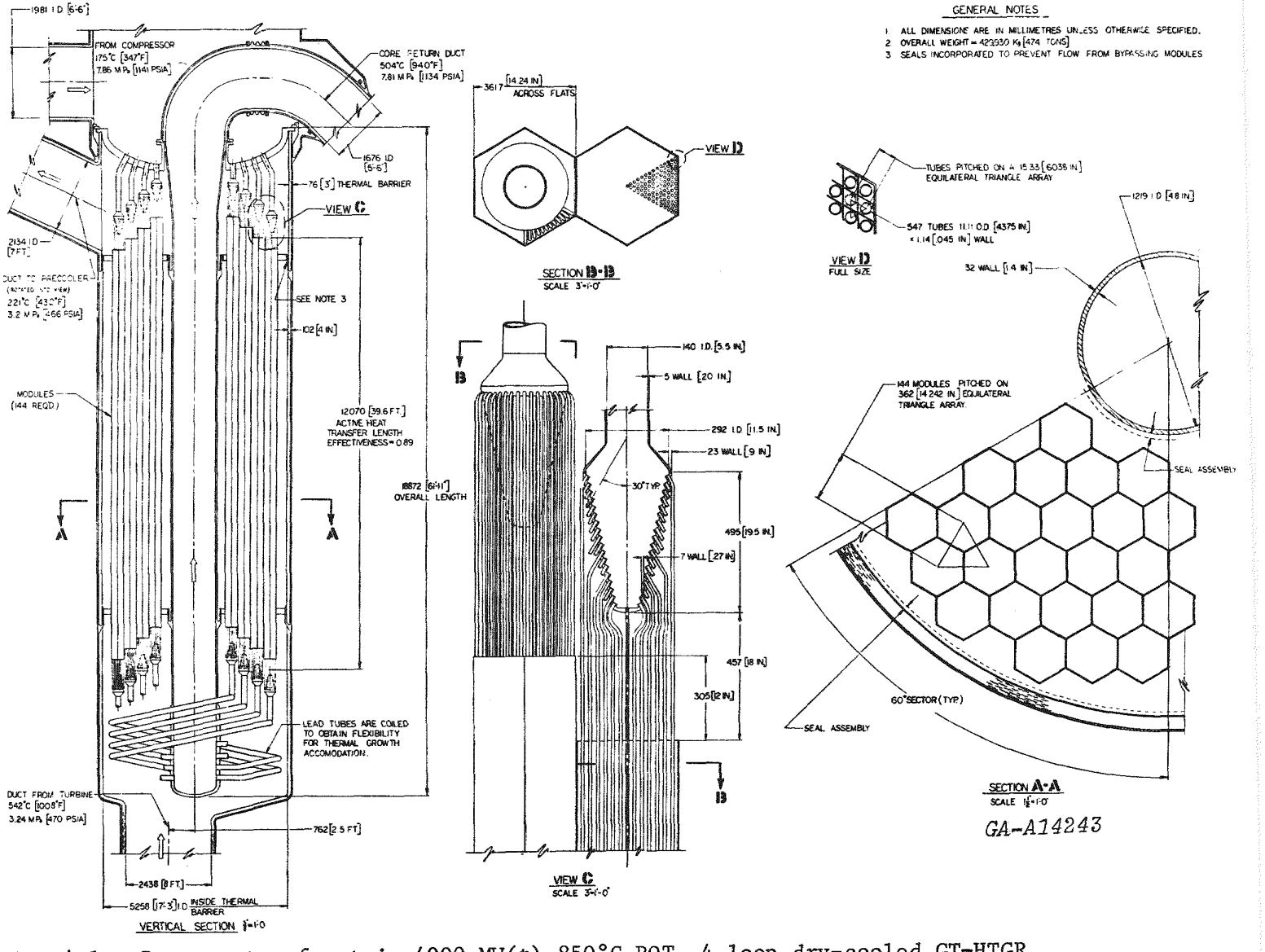

Fig. 4-1. Recuperator for twin 4000 MW(t) 850°C ROT, 4 loop dry-cooled GT-HTGR

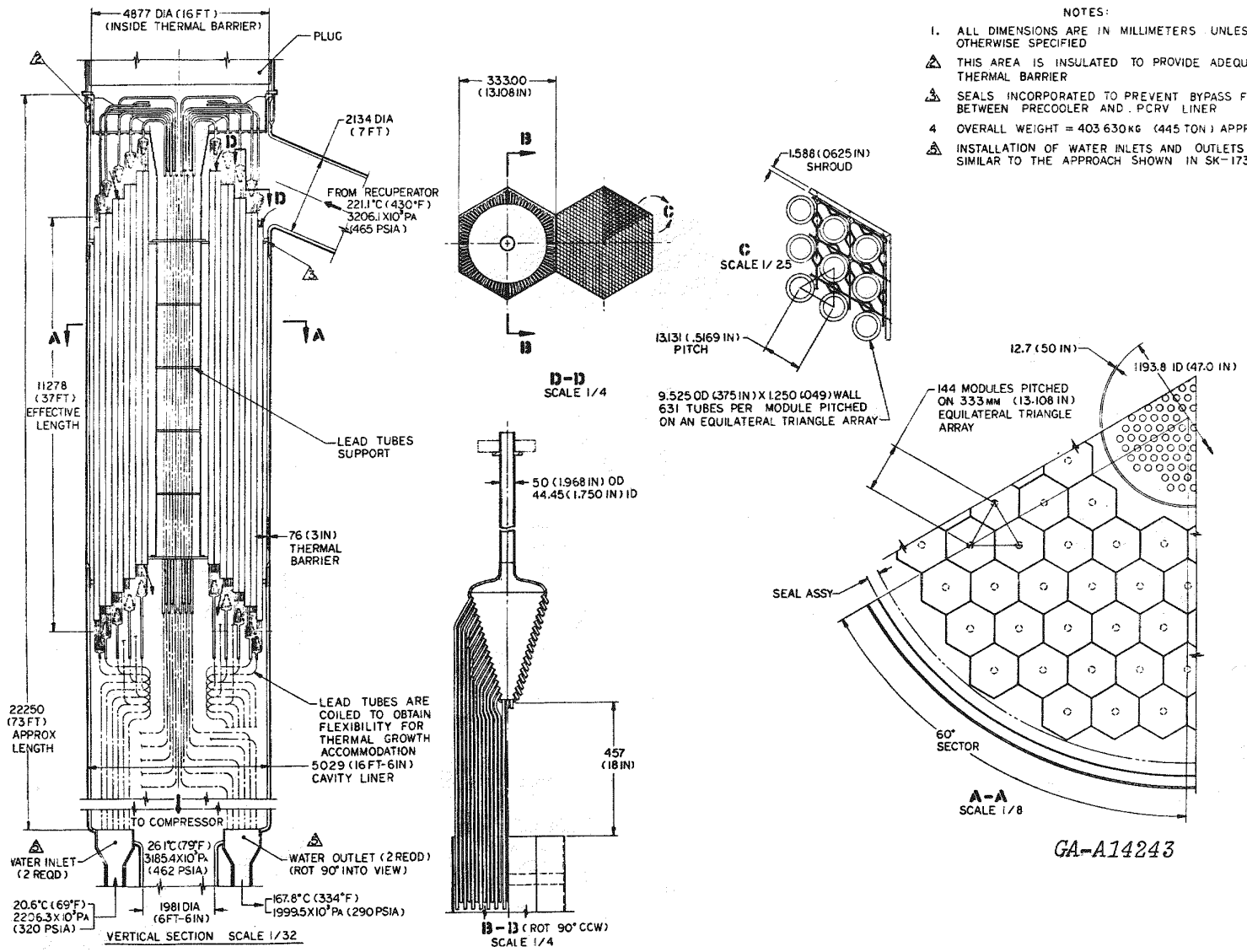

Fig. 4-2. Precooler for twin 4000 MW(t) 850°C ROT, 4 loop dry-cooled GT-HTGR

improve module packaging (by roughly 20%) or to accept the larger PCRV cavity diameter attendant to the more conventional flat tubesheet method. Preliminary GA engineering cost studies suggest that the conical subheadering method is preferable.

4.1.2.2 Analytical Procedures.

Heat Transfer Correlations. In view of the similarity in the GT-HTGR and HHT recuperator thermal design approaches, the agreement of both projects on a common set of heat-transfer correlations is being sought, and communications are currently being exchanged to advance this goal. A recent GA study, comparing the HHT and GT-HTGR correlations directly by applying them to the same flow geometry with the same operating conditions as that of the reference design GT-HTGR recuperator, indicated agreement on thermal size within approximately 4%. Considering the general uncertainty (typically ±10%) of the experimental data supporting these correlations, something approaching de facto HHT/GT-HTGR commonality in this area already exists, suggesting the joint adaption of common correlations as the probable result of further discussion.

Margins and Allowances. An exchange of views between the two projects on margins and allowances is currently in process. The GT-HTGR recuperator is designed to satisfy performance at beginning of life, and the only margin included at this time is a 10% allowance on surface area to cover flow maldistribution. No allowances are being made at this time for ensuring minimum performance later in life (i.e., no allowances for plugging or other time-dependent effects).

Shell-side helium leakage past the recuperator peripheral seals in the GT-HTGR design is currently estimated to be 0.50% of the inlet flow. The low leakage figure is attributable to the contiguous packaging approach that eliminated the bypass leakage paths between modules. The peripheral seal designs for these heat exchangers employ the technology developed

for the Philadelphia Electric Company Peach Bottom Generating Station reactor top core seal, which essentially comprises an assembly of spring-loaded graphite circular segments.

Pressure Loss Considerations. Figure 4-3 schematically portrays the GT-HTGR recuperator boundaries and identifies the constituent pressure losses analyzed within these boundaries.

The chief differences in the GT-HTGR and HHT heat exchanger pressure loss predictions are in the tube surface roughness assumed for friction loss calculations and in the way tube supports are handled.

General Atomic calculations are based on surface roughnesses consistent with U.S. tube manufacturer recommendations for commercial grade tubing; it is understood that considerably higher roughnesses are being used by the HHT project. This issue may be influenced by philosophical considerations as to whether the calculations should assume beginning-of-life or end-of-life conditions. Both projects compute shell-side pressure losses at the tube supports by the same general method, but use different loss coefficients and locate the tube supports at different axial intervals. Efforts to clear up the differences in these areas are in progress.

4.1.2.3 Follow-On Effort. Information exchange and discussions are planned to achieve a thorough exchange of views on all aspects of the heat exchanger designs being pursued for the GT-HTGR and HHT; the goal is to reach the maximum possible extent of design commonality.

4.1.3 Integral Return Tube Recuperator Design

Additional studies have been carried out on the integral return tube (IRT) recuperator design approach discussed in Ref. 1. Further investigation of this concept was warranted when the initial study results indicated that the apparent virtues of this design alternative could be obtained without unacceptable pressure loss penalty and heat leak while providing

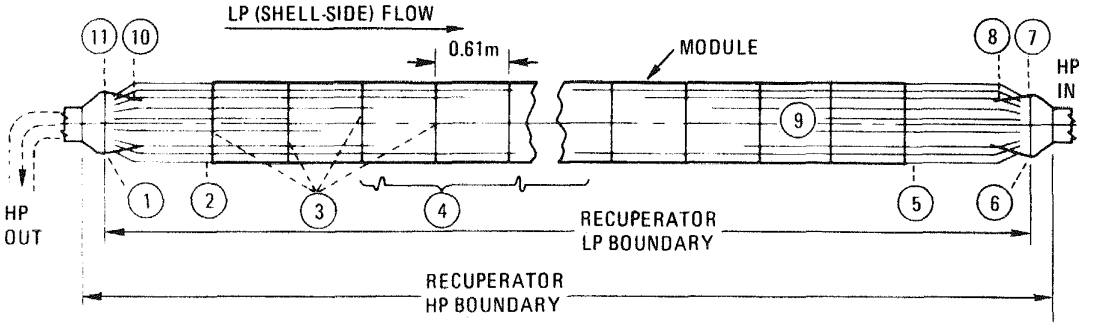

REGION		LOSS	ESTIMATED BY
LP LOSSES: (SHELL-SIDE)	(1)	ENTRY FLOW PAST SUBHEADERS	$\Delta P = 2 \cdot q$ in. (q = velocity head $= \rho \frac{V^2}{2g}$)
	(2)	MODULE ENTRY	$\Delta P = 2q_{bundle\ (in)}$
	(3)	TUBE SUPPORT DRAG	$\Delta P = N \cdot F_s \cdot q_{bundle\ (avg)}$ { N = no. of spacers; $F_s = \frac{S(1+S)}{(1-S)^2}$
	(4)	TUBE BUNDLE FRICTION AND ACCELERATION	$\Delta P = \left[\frac{fL}{d_h} + \frac{\Delta T}{Tm}\right] q_{bundle\ (avg)}$
	(5)	MODULE EXIT	$\Delta P = 2q_{bundle\ (out)}$
	(6)	EXIT FLOW PAST SUBHEADERS	$\Delta P = 2 \cdot q_{out}$
HP LOSSES: (TUBE-SIDE)	(7)	UPPER LEAD TUBE TO SUBHEADER	$\Delta P = K_e\ q_{lead\ (in)}$
	(8)	TUBE BUNDLE ENTRY	$\Delta P = K_c\ q_{bundle\ (in)}$
	(9)	TUBE BUNDLE FRICTION AND ACCELERATION	$\Delta P = \left[\frac{fL}{d_i} + \frac{\Delta T}{Tm}\right] q_{bundle\ (avg)}$
	(10)	TUBE BUNDLE EXIT	$\Delta P = K_e\ q_{bundle\ (out)}$
	(11)	SUBHEADER TO LOWER LEAD TUBE	$\Delta P = K_c\ q_{lead\ (out)}$

GA-A14243

Fig. 4-3. GT-HTGR recuperator boundaries for ΔP computations

the possibility for recuperator height reduction and mechanical design simplification at the bottom end. The integral return tube (IRT) approach revises the high-pressure helium flow path within the recuperator such that the hot high-pressure helium is returned to the top of the recuperator via return pipes within the modules, instead of collecting all the module high-pressure discharge flow at the bottom and returning it upward via a single, large high-pressure duct and coiled (for differential expansion) subheadering lead tubes that connect the duct to the modules. Thus the IRT approach will eliminate a source of a possible depressurization accident for high-pressure helium into the recuperator matrix, and offer the aforementioned prospects for height savings and design simplification through elimination of the coiled lead tube envelope.

Figure 4-4 depicts the IRT recuperator design evolved for the 850°C ROT, dry-cooled, 1000-MW(t)/loop GT-HTGR plant, revised in accordance with the additional design information developed during this report period. The flow circuitry for this design remains the same as that previously reported: cold high-pressure helium from the compressor discharge enters the recuperator via a sidewall opening in the PCRV cavity between the upper and lower tubesheets and flows downward through the annuli formed by the lead tubes and their associated return tubes to the modules. During its downward passage inside the module tubes, the high-pressure helium is preheated by the low-pressure turbine discharge helium flowing upward on the shell-side of the tube bundles. At the bottom ends of the modules the hot high-pressure helium turns 180 deg, flows upward inside the return tubes, and discharges into a plenum connected to the core return ducting above the uppermost tubesheet. The hot turbine discharge helium enters the recuperator at the bottom of the cavity and, after transferring its heat to the high-pressure helium in counterflow, leaves the recuperator cavity via a side-wall opening beneath the torospherical tubesheet.

The follow-on studies focused on two basic areas peculiar to the IRT concept that will significantly influence its ultimate adaptability to the GT-HTGR application, which is to prevent heat leaks and accommodate thermal

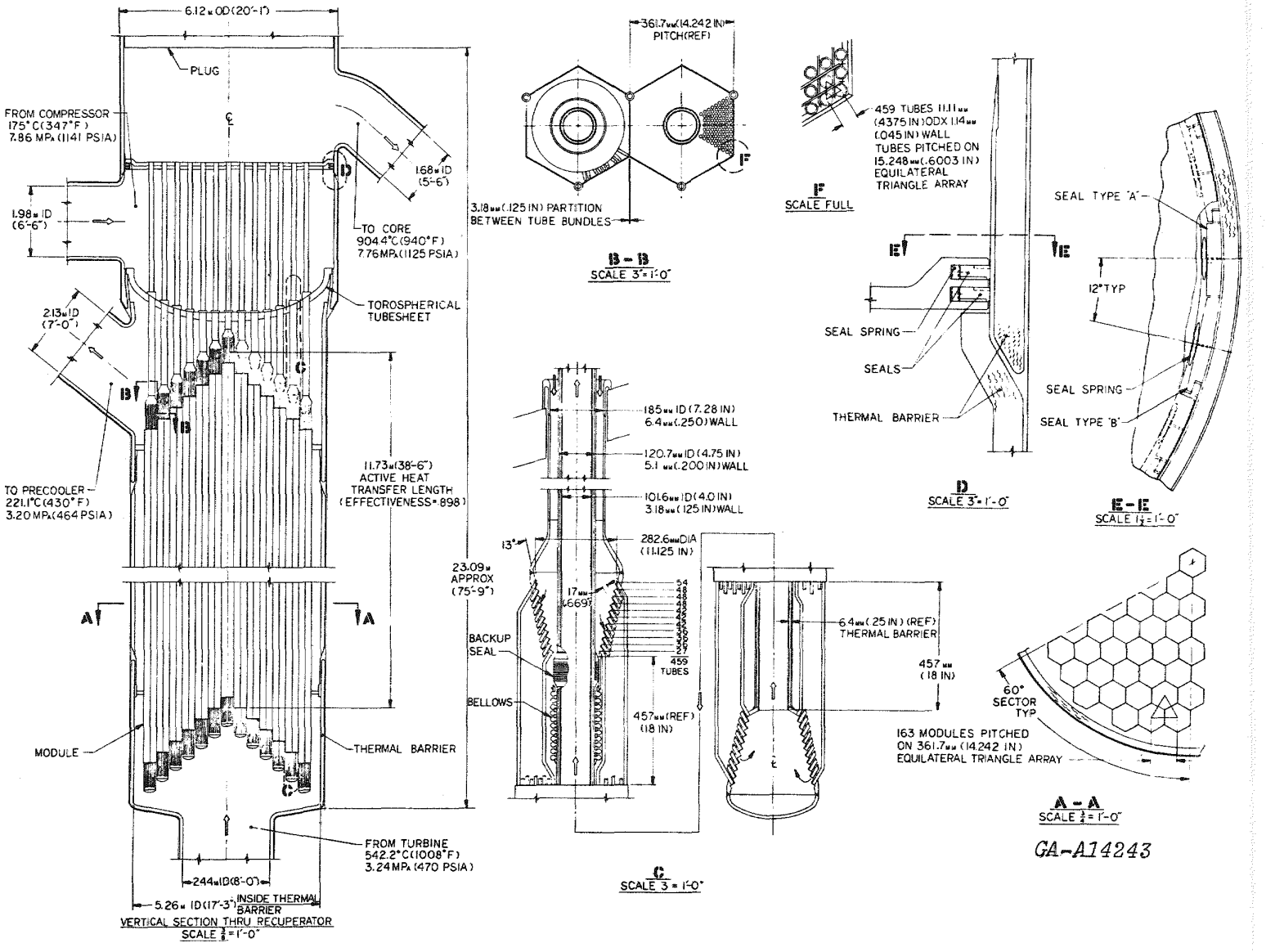

Fig. 4-4. Layout of integral return tube recuperator

growth between the return tube and its adjacent module tube bundle. Previous analyses revealed that recuperator performance degradation through heat leak from the hot high-pressure helium in the return tubes to the cooler low-pressure helium flowing on the shell side can be minimized through relatively simple thermal barrier measures, such as a stagnant helium buffer layer. A survey of thermal barrier prior art, notably the British and French experience in attempting to achieve stagnant fluid conditions within metallic thermal barriers for gas-cooled nuclear reactors, indicates that positive measures approaching that of conventional insulation are required to keep internal natural-convection effects at an acceptable minimum. For this reason, a thermal barrier comprising conventional MgO or Kaowool insulation was assumed for this study, which was expanded to examine the magnitude of the heat leak in the lead tube area above the modules. The results indicate that the greatest potential for heat leak in the IRT recuperator design exists in the annular flow areas formed by the hot high-pressure return tubes when they are passed concentrically inside the cold high-pressure inlet tubes, due to the combined effects of pure counterflow heat transfer, relatively high helium velocities, significant length, and a large approach temperature difference. Although there are comparable temperature differentials above the primary tubesheet and the cold high-pressure helium is flowing across, rather than parallel to, the bank of return tubes, the potential for a heat leak is considerably less, owing to the low velocity of the cold helium.

The annular region described above thus governs the thickness of the uniform thermal barrier assumed for these studies, and preliminary estimates of the heat leak across this barrier within the IRT recuperator design shown in Fig. 4-4 indicate a loss of less than 0.5% on recuperator heat transfer. For this study this loss was considered acceptable, and no compensatory UA margin was taken in the thermal sizing.

While heat leakage is important in the IRT approach, which essentially calls for a bayonet-tube heat exchanger design, the differential thermal growth accommodation between the return tube and tube bundle is also a

fundamental consideration. In the initial study it was assumed that the expansion of the return tubes relative to their adjacent module tube bundles could be accommodated with a sliding seal, using an approach similar to that employed between the steam inlet and inner shell of a conventional steam turbine, recognizing that the recuperator, which operates with the same fluid on both sides, can tolerate small amounts of leakage. Results of the follow-on studies, however, which considered various seal styles and their related performance, indicate that it will be difficult to confine leakage to acceptable levels with virtually any kind of sliding seal, owing to the large high- to low-pressure differential across the seal (approximately 700 psi), which demands near-perfect compliance between the seal and its gland throughout its stroke, if leakage rates are to be maintained below 1% of the inlet flow (considered to be maximum from a system standpoint). Figure 4-5 depicts the relative performance of the candidate seal configurations; unfortunately, labyrinth seals, which show the best performance, are considered impractical for this application due to their exacting tolerance requirements and relatively delicate construction. Piston rings have possibilities, but their compliance, material compatibility for sliding contact in a hot helium environment, and general performance as pure gas seals to limit helium leakage at these high-pressure differentials are not known with sufficient certainty to warrant their adoption for this critical design application. In summary, it appears that any nonhermetic, sliding seal proposed for this role in the IRT recuperator design will require early experimental confirmation of its performance before it can be adopted.

With nonhermetic seals ruled out for now, consideration was given to accommodating the return tube-to-module tube bundle differential expansion by conventional hermetic methods. The IRT recuperator design shown in Fig. 4-4 employs a bellows as the primary interface with a sliding seal (the exact type of which is yet to be determined) as its backup. This installation uses two design features to help ensure the proper operation and reliability of the bellows: the center high-pressure return tube prevents direct exposure of the convolutions to flow, reducing vibration, and serves as a bellows guide to eliminate squirm. Since the service

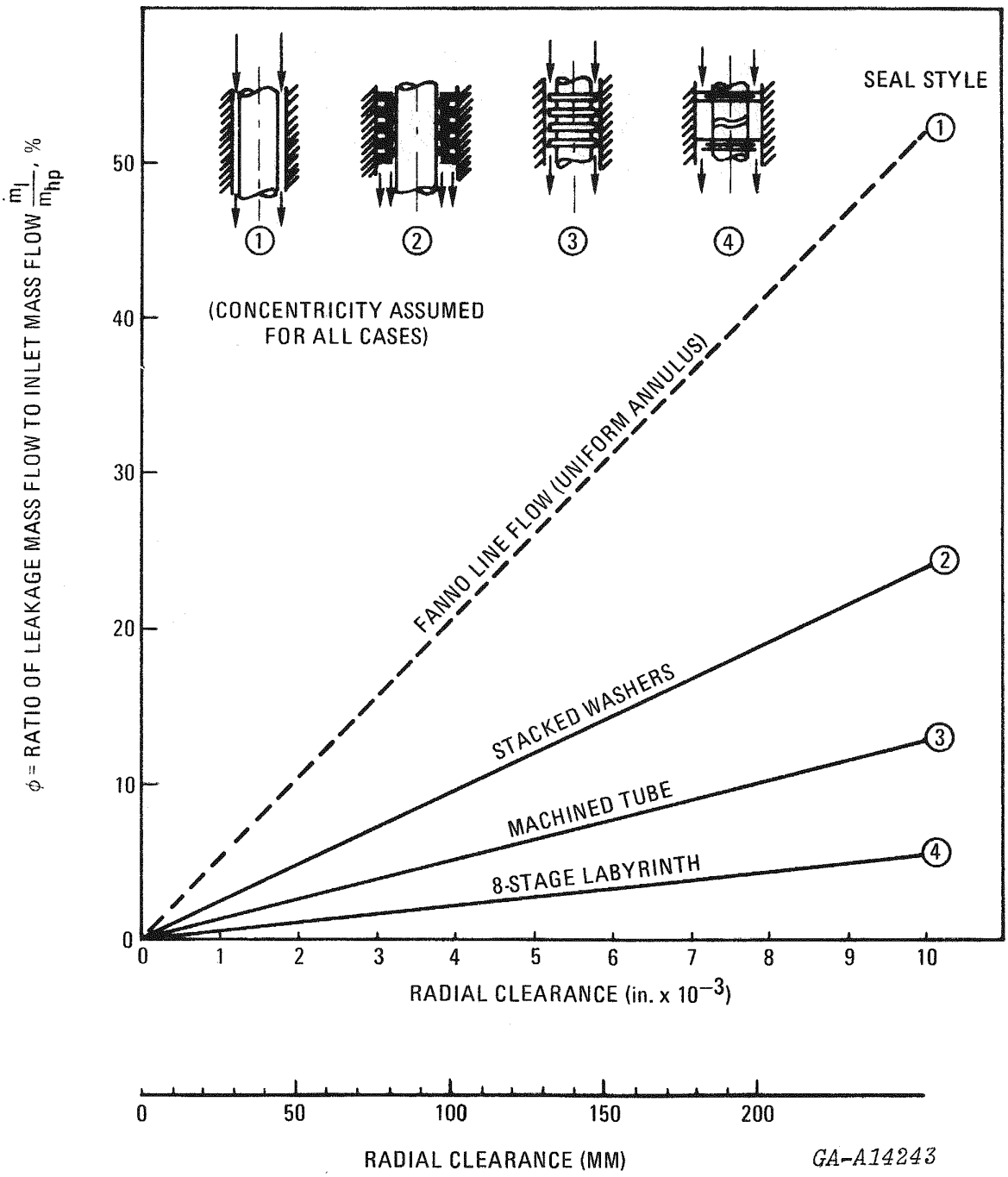

Fig. 4-5. Influence of high-pressure return tube seal design upon leakage in the IRT recuperator

requirements for this bellows are relatively severe [510°C (950°F) metal temperature, 31.8 mm (1.25 in.) stroke, 4.82 MPa (700 psid) pressure differential, at least 5000 cycles, smallest diameter envelope consistent with 102 mm (4 in.) i.d. return tube, etc.], preliminary confirmation of the feasibility of this bellows vendor. Layout studies then established the number of tubes that would have to be removed from each module to accommodate the bellows installation below the knuckle of the upper module subheader. These layouts revealed a virtue of the conical subheader concept that appears particularly suited for this application, i.e., the tube bends required to permit the innermost ring of module tubes to approach the conical subheader tubesheet at the desired angle create considerable annular space around the return tube where it penetrates the subheader. Unlike flat tubesheet subheader designs, this inherent local space allowance nearly eliminates the impact of the bellows envelope upon the available tube pattern, thus producing a relatively higher tube packing efficiency for the recuperator. To accommodate the bellows feature in this IRT recuperator design, it was necessary to remove only 24 tubes from the original 483-tube module pattern. The influence of this reduction manifested itself in a slight increase in effective length [from 11.6 m (38 ft) to 11.8 m (38.6 ft)] and a somewhat higher pressure loss (from 2.59% to 2.72% based on expanded boundaries) than that estimated for the original IRT design discussed in Ref. 1.

While additional mechanical design studies are required to establish the final configuration and sealing approach for the cold high-pressure helium to hot high-pressure helium boundary above the primary tubesheet of the recuperator, this area, which senses only the pressure differential developed across the high-pressure side of the recuperator, is not now viewed as a design problem. The design shown in Fig. 4-4 calls for the high-pressure return tubes to be welded to a flat tubesheet, which will be permitted to float through the use of a circumferential sliding seal similar in design to the antibypass seal employed around the periphery of the modular array. This approach permits the use of straight high-pressure return tubes (a fabrication and maintenance advantage) and further exploits the pressure

containment role of the PCRV cavity to eliminate the parasitic structure associated with an upper drum header. Considerations to be addressed later include tube-to-tube differential expansion, options for transferring the sliding seals to the tube/tubesheet interface, tradeoff incentives (if any) for a dished, rather than flat, tubesheet, etc.

Table 4-2 summarizes the present features of the IRT recuperator design and includes a comparison of its more significant aspects with those of the current GA recuperator reference design with which it is competing.

4.1.4 Precooler Conceptual Studies

Previous investigations have shown the merit of changing the precooler design to a bottom-supported arrangement. Moving the support plane to the bottom of the cavity, where precooler physical attachments to the PCRV already exist by virtue of inlet and outlet water headering connections, eliminates the need for accommodating the thermal growth between two widely separated attachment points, as is now incorporated in the top-supported reference design. The water piping, which is coiled below the modular array to produce the flexibility required for thermal growth accommodation, in the top-supported design is not only a complex installation problem as such, but it also creates a parasitic loss of PCRV cavity envelope; by shifting the active precooler heat transfer matrix upward, it complicates the helium cross-duct connection between the recuperator and precooler. While it has long been recognized that a bottom-supported precooler would be a considerably simpler design in these areas, early considerations of installation and removal reinstallation of the precooler without requiring mandatory man-access militated against it. This ground rule was modified recently to take more appropriate account of the low activity rates forecast for the bottom end of the precooler and the fact that replacement of a precooler will be, in any case, a very infrequent, nonroutine event. Relaxation of this design rule is consistent with the precooler approach adopted by the HHT project, which has considered man-access to be mandatory for the installation, removal/reinstallation, maintenance, and repair of its bottom-supported

TABLE 4-2
RECUPERATOR DESIGN SUMMARY

Design Reference	IRT Approach TBD	Reference Design 3227-SK-85
Thermal Requirements:		
Q, MW(t)/Hx	954	
E	0.8975	
LMTD, °C (°F)	41.8 (75.3)	
UA, MW/°C per Hx	22.8 (43.3×10^6)	
UA Margin, %	10	
Physical Characteristics:		
Effective Length, m (ft)	11.8 (38.6)	12.13 (39.8)
Hx o.d. (ITB), m (ft)	5.26 (17.25)	5.26 (17.25)
Overall Length, m (ft)	TBD	18.9 (62)
No. of Modules/Hx	163	144
Module Type	Hexagonal	Hexagonal
Module Pitch, mm (in.)	362 (14.24)	362 (14.24)
Tubes per Module	459	547
Tube p/d	1.38	1.374
Tube o.d. x Wall, mm (in.)	11.1 x 1.14 (0.4375 x 0.045)	11.1 x 1.14 (0.4375 x 0.045)
Total Tubes/Hx	74,817	78,768
Pressure Losses[(a)]		
$(\frac{\Delta P}{P_1})$ HP	0.0145	0.0090
$(\frac{\Delta P}{P_1})$ LP	0.0127	0.0128
$\Sigma\ (\frac{P}{P_1})$	0.0272	0.0218

[(a)] Boundaries adjusted for common basis of comparison.

precooler design. Man-access aspects of the gas turbine heat exchanger installation and maintenance philosophy are discussed further in Sections 4.1.5 and 4.1.6.

There is potential benefit from the precooler standpoint of lowering the water outlet temperature and reducing surface area (and thus cost). The reference design precooler for the dry-cooled, 850°C (1562°F) ROT, 1000 MW(t) per loop, GT-HTGR plant is based on a water outlet temperature of 168°C (334°F), which was selected from a computerized plant optimization study that considered the tradeoff between precooler size and dry cooling tower size. It was recognized, however, that this value is the least definite of the precooler independent design variables, because a reference design for the dry cooling towers has not been completed. This uncertainty, in conjunction with the relatively flat variation of water outlet temperature about its selected optimum point, suggests that it may be possible to lower the precooler water outlet temperature without hurting plant performance or cost.

A brief study was undertaken to investigate the benefits of combining these two design options to produce a bottom-supported precooler with a 132°C (270°F) water outlet temperature, which is considered the low end of the optimum range. The remainder of the operating conditions corresponding to this water outlet temperature were obtained from the plant optimization code; the parametric survey shown in Fig. 4-6 was then generated to show the available combinations of precooler effective length and tube diameter at this design point. Simplifying assumptions included the same module number and size as the reference design, the same tube pattern p/d for all cases (1.40), and a constant tube o.d.-to-thickness ratio; in addition, the general reference design ground rules of 10% UA margin, inside surface enhancement to give twice the plain tube coefficient, and inside fouling coefficient of 56,770 $W/m^2°C$ (10,000 $Btu/hr\text{-}ft^2°F$) were followed. With this information, layout studies were made to determine the extent of recuperator-to-precooler cross-duct simplification (an optimum would be a horizontal cross-duct) and precooler tube o.d. increase (reduced number of

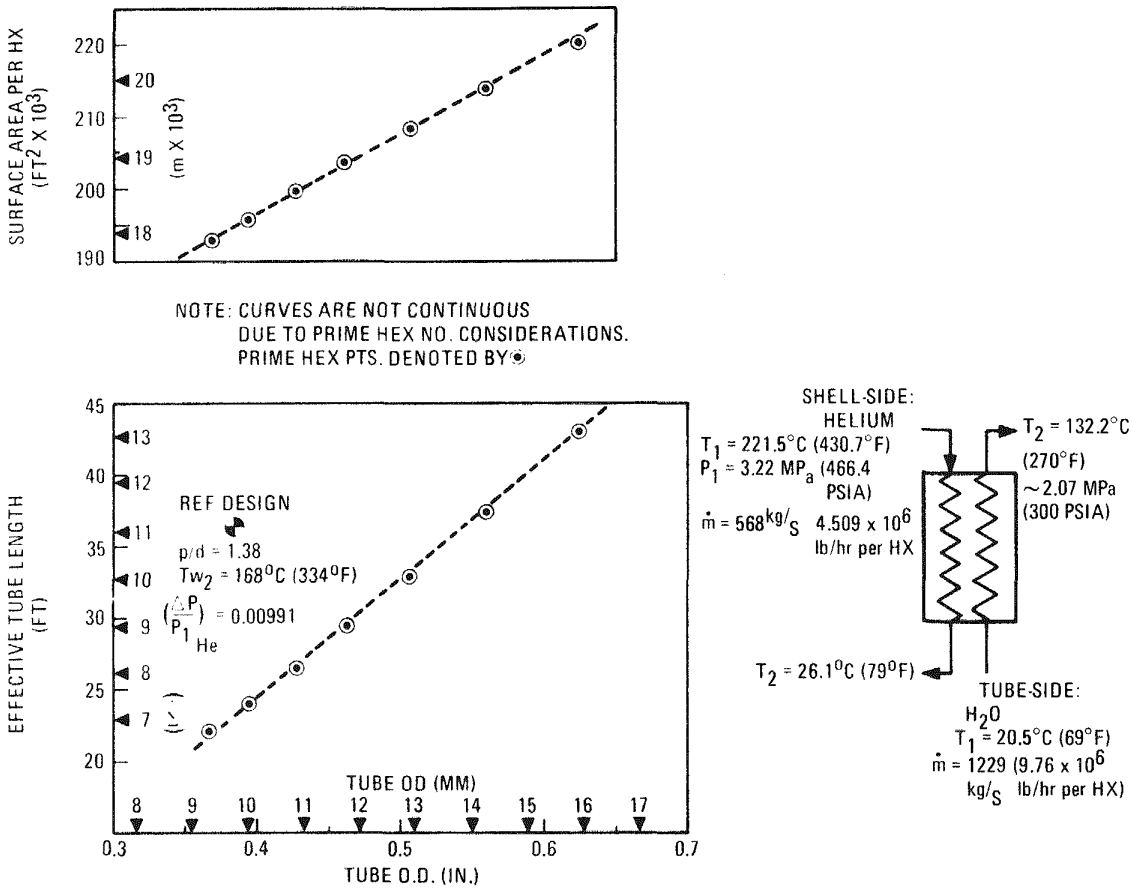

NOTES

- 144 HEX MODULES @ 333 MM (13.108 IN.) PITCH
- p/d = 1.40 EQUILATERAL △
- TUBE OD/THICKNESS = 7.653
- 10% UA MARGIN
- FOULING h = 10,000 $\frac{BTU}{hrft^2°F}$ (inside)
  (56770 $W/M^{2°}C$)
- INSIDE SURFACE ENHANCED TO GIVE 2 X h_w
- $(\frac{\Delta P}{P_1})_{He}$ = 0.00706 FOR ALL CASES

GA-A14243

Fig. 4-6. Effect of tube outside diameter on length for precooler with 132°C outlet water

tube ends) that would be available. When the layout work revealed that the minimum effective length was not compatible with a horizontal recuperator-to-precooler crossduct configuration, attempts at simplifying this crossduct configuration relative to that of the reference design were abandoned. Attention was focused instead on identifying the maximum tube o.d. available within the existing envelope. The results of this effect are shown in Fig. 4-7 which reveals the following advantages:

1. The tube o.d. can be increased from its present 9.5 mm (0.375 in.) to 14.2 mm (0.559 in.), reducing the number of tubes required per precooler from 90,864 to 39,024. Both results should have fabrication and cost benefits.

2. The overall precooler length can be shortened by approximately 1.6 m (5.25 ft).

4.1.5 Recuperator Installation and Removal

The GT-HTGR recuperator shown in Fig. 4-1 is a straight tube exchanger with an overall length of 18.9 m (62 ft), diameter of 51.m (16.75 ft), and weight of 430,000 kg (474 tons). Installation and the postulated removal of this heat exchanger from the PCRV will be a substantial task. With proper design and planning, however, it can be accomplished within significant impact on construction or repair schedules, with existing state-of-the-art technology, and with insignificant capital equipment investment. A summary of the sizes and weights of the GA-designed heat exchangers is given in Table 4-3. While in-depth installation and removal studies for the recuperator have not been carried out, a discussion on the envisioned procedures is given below.

The lifting and placement of components that are similar in size and weight to the GT-HTGR recuperators has been accomplished numerous times. The placement of a 567,150 kg (625-ton) BWR vessel using a 55 m (180-ft) tall hoist beam with a pair of 93.3 kW (125-hp) hydraulic motors for power

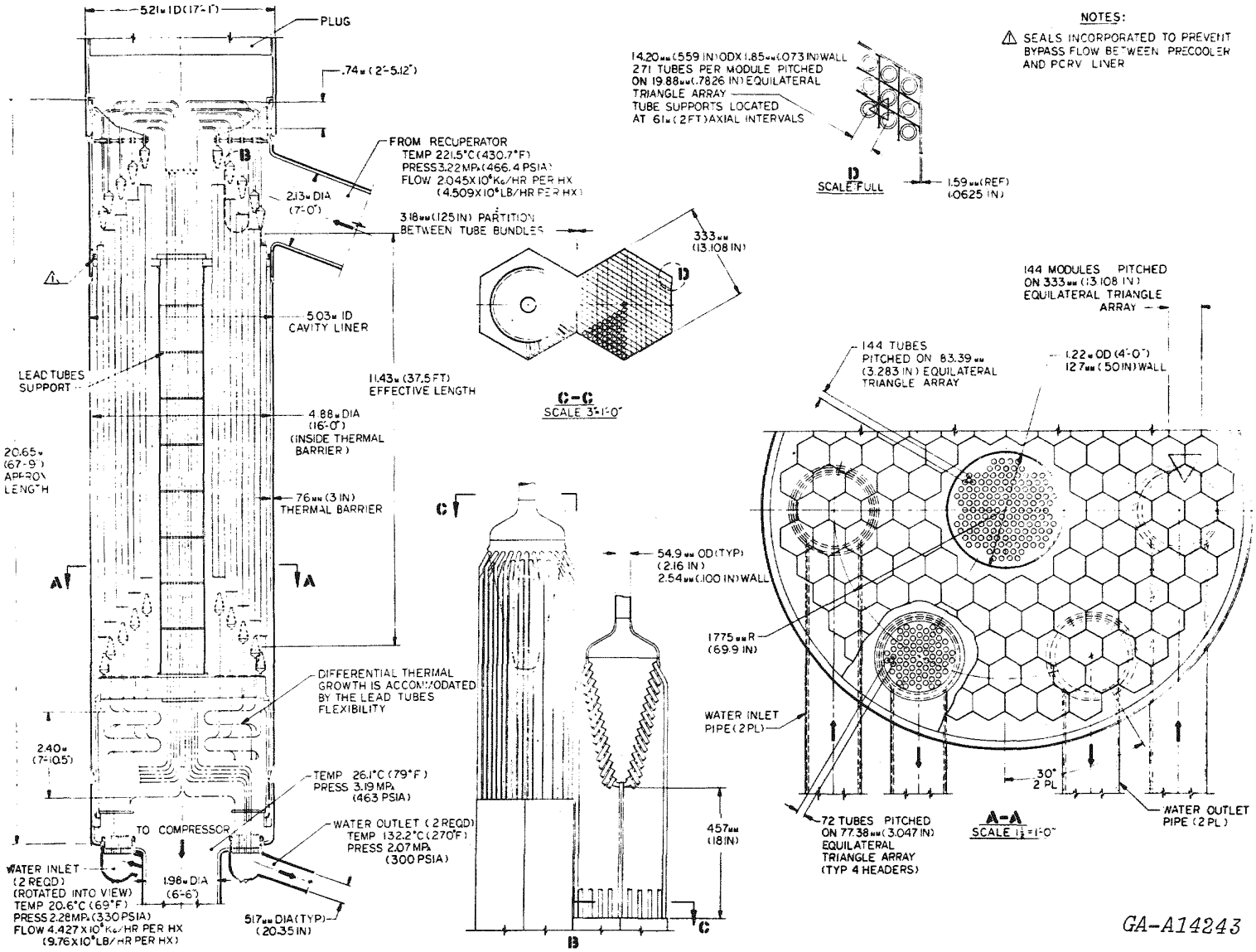

Fig. 4-7. Bottom supported precooler design with 132°C outlet water

TABLE 4-3
SUMMARY OF HEAT EXCHANGER PRELIMINARY DESIGNS FOR GT-HTGR

	Type		
	Exchanger	Recuperator	Precooler
	Number per Reactor	3	3
	Matrix Type	Tubular	
	Flow Configuration	Axial Counterflow	
	Construction	Modular	
Surface Geometry	Tube Outer Diameter, mm (in.)	11.1 (7/16)	9.5 (3/8)
	Tube Wall Thickness, mm (in.)	1.14 (0.045)	1.24 (0.049)
	Maximum Metal Temperature, °C (°F)	520 (968)	81 (357)
	Internal Pressure Differential, MPa (psi)	4.61 (670)	1.03 (150) He > H_2O
	Tube Material Type	Ferritic, 2 1/4 CR - 1 MO	Medium Carbon Steel
Module Details	Module Dimn. (across flats), mm (in.)	361 (14.2)	335 (13.2)
	Subheadering Type	Conical	Conical
	Modules per Unit	144	144
	Tubes per Module	547	631
	Effective Tube Length, m (ft)	12.13 (39.8)	11.3 (37.0)
	Surface Area/Reactor, m^2 (ft^2)	100,000 (1,080,000)	91,900 (990,000)
Overall Assembly	Approximate Overall Length, m (ft)	18.9 (62)	22.3 (73)
	Overall Diameter, m (ft)	5.1 (16.75)	4.72 (15.5)
	Module Weight, kg (lb)	2375 (5230)	2715 (5980)
	Approximate Assembly Weight, kg (ton)	430,000 (474)	404,000 (445)
	Fabrication Location	Factory	Factory

is described in Ref. 10. The hoist beam was supported by runway girders and lattice towers. The 17 m (56-ft) long reactor vessel was tilted up from the horizontal shipping position to vertical, hoisted vertically 31.7 m (104 ft) and trollied 29.6 m (85 ft) across the roof before being lowered 24.4 m (80 ft) into the well, where a flange-to-flange bolt-up was made. Reference 11 describes a 635-ton lift performed in Sweden using a lifting gantry, attached to the building, and hydraulic jacks with stranded lifting cables. This 18.9 m (62-ft)-high vessel was tilted to the vertical position, lifted 58 m (190 ft) and jacked horizontally 22.9 m (75 ft) before being lowered into its permanent position.

The recuperator is transported to the site in a horizontal shipping container to be positioned near the control and diesel building at the reactor site. For the initial placement of the GT-HTGR recuperator, preliminary work will entail the preparation of the lifting equipment and building. The lifting equipment will be mounted partially on the ground and partially on the supporting structure of the building. The upper floor of the control and diesel building will not be complete when the recuperator arrives, leaving the fuel-handling equipment track exposed for a length of approximately 30.5 m (100 ft). The recuperator in its cask will be lifted and placed on the track utilizing a system of dollies and trunnions.

Between the track and the cask will be two dollies, one of which has a trunnion about which the cask may be rotated to the vertical position. While still horizontal, the recuperator is rolled into the containment building to a turntable at the center of the refueling floor. The turntable is rotated to align the cask with the appropriate PCRV cavity.

Using a system of jacks as described in Refs. 12 and 13, the cask is rotated about the trunnion to vertical, positioned directly over the PCRV cavity. With the cask vertical and resting on the refueling floor, jacks are attached to the recuperator, which is then freed from the cask and lowered into the PCRV cavity. A detailed estimate of the time and cost involved in the installation of the heat exchangers is given in Ref. 14.

Presented therein is the Brown and Root engineering determination of the total installation time of each heat exchanger, which is 34 8-hr shifts.

Removal of the heat exchangers which may be radioactively contaminated by substantial service is essentially a reversal of the above procedure with two exceptions. First, the container used may require shielding to prevent excessive exposure to the workmen. If so, the shielding requirement can be expected to be similar to that required for HTGR steam generators, requiring a cask weighing approximately 280 tons. Because the recuperator is attached to the PCRV only at the upper support, no significant access problems are anticipated. Man access is not required in any potentially high irradiation area. The total lift weight for this operation is then about 762 tons, well within the maximum range of the lift jacks. The second exception is a minor one, regarding crane access to the fuel-handling equipment track. Since the building will cover the track at the time the cask is to be removed, the roof must be removed to expose the track and the crane mounting points. This is easily accomplished because the control and diesel building top floor is of the Butler-type construction. After the recuperator and cask are removed from the building, the recuperator is dismantled and shipped offsite.

4.1.6 Precooler Installation and Removal

The GT-HTGR precooler shown on Fig. 4-2 is a straight tube exchanger assembly with an overall length of 22.3 m (73 ft), diameter of 4.7 m (15.5 ft), and weight of 404,000 kg (445 tons). Installation and removal follows much the same procedure outlined above for the recuperator, since the units are approximately the same size and weight. A major difference between the handling of the two heat exchangers is that the precooler has water line connections. Since these connections are primary pressure boundaries and are below the precooler, some discussion of their installation is warranted.

A layout of the precooler water piping is shown in Fig. 4-8. It can be seen that the lower flange of the four precooler bundles is butt-welded

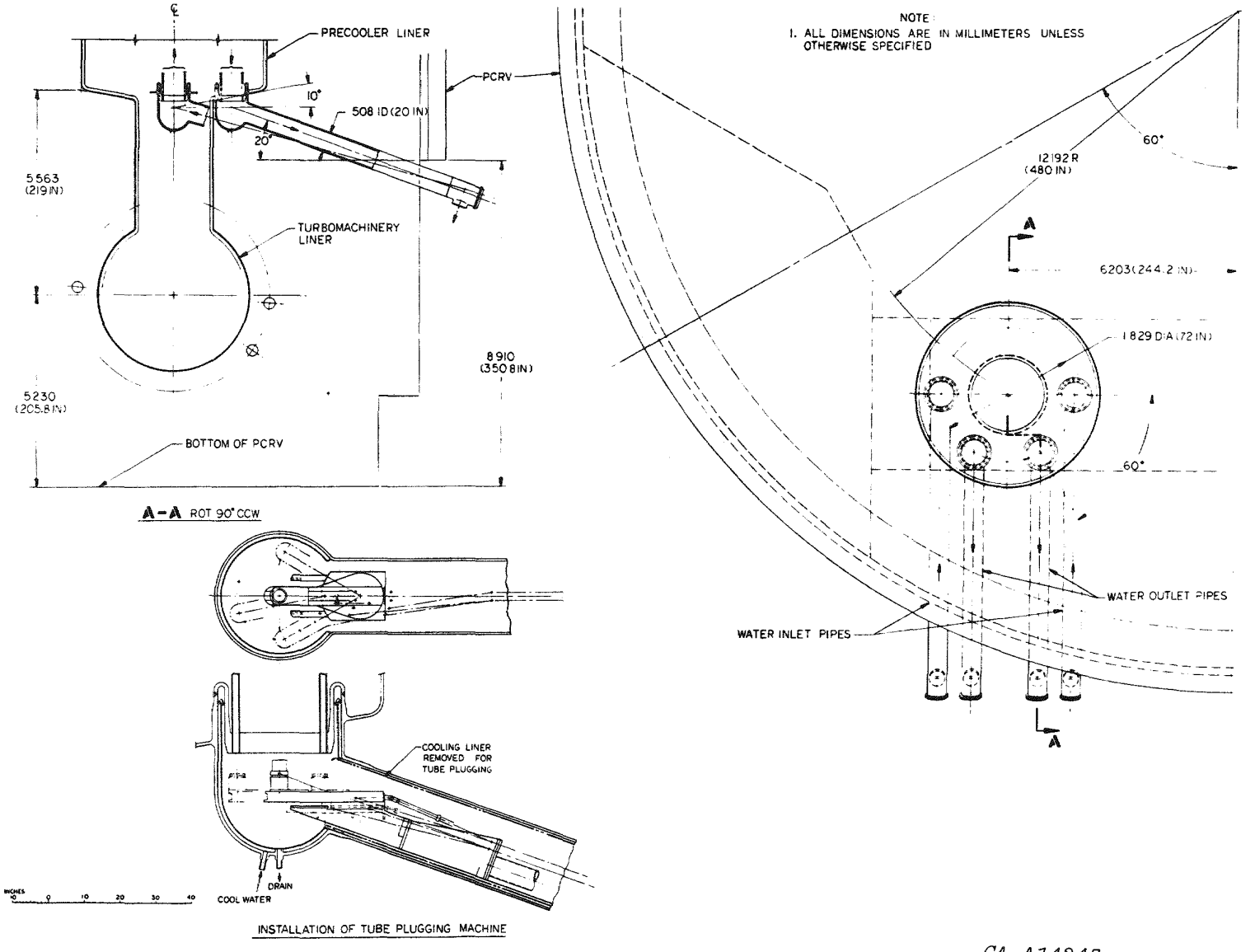

Fig. 4-8. Precooler water piping

circumferentially to the liner abutment provided for that purpose. This weld can be made manually, most probably with the use of fixtures for alignment, by a welder who can gain access to the lower cavity through the duct leading to the turbomachine cavity. Access through this duct is possible even with the turbomachine in place.

In the event that removal of a contaminated precooler is necessary, the welds attaching the water lines must be cut remotely. Access through the turbomachine cavity may be required for a remote cutting tool, which has yet to be designed. The large diameter ducts render this task relatively easy.

Installation of another precooler can be accomplished in much the same way as the original. A low activity level is expected in the cavity. Because of its placement in the loop, very low levels of metallic plateout will occur, probably from the decay of gaseous fission products absorbed in the thermal barrier. Protection of welding personnel can be accomplished by ordinary decontamination of the thermal barrier cover plate, and if necessary, by the use of segmented shielding around the cavity walls.

4.2 TURBOMACHINERY

In this phase of the program, work in the turbomachine area was limited to comparing the design features and performance of the gas turbine for the GA and HHT plant configurations. Even with different power rating, and for the HHT incorporation of intercooling, the machines bear substantial physical similarity, furthermore many of the mechanical design ground rules are the same (these aspects are discussed below). The respective turbomachinery companies, United Technologies Corporation (UTC) in the GA GT-HTGR program and Brown Boveri et Cie (BBC) in the HHT program, define their compressor and turbine efficiencies differently. Simple computations to normalize these for direct comparison are discussed below. Aspects of the turbomachinery performance, including seal leakages, are discussed in the context of supporting overall plant performance estimates and resolving computational differences.

4.2.1 Mechanical Design Features

4.2.1.1 Turbomachine for GA Reference Plant Design. The UTC machine, designed for the U.S. market, has a power rating of 400 MW(e) at 60 Hz. Three of these gas turbines are required per plant. As shown on Fig. 4-9, the machine is single shaft (i.e., compressor, turbine, and generator on the same shaft), nonintercooled, and has 18 compressor stages and 8 turbine stages. The rotor is of welded construction as opposed to earlier use of bolted rotor assembly. With the exception of the turbine inlet duct, which has a mechanical connection to the turbomachine, the other three gas inlet and exit boundaries (to and from the machine) utilize the PCRV cavity envelope and engine annulus geometry as the flow path boundary. While this eliminates the need for multiple remotely actuated flange connections, it necessitates compartmentalization of the turbomachinery cavity by peripheral seals as shown in Fig. 4-9.

Details of the salient mechanical design features of the UTC machine are given on Table 4-4. With the rotor supported on two journal bearings (state-of-the-art loading and peripheral speed) the overall length of the machine (excluding exhaust plenum) is 11.3 m (37 ft). The overall diameter of 3.5 m (11.5 ft) was a design constraint to facilitate rail transportation including the turbomachine when contaminated and installed in a shielded container. The overall machine weight is 277,000 kg (305 tons). From Fig. 4-9 it can be seen that rotor burst protection is incorporated in the machine design in the form of burst shields around the compressor and turbine rotor bladed sections. The machine design incorporates provisions for man access to both journal bearings. The drive to the generator is from the compressor end of the machine, and the thrust bearing is outside the PCRV to facilitate ease of inspection and maintenance. With a turbine inlet temperature of 850°C (1562°F) an existing nickel-base alloy (IN 100) has been selected for the turbine blades. The turbine blading lifetime goal of 280,000 hr can be realized without using turbine blade (rotor) and vane (stator) cooling. The turbine coolant flow (bled from the compressor) of 3.6% includes rotor and case cooling and internal leakages.

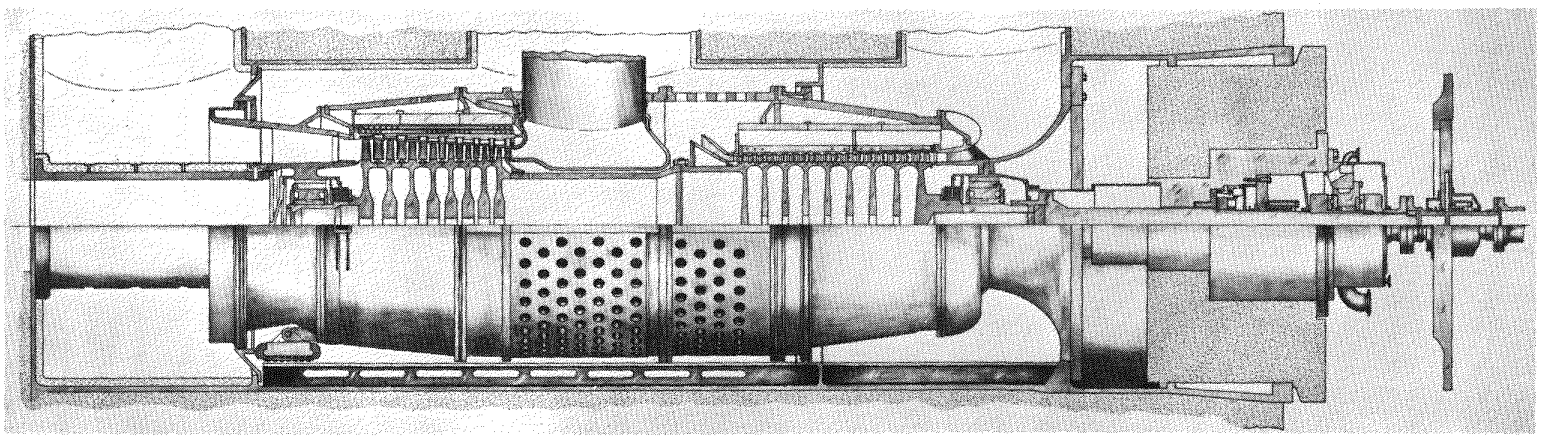

Fig. 4-9. Reference 400 MW(e), 60-Hz, nonintercooled helium gas turbine

TABLE 4-4

DETAILS OF REFERENCE 400 MW(e), 60-Hz, NONINTERCOOLED HELIUM GAS TURBINE

	Compressor		Turbine	
Inlet temperature, °C (°F)	26 (79)		850 (1562)	
Inlet pressure, MPa (psi)	3.17 (460)		7.6 (1109)	
Exit temperature, °C (°F)	177 (350)		533 (991)	
Exit pressure, MPa (psi)	7.93 (1050)		3.3 (476)	
Mass flow rate, kg/s (lb/s)	575 (1268)		542 (1195)	
Rotational speed, rpm	3600		3600	
Number of stages	18		8	
Stage number	1	18	1	8
Tip diameter, mm (in.)	1826 (71.9)	1735 (68.3)	1943 (76.5)	2184 (86)
Hub diameter, mm (in.)	1575 (62)	1575 (62.0)	1691 (66.6)	1590 (62.6)
Number of vanes, stator	78	121	90	50
Number of blades, rotor	77	120	124	68
Blade height, mm (in.)	126 (4.95)	80 (3.15)	125.7 (4.95)	297.2 (11.7)
Blade chord, mm (in.)	79 (3.1)	51 (2.0)	62.5 (2.46)	127 (5.0)
Vane height, mm (in.)	124 (4.9)	79 (3.1)	125.7 (4.95)	284.5 (11.2)
Vane chord, mm (in.)	76 (3.0)	48 (1.9)	110 (4.34)	211 (8.3)
Blade effective stress, MPa (psi)	--	--	107 (15,500)	214 (31,000)
Disk avg. tang. stress, MPa (psi)	407 (59,000)	358 (52,000)	294 (42,640)	248 (36,000)
Disk max. radial stress, MPa (psi)	476 (69,000)	517 (75,000)	335 (48,600)	331 (45,000)

Turbomachine Overall Data

Length overall, m (ft)	11.2 (36.84) (not including exhaust plenum)
Diameter overall, m (ft)	3.51 (11.5)
Rotor weight, kg (lb)	60,505 (133,500) (includes output shaft)
Stator and case weight, kg (lb)	216,140 (476,500) (includes plug seal assembly)
Total machine weight, kg (lb)	276,696 (610,000)
Bearings: Number of journal bearings	2
Type of journal bearings	5 pad tilting pad oil lubricated
Journal diameter, mm (in.)	508 (20)
Thrust bearing type	8 pad tilting pad, double-acting oil lubricated
Thrust bearing o.d., mm (in.)	762 (30)
Length of shaft over bearing centers, m (ft)	8.8 (29)

4.2.1.2 Turbomachine for HHT Plant Design (INT Configuration). The HHT turbomachine, designed for the German Utility market, has a power rating of 1200 MW(e) at 50 Hz, the INT embodying only one helium turbine with the 3000 MW(t) reactor. This large machine has a single shaft and a low-pressure and high-pressure compressor to realize an intercooled cycle (i.e., removal of compression heat after the low-pressure compressor). The low-pressure compressor, high-pressure compressor, and the turbine have 10, 12, and 9 stages, respectively. The rotor assemblies for this machine are welded and follow established BBC practice for industrial gas turbines and steam turbines.

Because of the large helium mass flow rate associated with the single turbomachine double-flow inlet and outlet ducts (to and from the heat exchangers and core) are necessary.

A comparison of the salient mechanical design features of the UTC and BBC turbomachine designs is given on Table 4-5. For the 1200 MW(e) HHT machine, the rotor is supported on three journal bearings. The size of these bearings [approximately 710 mm (28 in.) diam] is similar to those utilized in BBC steam turbines. The overall weight of this intercooled turbomachine is somewhat in excess of 816,000 kg (900 tons). Provision is made in the machine design for man access to all three journal bearings for inspection, maintenance, and replacement. The drive to the generator is from the turbine end of the machine. The thrust bearing is positioned at the (cold) compressor end of the machine, and since this is the free end of the rotating assembly, the shaft diameter is stepped down to allow use of a thrust bearing with a peripheral speed (and loading) similar to that used in large open-cycle gas turbines. With this arrangement, however, the thrust bearing and its associated service systems are positioned inside the PCRV.

With a turbine inlet temperature of 850°C (1562°F), an existing nickel-base alloy (713LC) has been selected for the turbine blades. The helium mass flow rate through the single BBC turbine, which is almost three times

TABLE 4-5
COMPARISON OF U.S. AND HHT TURBOMACHINE DESIGNS

Plant	GT-HTGR Reference Design (UTC)	HHT/INT Configuration (BBC)
Power Rating, MW(e)	400	1200
Frequency, Hz	60	50
Type	Nonintercooled	Intercooled
Overall diameter, m (ft)	3.5 (11.5)	4.4 (14.5)
Overall length, m (ft)	11.3 (37)	32 (105)
Approximate weight, ton	305	900
Type of Construction	Welded Rotor	Welded Rotor
Compressor Stages	18	10 (LP) + 12 (HP)
Turbine Stages	8	9
Turbine Blade Material	IN 100	713 LC
Blade Cooling	No	Yes, 3 or 4 Stages
Turbine Coolant Flow, %	3.6	2.2 + 1/2 to 1% leakage
Generator Drive End	Compressor	Turbine
Journal Bearings	2	3
Bearing Technology	From open-cycle gas turbine experience	Being developed for steam turbines (710 mm diameter)
Loading and Peripheral Speed	State-of-the-art	State-of-the-art
Thrust Bearing Location	Outside PCRV	Inside PCRV
Bearing Man Access	Yes	Yes, including center bearing
Turbine Inlets	1	2

that of the UTC machine (not exactly three because of the higher specific power of the intercooled cycle) necessitates a substantial increase in annulus flow area leading to higher stresses. The turbine blades (of nickel-base alloy) therefore must be cooled.

4.2.2 Seal Leakage

The performance of a closed-cycle gas turbine plant is sensitive to leakages in the system. Although detailed seal designs (in the vicinity of the turbomachine) were not prepared during this phase of the program, approximate seal leakage was estimated for inclusion in the cycle calculations as outlined below for the GA plant design embodying three 400 MW(e) gas turbines.

4.2.2.1 Turbine Inlet Duct Seals. The only mechanical duct attachment to the turbomachine is the turbine inlet duct. A tapered clamp flange is used for this application, with an extension rod penetrating either the compressor discharge duct closure or the PCRV concrete for remote actuation. A face seal is employed at each end of the movable duct section. The lower seal is held rigidly by the clamp. The upper seal can be a face seal because of the flexibility of the bellows integrated into the movable duct section. The duct bellows will allow relative movement between the duct and the turbomachine without disengaging either seal. Seal packings will be required at the two face joints to hold helium leakage rates to acceptable values. The packing material has been tentatively identified as pyrolitic graphite, which has the necessary resilience. When compressed, the graphite forms a good seal at the metallic interface because it conforms to the actual metal profile and decreases the permeability of the seal itself. The pressure difference across this mechanically clamped seal is low (recuperator ΔP + core ΔP) and a secondary leakage value of 0.14% of loop flow is estimated.

4.2.2.2 Turbomachine Cavity Casing Seals. The two casing seals in each turbomachine cavity seal compressor discharge gas from the compressor inlet

gas and turbine exhaust gas. These seals have not been designed in detail, but conceptual designs have been formulated and analytically modeled for computation of leakage rates. These seals are about 3.56 m (140 in.) in diameter, and since both the turbomachinery cavity liner and the gas turbine structure itself will change dimensions during plant operation, it is necessary to decouple the sealing surfaces to achieve small leakage rates. The principle of decoupling the seal surfaces from turbomachine and cavity liners has been modeled. It is postulated that a machined split-ring arrangement will be compliant so that gas pressure differential across the seal, assisted by springs, will tend to close gaps from waviness of sealing surfaces in the event of warpage. The ring assembly will be mounted in a seal housing bolted to the turbomachine. Both the ring assembly and seal housing will be withdrawn with the machine permitting servicing or replacement when the machine is removed for inspection or overhaul. In an actual seal design, more than one pair of compliant seal rings would be utilized.

Warpage of the sealing surfaces in service will no doubt occur. At this stage of the design, warpage is not an analyzable quantity. Since experience with similar seals is not available, the extent can only be conjecture. Advantages of these seals are that the inner seal rings are compliant, the pressure differential assists in compensating for warpage, and all members of the seal assembly will operate well below their yield stress. A preliminary estimate of the leakage through each casing seal of 0.4% of the loop helium flow has been incorporated in the plant cycle performance calculations. To minimize primary leakage in the system (i.e., high-to-low pressure), studies may lead to the adoption of another type of seal. Alternative possibilities are magnetic seals, or flexible face-to-face seals (possibly bellows-mounted) that use the large gas-pressure differential to load the seal with an appropriate resilient packing.

4.3 PRIMARY SYSTEM PRESSURE BOUNDARY

4.3.1 Revised Tendon Layout

Revision C to dwg SK92 (Fig. 4-10) illustrates recent PCRV geometry changes. The entire longitudinal prestress system has been revised; a new vertical tendon layout is shown on Sheet 1 and a new horizontal tendon layout is shown on Sheet 3.

4.3.1.1 Vertical Tendons. Recent plant optimization studies show an overall economic benefit when higher maximum power-conversion loop helium pressures are used. These higher pressures result in a higher maximum cavity pressure, necessitating increased vertical tendon load. Furthermore, some small changes to cavity dimensions have been made since previous tendon studies were made. It was discovered that the bypass valve control system ducting was responsible for much of the total vertical PCRV gas pressure load on the tendons, so the system was redesigned as reported in Section 4.3.2. The resulting top head vertical tendon geometry is shown in Sheet 1 of Fig. 4-10. Tendon placement was chosen to satisfy load requirements regardless of geographical location and to avoid cross ducts as well as sharp tendon bends.

The new vertical tendon layout provides for 624 tendons, of which 522 react against cavity pressure forces. Seventy-two tendons at the periphery of the PCRV react against the PCRV thermal-induced stress loads. The previous design employed a total of 545 vertical tendons, as discussed in Ref. 1.

It will be necessary to retension the tendons once during the plant lifetime. This will be done one year after initial tensioning to counteract the effects of concrete and tendon creep. No changes have been made to the design requirements of the tendons over those given in Ref. 15.

4.3.1.2 Horizontal Tendons. One result of the finite element PCRV stress analysis studies performed on the delta PCRV layout was that high concrete

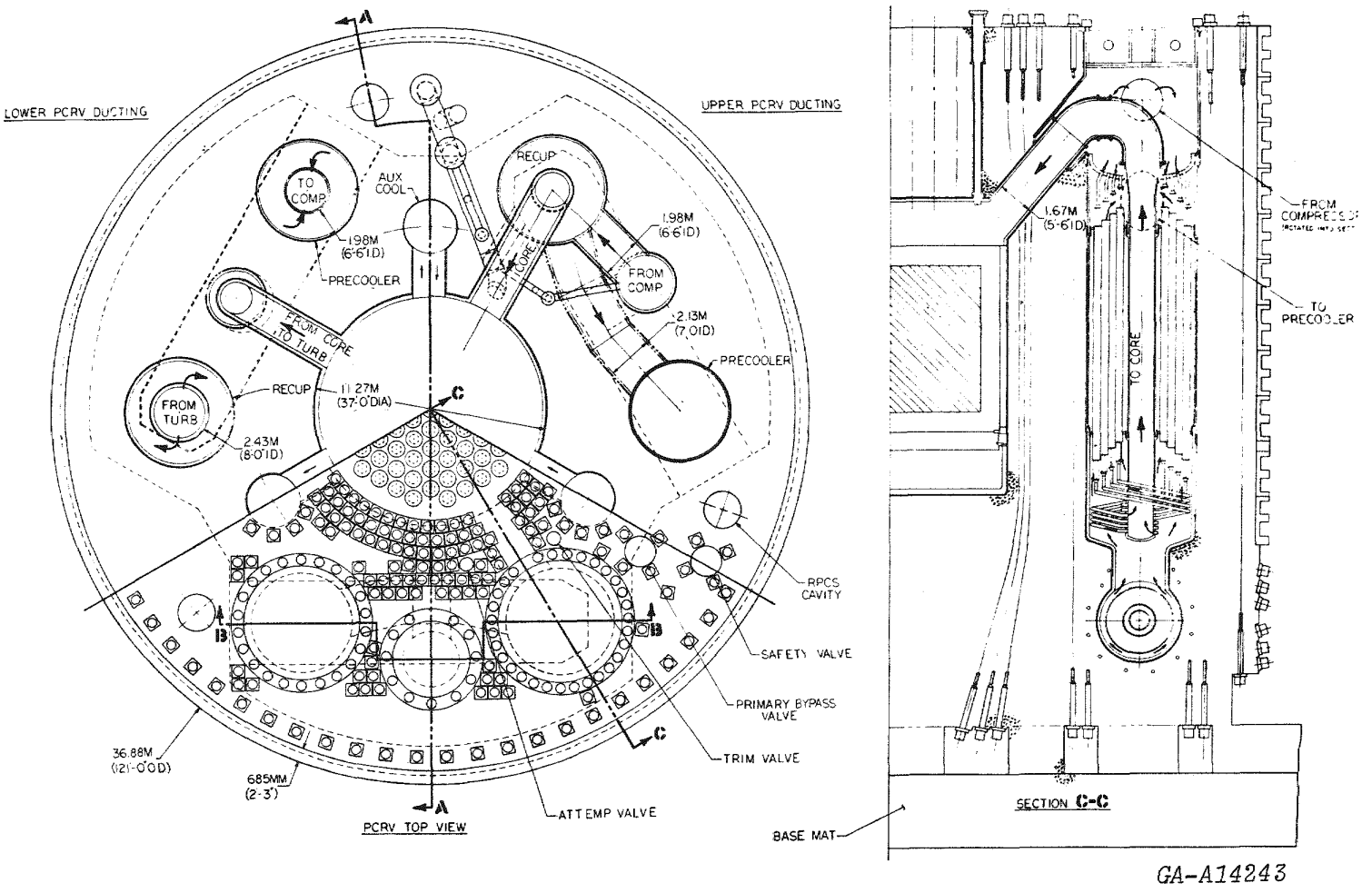

Fig. 4-10. Revised Delta layout of 3 loop 3000 MW(t) GT-HTGR (Sheet 1 of 3)

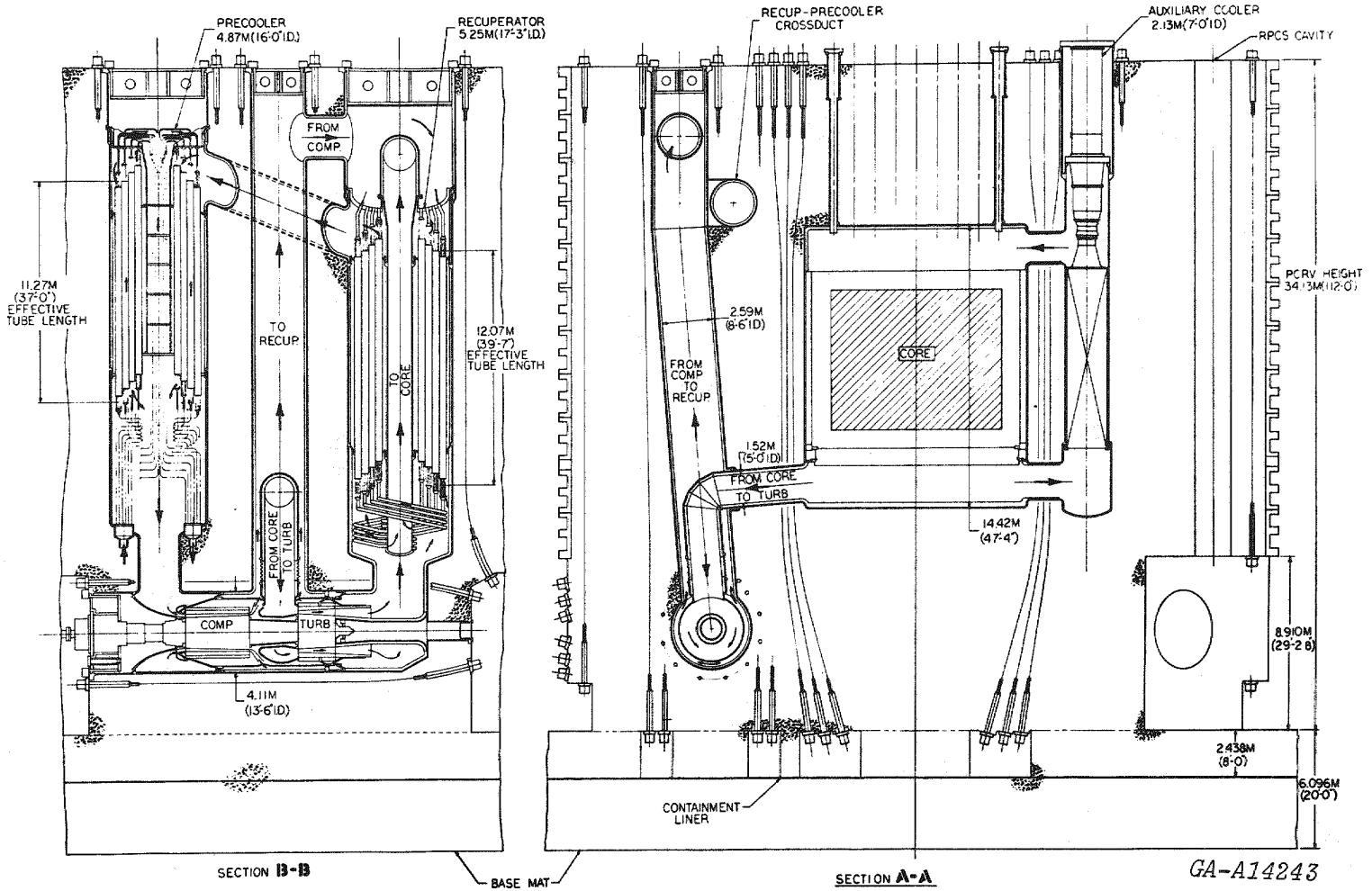

Fig. 4-10. Revised Delta layout of 3 loop 3000 MW(t) GT-HTGR (Sheet 2 of 3)

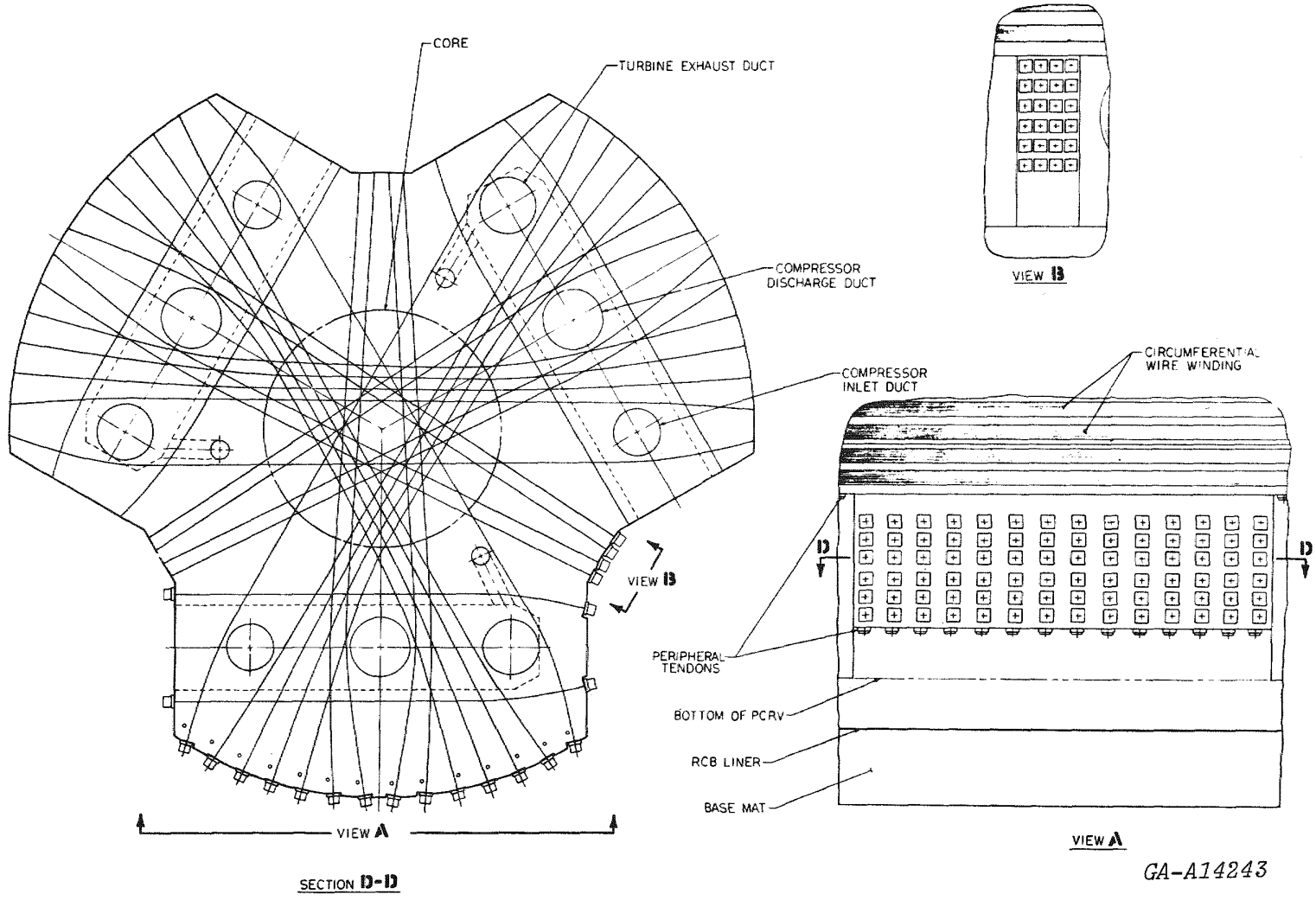

Fig. 4-10. Revised Delta layout of 3 loop 3000 MW(t) GT-HTGR (Sheet 3 of 3)

compressive stresses occurred at the turbomachine level. These stresses were caused by excessive forces applied by the horizontal or diagonal tendons that replace the circumferential wire wrap in that location. A new horizontal tendon layout employs a (smaller) total of 198 tendons, of which 162 span the PCRV diametrically, and 36 span chordally to provide longitudinal turbomachine cavity prestress. The layout is shown in Fig. 4-10. This new layout eliminates the high compressive stresses discussed above.

4.3.2 Revised Control Valve Arrangement

While vertical tendon layout studies, reported in Section 4.3.1, were being conducted, it was noted that the existing bypass control valve system duct geometry placed unnecessarily high vertical gas pressure forces on the PCRV. The system geometry was redesigned, shortening the valve ducting and placing the valve outlet ducting under the inlet duct and the core cavity inlet duct. The total vertically projected duct area was thereby reduced, as were the requirements for vertical tendons.

The resulting bypass control valve system duct geometry is shown in Fig. 4-11. The system is functionally unchanged; the system operational characteristics should be slightly improved, however, because the shorter, lower-loss ducting contains less helium. In the previous design, the valve outlet duct and the attemperation duct were routed outboard and around the recuperator cavity, as explained in Ref. 1.

4.3.3 Potential PCRV Size Reduction

As reported in Section 4.4 of Ref. 1, there is a potential for a PCRV diameter reduction from the 37.3 m (122.5 ft) shown to 34.4 m (113.0 ft). This change depends on an interpretation of ASME Boiler and Pressure Vessel Code Section III, Division 2. A formal inquiry to the proper code committee has been initiated to clarify the rules and to institute a special code case, if required.

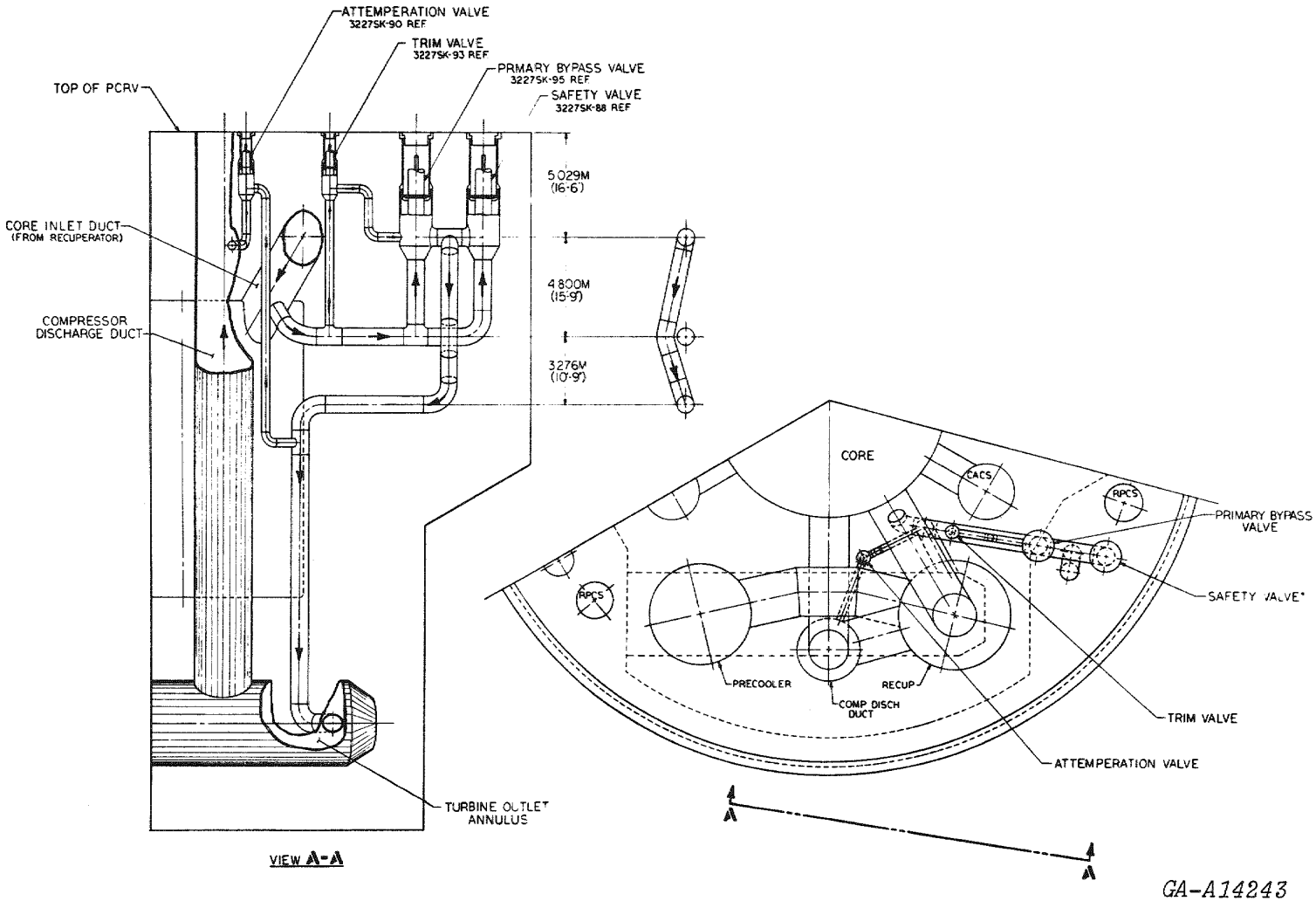

Fig. 4-11. Revised scheme for integrating bypass valves into PCRV

4.3.4 Cool and Warm Liner Arrangement

The low-pressure cool liner concept was first discussed in Section 4.2.1 of Ref. 1. A sketch of the flow paths involved with the low-pressure cool liner is shown in Fig. 4-12. For full flow, the entire flow returns via the cross duct and recuperator cavity. For partial flow, 90% of the flow enters directly into the compressor inlet through the precooler compressor inlet duct and the remaining 10% flows to the compressor inlet via the cross duct, etc. A flow restrictor in the precooler/compressor inlet duct provides the differential pressure required to cause 10% of the flow to return via the cross duct.

A low-pressure warm liner approach shown in Fig. 4-13 was also studied. In this approach, the outlet gas from the recuperator flows down around the outside of the recuperator, outside the turbine cavity, and up around the outside of the precooler to enter the precooler at the top. This scheme requires a warm PCRV liner, because the recuperator outlet operates at 222°C (431°F). Internal insulation would probably only be required in the area of the precooler outlet and the compressor inlet to prevent recuperation that would raise the compressor inlet temperature and decrease the plant efficiency. If the same annular gap widths are chosen for the warm liner as was chosen for the cold liner, the pressure drop will increase for the warm liner, since the higher temperature results in a lower density and therefore a higher flow velocity.

The use of high-pressure cooling was discussed briefly in Section 4.2.2 of Ref. 1. It is currently recommended that a bleed flow of about 1% from the compressor outlet be used to cool the core seismic restraint structure. This would probably be necessary even if the warm liner concept were adopted.

If a warm liner is adopted, it appears that full flow around the core shroud is not the recommended solution due to the performance loss and the liner heating load. About 10% of the flow should be bled around the core

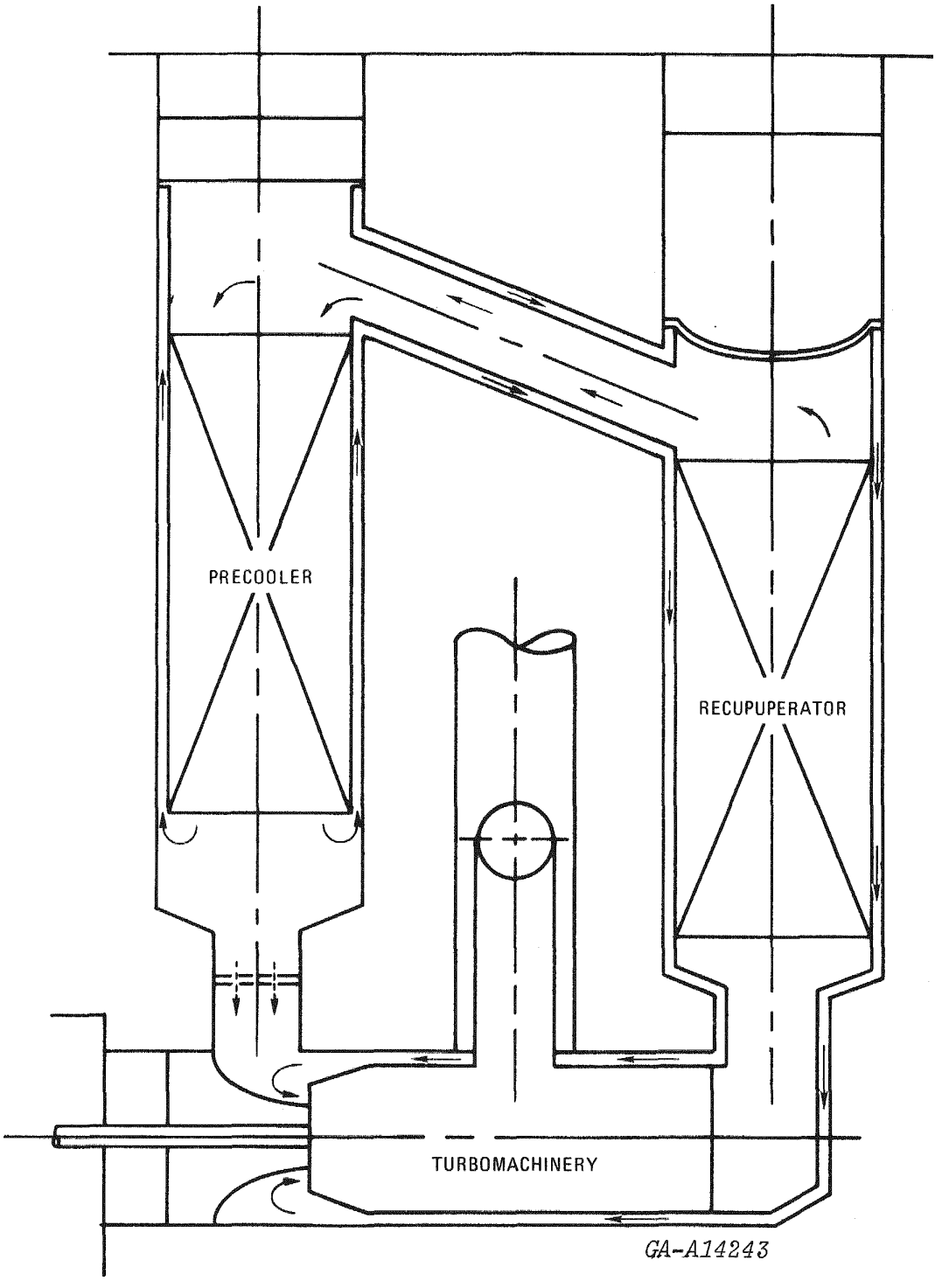

Fig. 4-12. Low-pressure cool liner arrangement

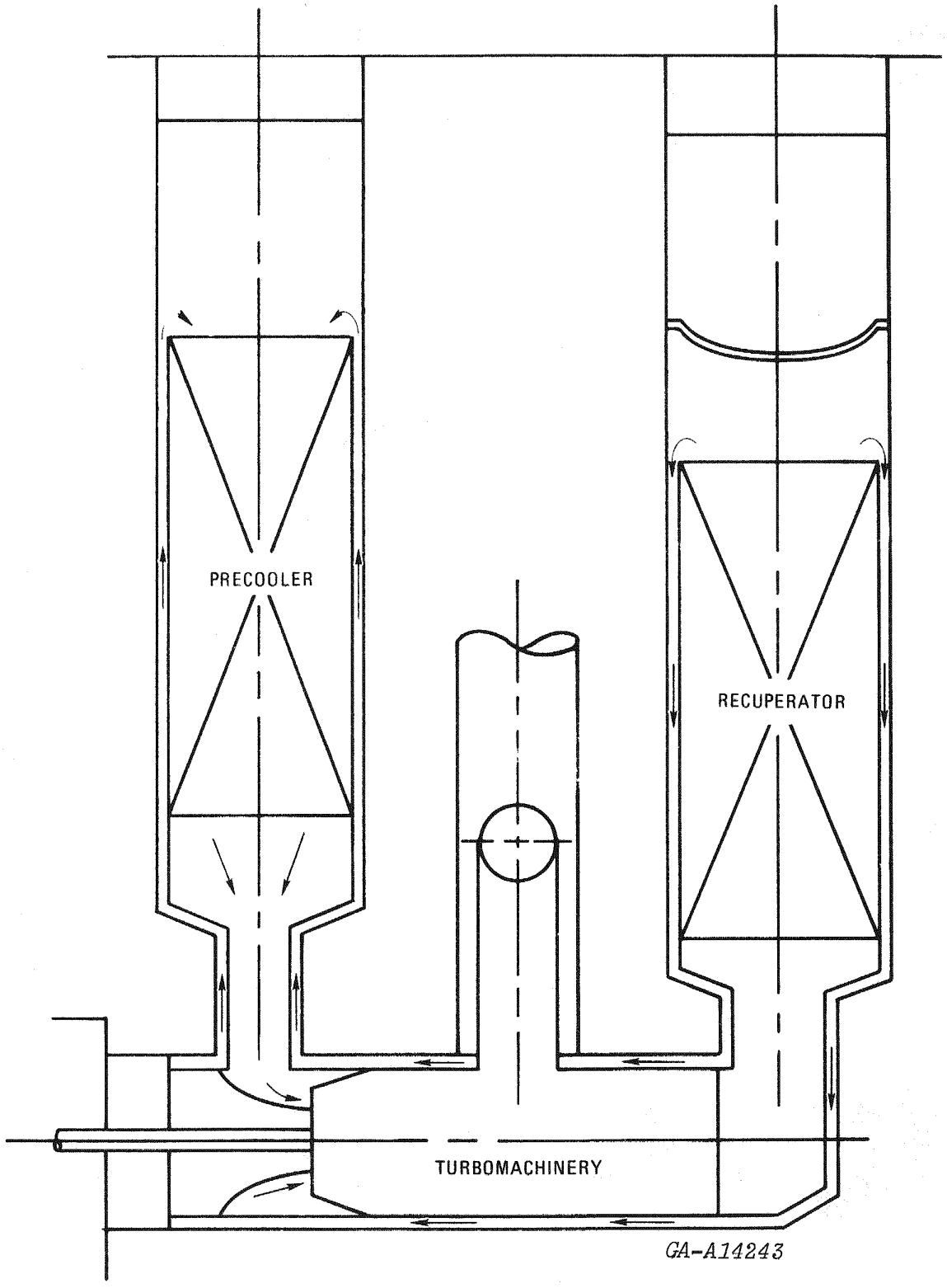

Fig. 4-13. Low-pressure warm liner arrangement

shroud to prevent overheating the core cavity liner and the remainder passed up the vertical compressor outlet duct as shown in Fig. 4-14. This will minimize both pressure losses and safety problems. Details of this system have not been completed.

Table 4-6 compares the system performances of cooled and warm liner arrangements with the standard GT-HTGR layout. The pressure drop penalty shown for the low-pressure warm liner is based on slightly larger flow passages, which are partially reflected in an additional increase in PCRV diameter. The last two columns, which are for full and partial flow high-pressure warm liner, are based on approximations because the warm liner studies have not been completed. The partial flow column under warm liner refers to the 10% flow around the core shroud and 90% through vertical compressor outlet duct.

A combination not yet investigated is cooled liner on the low-pressure side and a warm liner on the high-pressure side, with partial flows for both. Such a combination should lead to a minimum penalty if the thermal barrier is to be eliminated throughout the plant.

4.3.5 Core Cavity Cooling with Down Loops

Section 4.2 of Ref. 1 reported study results related to core outlet duct and core cavity annulus cooling; a compressor discharge bleed scheme was selected. This section reports results of a continued study to evaluate the cooling effectiveness provided to the core cavity annulus when the reference plant is run with one loop inoperative at 100% helium inventory and maximum reactor outlet temperature of 850°C.

The results of the recent study show that when properly designed, the selected cooling scheme will cool the core annulus without hot streaks and with about 2/3 normal annulus cooling flow where one loop is shut down. A key to successful bleed cooling system operation is the use of a coolant distribution manifold located at the core cavity annulus log seal as shown in Fig. 4-15.

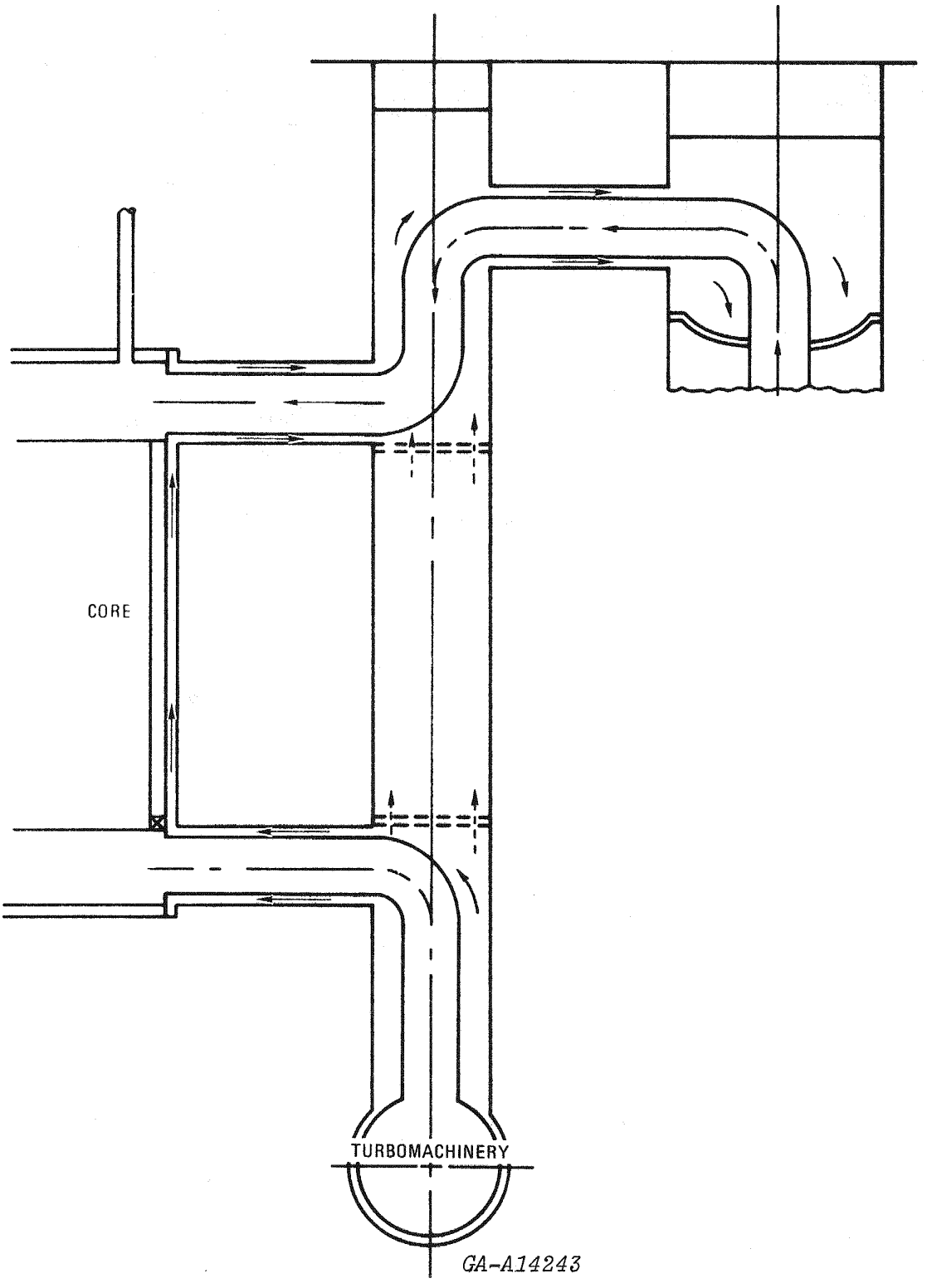

Fig. 4-14. High-pressure warm liner arrangement

TABLE 4-6
COMPARISON OF COOL AND WARM LINER DESIGN APPROACHES WITH REFERENCE INSULATED LINER DESIGN

Item	Cooled Liner		Warm Liner		
	Full	Partial	Low Pressure Only	Full[a]	Partial[a]
Δ Efficiency, %	-0.6	-0.05	--	--	--
Δ $\left(\frac{\Delta P}{P}\right)$ %	+1.112	+0.015	+0.453	+1.0	+0.62
Δ PCRV Diameter, m (ft)	0.701 (+2.3)	0.61 (+2.0)	0.91 (+3.0)	2.3 (+7.5)	2.13 (+7.0)
Δ PCRV Height, m (ft)	(+0.5)	0.15 (+0.5)	0.31 (+1.0)	0.91 (+3.0)	0.91 (+3.0)

[a]Preliminary estimates only.

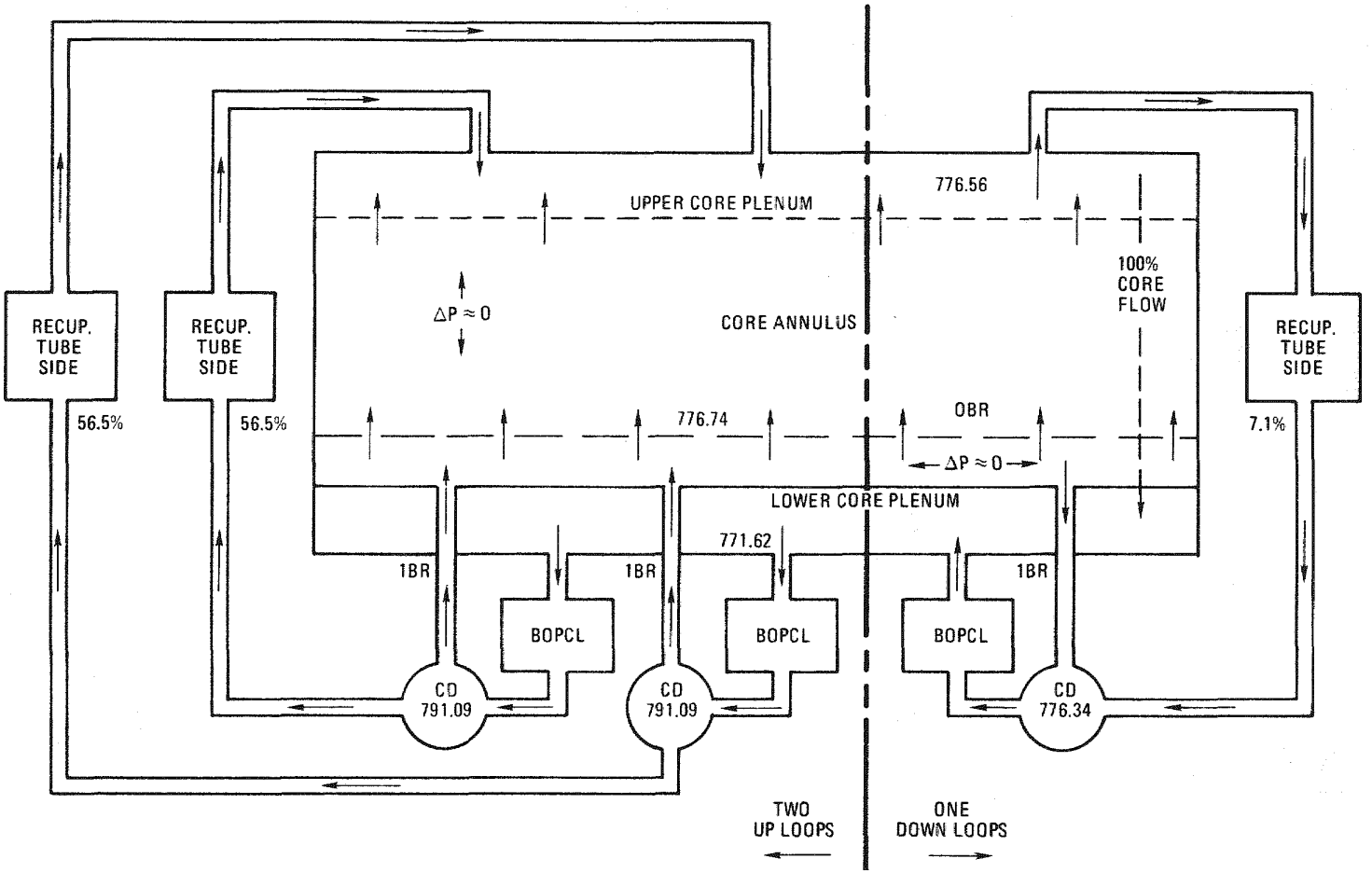

LEGEND

BOPCL = BALANCE OF POWER CONVERSION LOOP
CD = COMPRESSOR DISCHARGE
IBR = INLET BLEED RESISTANCE
OBR = OUTLET BLEED RESISTANCE

NOTE:

ALL VALUES (E.G., 776.56) ARE IN PSIA
PERCENTAGE VALUES INDICATE FLOW RATES COMPARED WITH CORE FLOW, WITHOUT COOLANT BLEEDS

GA-A14243

Fig. 4-15. Schematic of core annulus cooling with an inoperative loop

Core cavity annulus cooling by compressor discharge bleed without a bleed manifold would result in undercooled regions between the three turbine inlet ducts during normal operation, because of a lack of flow potentials there. During single-loop shutdown operation, an additional hot region would occur above the down-loop bleed port.

The normal function of the coolant distribution manifold is to receive compressor discharge bleed coolant from the three turbine inlet cross duct coolant annuli and to provide for low-pressure loss coolant distribution around the core periphery before metering the coolant upward into the cavity annulus. During single-loop shutdown operation, this design prevents annulus hot streaks by supplying high-pressure gas to the down loop reverse flow bleed orifice through the coolant distribution manifold. The core inlet plenum gas is not exposed to the reverse bleed in the down loop because of the coolant manifold, which provides a rather uniform, reduced flowrate coolant flow around the core cavity annulus.

Figure 4-15 is a flow schematic of the subject plant and conditions. Pressure and flow data were derived from REALY2 code (Ref. 5) run output. It was calculated that the pressure losses caused by coolant manifold flow and by core cavity annulus flow are low compared to the available flow potentials (1/4 ft^2 manifold flow area used). The coolant manifold pressure can be selected by specifying the inlet and outlet flow resistances. It is evident by inspection of Fig. 4-15 that use of high manifold inlet and outlet resistances will result in a low manifold pressure and reduced reverse bleed flow into the down loop compressor discharge duct. Improved core annulus cooling through a higher net flow rate would result without affecting the normal operation bleed flows. Fortunately, it will be mechanically easier to provide this desirable flow resistance ratio (high inlet/low outlet) than the reverse, as can be seen in Fig. 4-16.

4.3.6 Two-Loop PCRV Arrangement

Two-loop nonintercooled PCRV arrangements of the 3000 MW(t) GT-HTGR were investigated briefly in an effort to come closer to the current

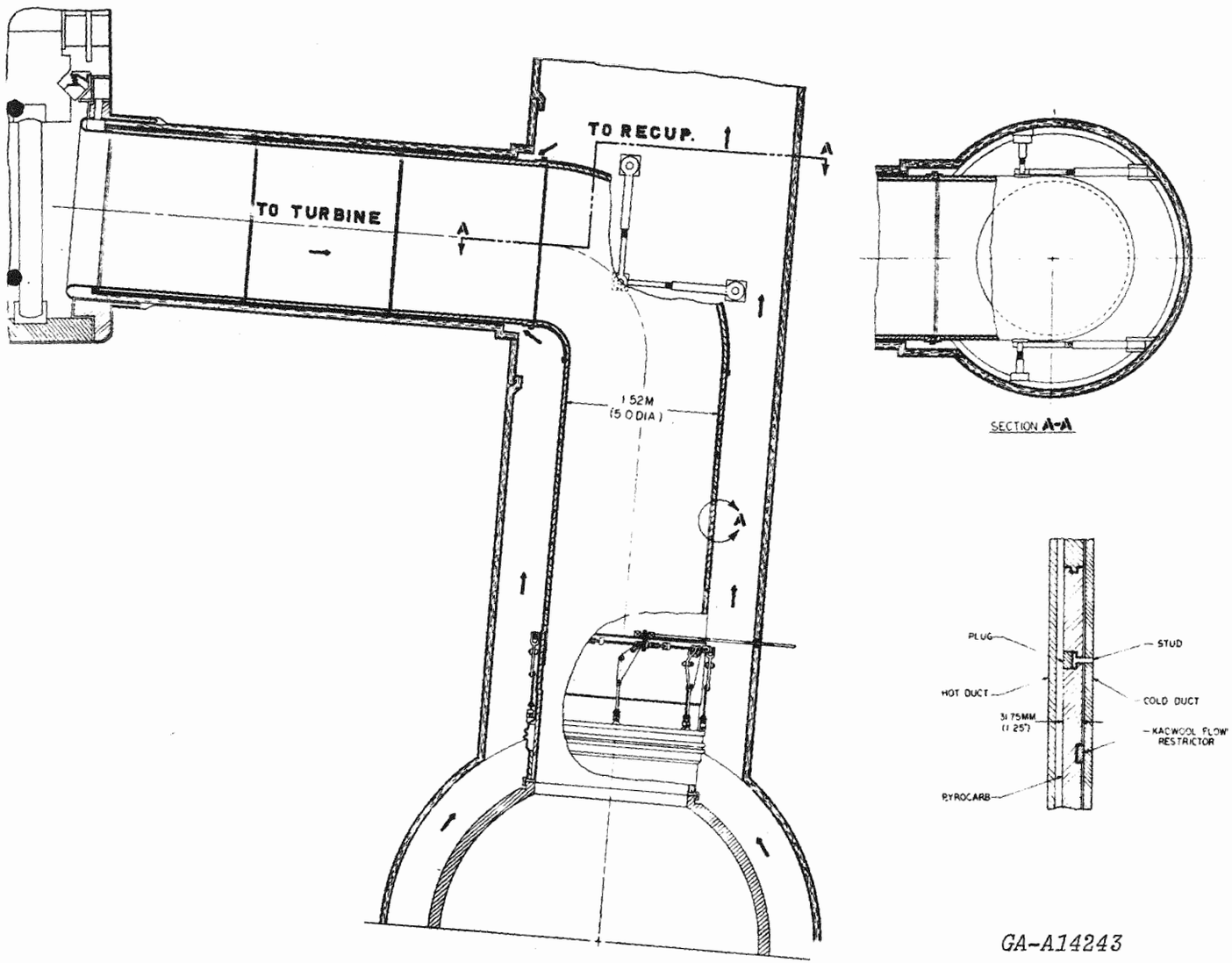

Fig. 4-16. Supply to core annulus coolant manifold

European direct-cycle reference designs. A comparison of the two arrangements studied and the current 3-loop design is shown in Fig. 4-17.

Arrangement 1 of Fig. 4-17 is one in which both the recuperator and precooler for each loop have separate cavities. This arrangement results in a minimum diameter PCRV, but the ducting arrangement for the system is quite complicated.

Arrangement 3 of Fig. 4-17 shows the conventional approach to a 2-loop arrangement. In this arrangement, only a single recuperator and precooler is used for each loop. This arrangement is stress limited because of the size of the single recuperators and results in 3.9 m (13 ft) increase in PCRV diameter over arrangement 1 and a 2.7 m (9 ft) increase over the conventional 3-loop arrangement, shown in arrangement 2, when the diameters are calculated on the same basis.

More detailed work must be done on the ducting arrangement and system pressure drops before a choice between the two systems can be made. It is now estimated that the cycle efficiency loss penalty associated with arrangement 1, due to increased system pressure drop, along with the increased cost of PCRV liner and thermal barrier, will more than offset the cost from the increased diameter of arrangement 3. Further investigations of the 2-loop designs are contemplated.

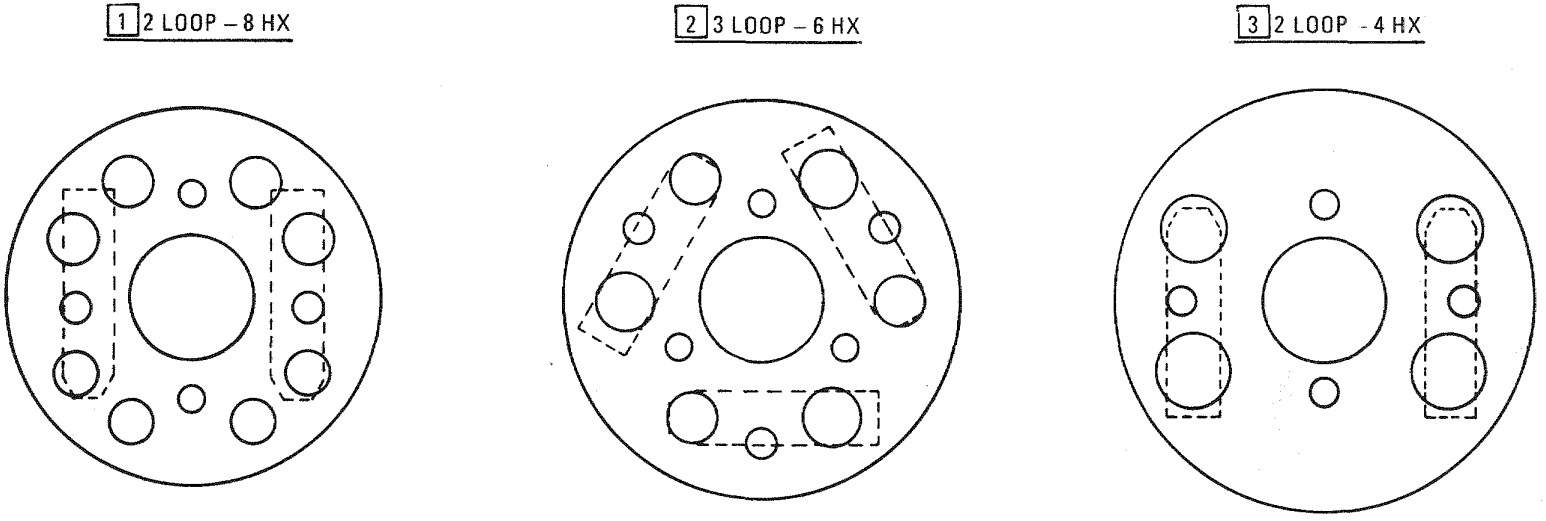

	NO.	METER	FT – IN.	NO.	METER	FT – IN.	NO.	METER	FT – IN.
CORE CAVITY DIAM	1	11.28	37 – 0	1	11.28	37 – 0	1	11.28	37 – 0
RECUPERATOR DIAM	4	4.80	15 – 9	3	5.46	17 – 11	2	6.65	21 – 0
PRECOOLER DIAM	4	4.39	14 – 5	3	5.03	16 – 6	2	6.10	20 – 0
VERTICAL DUCT DIAM	2	3.40	11 – 2	3	2.82	9 – 3	2	3.40	11 – 2
LOW PRESSURE CROSS DUCT DIAM	2	2.82	9 – 3	3	2.36	7 – 9	2	2.82	9 – 3
HIGH PRESSURE CROSS DUCT DIAM	2	2.67	8 – 9	3	2.21	7 – 3	2	2.67	8 – 9
CORE INLET DUCT DIAM	4	1.75	5 – 9	3	1.98	6 – 6	2	2.36	7 – 9
CORE OUTLET DUCT DIAM	2	2.21	7 – 3	3	1.88	6 – 2	2	2.21	7 – 3
TURBINE OUTLET DUCT DIAM	4	2.44	8 – 0	3	2.82	9 – 3	2	3.35	11 – 0
COMPRESSOR INLET DUCT DIAM	4	1.83	6 – 0	3	2.13	7 – 0	2	2.59	8 – 6
TURBOMACHINE CAVITY DIAM	2	4.11	13 – 6	3	4.11	13 – 6	2	4.11	13 – 6
PCRV OUTER DIAM (MPC = 6.033 MPa)		32.92	108 – 0		34.90	114 – 6		36.88	121 – 0
PCRV HEIGHT		34.14	112 – 0		34.14	112 – 0		34.14	112 – 0
GT-HTGR 3000 MW(t)		1			2			3	

GA-A14243

Fig. 4-17. Comparison of 3-loop plant with conceptual 2-loop arrangements (nonintercooled)

REFERENCES

1. "Gas Turbine HTGR Program, Quarterly Progress and Task Closeout Report for the Period Ending September 30, 1976," U.S. ERDA Report GA-A14097, General Atomic Company, October 1976.
2. "Gas Turbine HTGR Program, Semiannual Progress Report for the Period January 1, 1976, through June 30, 1976," U.S. ERDA Report GA-A13950, General Atomic Company, July 30, 1976.
3. "Gas Turbine HTGR Program, Semiannual Progress Report for the Period July 1, 1975, through December 31, 1975," U.S. ERDA Report GA-A13740, General Atomic Company, January 29, 1976.
4. "Gas Cooled Reactor Assessment," report prepared for U.S. ERDA by A. D. Little, Inc., United Engineers and Constructors, and S. M. Stoller, August 1976.
5. Croft, M. Z., "REALY2, The GT-HTGR Transient Performance Analysis Program," U.S. ERDA Report GA-A13880, General Atomic Company, March 31, 1976.
6. Schoene, T. W., "The Potential Effects of Wet/Dry Cooling on the Economic Incentives for the Gas Turbine HTGR," U.S. ERDA Report GA-A14192, General Atomic Company, December 1976.
7. "Engineering and Economic Evaluation of Wet/Dry Cooling Towers for Water Conservation," United Engineers & Constructors, Incorporated, Report UENC-ERDA-761130, November 1976.
8. GT-HTGR Design Criteria GCT-24-1 "Helium Storage System, 1/22/74," General Atomic Company unpublished data.
9. Bathe, K., et al., "A Structural Analysis Program for Static and Dynamic Response of Linear Systems," Report No. EERC 73-11 University of California, Berkeley, June 1973.
10. Electrical World, July 13, 1970, McGraw Hill.
11. "635 Ton Lift," Transportation Engineer, April, 1976.
12. "Jacks Install 462 Ton Stator," Engineering News Record, January 1, 1976.
13. Heede Lift Climbers (Brochure) Heede International Inc., Burlingame, California.

14. Correspondence from Brown & Root to General Atomic on GT-HTGR Heat Exchangers, unpublished data, January 15, 1975.
15. "GASSAR-6," General Atomic Standard Safety Analysis Report, February 5, 1975 (NRC Docket STN 50-535).